

BOOK OF ABSTRACTS

SCIENTIFIC CONFERENCE FOR YOUNG RESEARCHERS

COMMUNICATING IN SCIENCE



CUTTING
EDGE **2019**

Tuesday

17. 9. 2019

Faculty of Chemistry and
Chemical Technology,
University of Ljubljana

Organizator in založnik zbornika

Fakulteta za kemijo in kemijsko tehnologijo, Univerza v Ljubljani

Kraj prireditve

Fakulteta za kemijo in kemijsko tehnologijo, Univerza v Ljubljani

Urednika

Jakob Kljun, Tina Paljk

Organizacijski odbor

Sara Drvarič Talian, Aljaž Gaber, Monika Horvat, Marina Klemenčič, Marija Kisilak, Jakob Kljun, Tina Paljk, Nejc Petek, Aleš Ručigaj

Grafično oblikovanje

Miha Koželj

Tisk

TISKARNA PRINT POINT marketing in oglaševanje d.o.o.

Naklada

50

Publikacija je dostopna na spletu

www.fkkt.uni-lj.si

CIP - Kataložni zapis o publikaciji
Narodna in univerzitetna knjižnica, Ljubljana

54:66(082)

SCIENTIFIC Conference for Young Researchers (2019 ; Ljubljana)

Communicating in science : book of abstracts / Scientific Conference for Young Researchers, 17. 9. 2019 ; [organizator Fakulteta za kemijo in kemijsko tehnologijo, Univerza v Ljubljani ; urednika Jakob Kljun, Tina Paljk]. - Ljubljana : Fakulteta za kemijo in kemijsko tehnologijo, 2019

ISBN 978-961-7078-04-6

1. Gl. stv. nasl. 2. Kljun, Jakob

COBISS.SI-ID 301631744



Odd years are the Cutting Edge years and this one is an especially special one!

This year's Cutting Edge was organized within the celebration of 100th anniversary of University of Ljubljana in collaboration with the National Institute of Chemistry, the National Institute of Biology and the Jožef Stefan Institute.

We started already on Monday, 16. 9. 2019 at 7pm at the atrium ZRC SAZU (Novi trg 2, Ljubljana) where we in collaboration with the Science on the Street team organized the first Cutting Edge Science Slam. There were 8 presenters with 8 very cool topics who were given only 5 minutes to present them!

The unforgettable Cutting Edge 2019 conference took place the next day, Tuesday, 17. 9. 2019, and lasted from 9am till eternity (6pm officially) at UL FKKT. This year's topic was Communicating in Science. For this reason, we invited **Alok Jha**, currently science and technology correspondent at The Economist, previously journalist for ITV News, the Guardian and the BBC to give a plenary lecture.

There were more than 150 participants!

106 of them presented their research in two poster sessions, while the rest of them came as passive participants to listen to three invited speakers: **Andreja Kutnar**, the only Slovene COST action holder, who talked about what COST actions are, what the benefits of being involved in them are and how to join them, **Katerina Peterkova**, an ITN Marie Curie PhD fellow, who shared with us her experience about ITN-MSCA programmes and why to choose to study abroad and **Matevž Dular**, holder of an ERC consolidator grant who talked about ERC funding, his exciting research and how to plan and build your research career.

In the afternoon two parallel workshops were organized; one held by **Noah Charney**, who told us more about narration and storytelling in communicating research results and the second one, held by **Barbara Luštek Preskar**, who focused on graphical aspects of presenting research.

We finished by giving awards to the best posters and a mingled into the evening.

The conference could not have been organized at the level as it was without the help of several students of the Faculty of Chemistry and Chemical Technology. We thank Teja Antončič, Lucija Belingar, Veronika Bračić, Maša Brulc, David Ciriković, Matej Kolarič, Jana Krušič, Ervin Rems and Klemen Zupančič for their efforts.

We sincerely thank the Faculty of Chemistry and Chemical Technology and the Unit for Researcher Support and Promotion of University of Ljubljana for organizational help.

We look forward to the next odd year ;)

The Cutting Edge team



CUTTING
EDGE **2019**

8.00 - 9.00	<i>Registration</i>		
9.00 - 9.20	<i>Opening</i>		
9.20 - 10.20	Plenary lecture	Alok Jha, <i>2014 Science Communication Award</i>	
10.20 - 11.00	<i>Poster session & Coffee break</i>		
11.00 - 11.40	ITN Marie-Curie	Katerina Peterkova, <i>PhD student, LightDyNAMics MSCA ITN</i>	
11.40 - 12.20	COST actions	Andreja Kutnar, <i>chair, COST action ModWoodLife</i>	
12.20 - 13.20	<i>Lunch</i>		
13.20 - 14.00	ERC grant	Matevž Dular, <i>Consolidator ERC grant holder</i>	
14.00 - 15.00	<i>Poster session & Coffee break</i>		
15.00 - 18.00	Workshops	1. Noah Charney <i>Narration and storytelling in communicating research results</i>	2. Barbara Luštek Preskar <i>How to make presentations in science more engaging</i>
18.00 - ____	<i>Closing ceremony</i>		

TABLE OF CONTENTS

POSTERS



KOPRIVNIKAR KRAJNC MIHA: The role of chemokine CCL5 and its receptor CCR5 in glioblastoma	1
UTROŠA PETRA: In situ simultaneous interpenetrating polymer networks as the precursors to porous polystyrene monoliths	2
LAVRIHA PIA: DARPin C4 mimics adenylyl cyclase 9 activation by $G\alpha_s$	3
PLAVEC TINA VIDA: Tumor cell lines-targeting by <i>Lactococcus lactis</i>	4
MOŽE MATIC: Transition of surface chemistry and morphology of laser-textured copper surfaces due to exposure to boiling critical heat flux	5
ROČNIK TINA: Biodegradability study of chitosan-based films with added chestnut extract in an aqueous environment.....	6
ŠUŠTARIČ ARIANA: Optimization of HFME for determination of benzotriazoles in environmental waters	7
NOVAK VALENTINA: Is transportin 1 involved in nuclear import of annexin A11?.....	8
BRADIĆ BOJANA: Fractionation of shrimps shells biomass by choline chloride/lactic acid deep eutectic solvent.....	9
HABIČ ANDREJA: A novel method for discovery of DNA-protein interaction partners	10
GORIČAN TJAŠA: Development of allosteric modifiers of cathepsin S based on the scaffold of a cathepsin K effector	11
LATYSHEVA DARIA, PREŠERN UROŠ AND ŠKRINJAR PETER: EpCAM – A shift from cell-cell adhesion to signaling	12
ZUPANČIČ DEJA: Physico-chemical and qualitative properties of Slovene honey	13
CERAR JURE: Structure–dynamics relationship in aqueous tert-butanol solutions	14
ROZMAN ULA: Characterization of waste fungal biomass – an effective adsorbent for heavy metals.....	15
STOJANOV SPASE: Engineering fluorescent probiotic bacteria	16
ANTONČIČ TEJA: Degradation of antibiotics by ozone-based reactions.	17
MAKSIMOVIĆ OLIVERA: New methods to reveal pathogenic viruses in food and water sources	18
VRABEL MARTIN: Degradation of antibiotic mixture by ozone-based reactions.	19

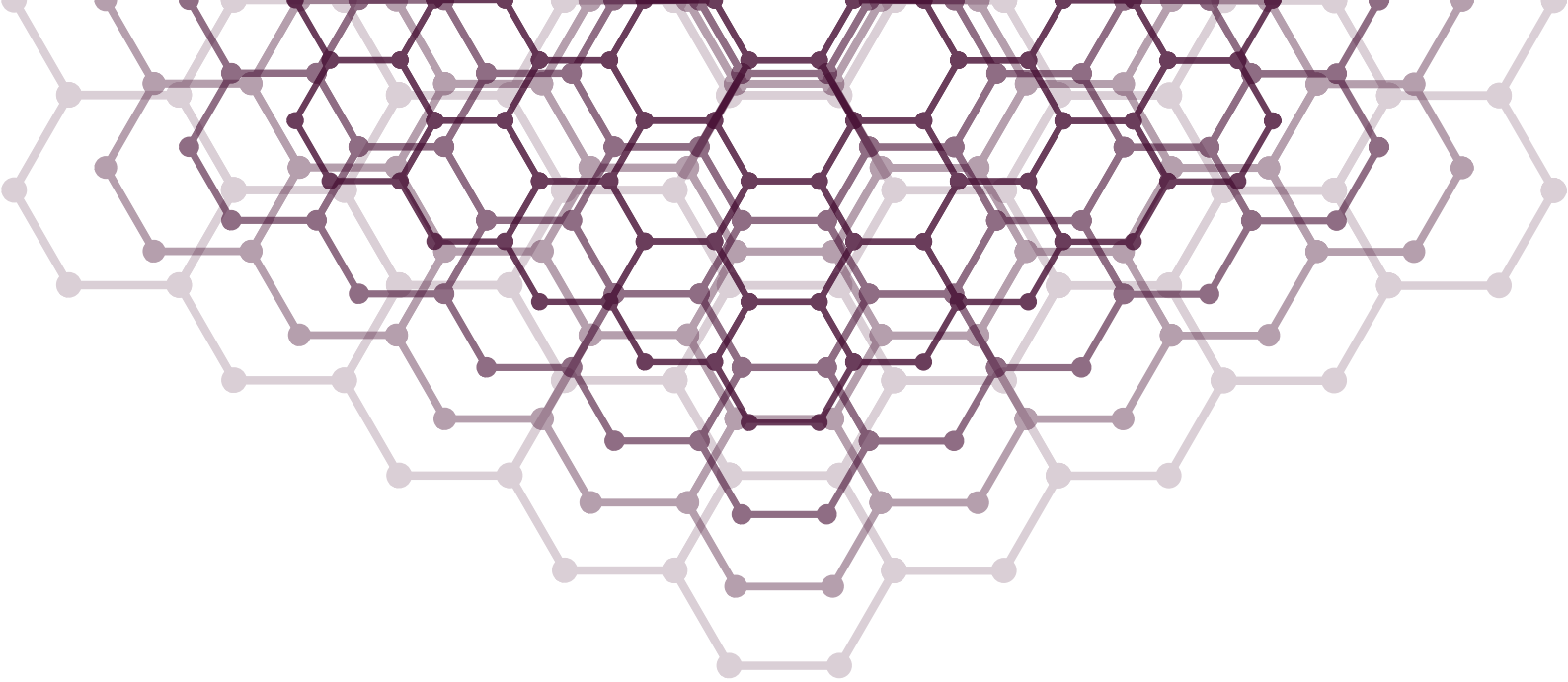
BRUDAR SANDI:	In silico investigation of hen egg-white lysozyme self-association in aqueous solutions.....	20
SIMONČIČ MATJAŽ:	The effect of sucrose and sucralose on cloud point temperature of lysozyme solutions.....	21
SEME TANJA:	Degradation of antibiotic amoxicillin by hydrodynamic cavitation...	22
LEGAN MAŠA:	The use of electronic devices and musculoskeletal discomfort among university students at the Faculty of chemistry and chemical technology in Ljubljana.....	23
JERMAN LARA:	Caspase cleavage frequency at human protein exon junction sites	24
ĐURIČIĆ TIJANA:	Corrosion testing and efficiency of benzotriazole based inhibitor on stainless steel and copper.....	25
HOČEVAR BRIGITA:	The effect of the catalyst type and the reaction conditions on hydrodeoxygenation of aldaric acid	26
JURJEVEC SARAH:	π -Conjugated polyHIPEs.....	27
POŽEK KITY:	Expression of cystatin C in the PC12 cell model of Alzheimer's disease after exposure to amyloid beta peptide 25-35	28
KOVAČIČ ŽAN:	Mechanical properties and curing kinetics of aromatic epoxides with aminomaleimide.....	29
JASIUKAITYTE GROJZDEK EDITA:	Typical lignin bond cleavage in acidified aqueous and non-aqueous alcohols.....	30
STANTIČ METKA:	Antibodies glycan analysis using recombinant prokaryotic lectins .	31
TUŠEK MARTIN:	Modelling water with rose functions	32
VEHAR ANJA:	Disinfection of wastewater – tertiary treatment in municipal wastewater treatment plant with peracetic acid.....	33
RIJAVEC TJAŠA:	Development of an amperometric biosensor for the detection of biogenic amines.....	34
RAVNIK VID:	The effect of ion size on the electrolyte distribution near a charged wall. A Poisson-Boltzmann and Monte Carlo study	35
LOKAR KRISTA:	The effect of drying conditions on mechanical properties of alginate-based films	36
MAKLIN ANA:	Optimizing expression of human wild type ANXA11.....	37
KOJČINOVIĆ ALEKSA:	Influence of molybdenum-oxides' oxidation state and morphology on furfural hydrodeoxygenation	38
KREJAN EVA:	Comparison of organic and ruthenium dyes in dye-sensitized solar cells.....	39

SUPEJ ŠPELA:	Isolation and characterization of ANXA11 mutants D40G and dN1-118.....	40
SRNKO MARIJA:	Introduction of surface exposed thiol groups on filamentous virus like particles.....	41
PETROVČIČ JAN:	Can we recycle reagents for nucleophilic fluorination.....	42
ČERNE URŠKA:	Effect of M33 nanobody on cell death caused by MLKL protein ...	43
HLADNIK LUCIJA:	Extraction of flavonoids from lignocellulosic biomass as the first valorization step in a biorefinery.....	44
KRAVOS ALEKSANDER:	Aerobic iodochlorination of alkenes with iodine and hydrochloric acid catalysed by sodium nitrite	45
BELINGAR LUCIJA AND KAPŠ ŠPELA:	Biochar from beechwood: Preparation and characterization	46
OBERLINTNER ANA:	Chitosan-based films with incorporated natural extracts.....	47
JAKLIN MATEJ:	The influence of buffer identity on the hydrodynamic radius and zeta-potential of hen egg white lysozyme molecule.....	48
SILJANOVSKA ANA:	Synthesis of stable diazonium salts	49
HABIČ ANAMARIJA:	Characterisation of human retrotransposon L1 ORF1p clusters....	50
HABIČ ANAMARIJA:	Variation within ultraconserved elements in the human genome ...	51
SEDEJ NELI:	Natural variants of human CYP51: a molecular dynamics study....	52
KOPAČ TILEN:	Designing hydrogels for controlled drug delivery.....	53
BRENČIČ KATJA:	Dyeing cotton with dyes obtained from invasive alien plants.....	54
ČUK NINA:	In situ phytosynthesis of silver nanoparticles on cellulose fibers with Fallopia japonica extract.....	55
TITOVŠEK DAVID, CAFUN AJDA AND IVANOVSKI ANDREJ:	Calcium binding properties of α -actinin.....	56
GORŠEK NIKA:	Intracellular responses of the model alga, Chlamydomonas reinhardtii, to oxidative and salt stress.....	57
LISAC ANA:	The influence of physiological state of bacteria Escherichia coli in occurrence of hibernation mode in formation of bacteriophages...	58
OŠTREK ANDRAŽ:	Novel inhibitors of the Plasmodium falciparum dihydroorotate dehydrogenase.....	59
KASTELEC LEA:	In-vitro model for measurements of ionized calcium using ion-selective electrode	60
JARC RYDZI MATEJ:	Compounds obtained by $K_3[Fe(C_2O_4)_3] \cdot 3H_2O$ and bis(3,5-dimethylpyrazol-1-yl)acetate.....	61

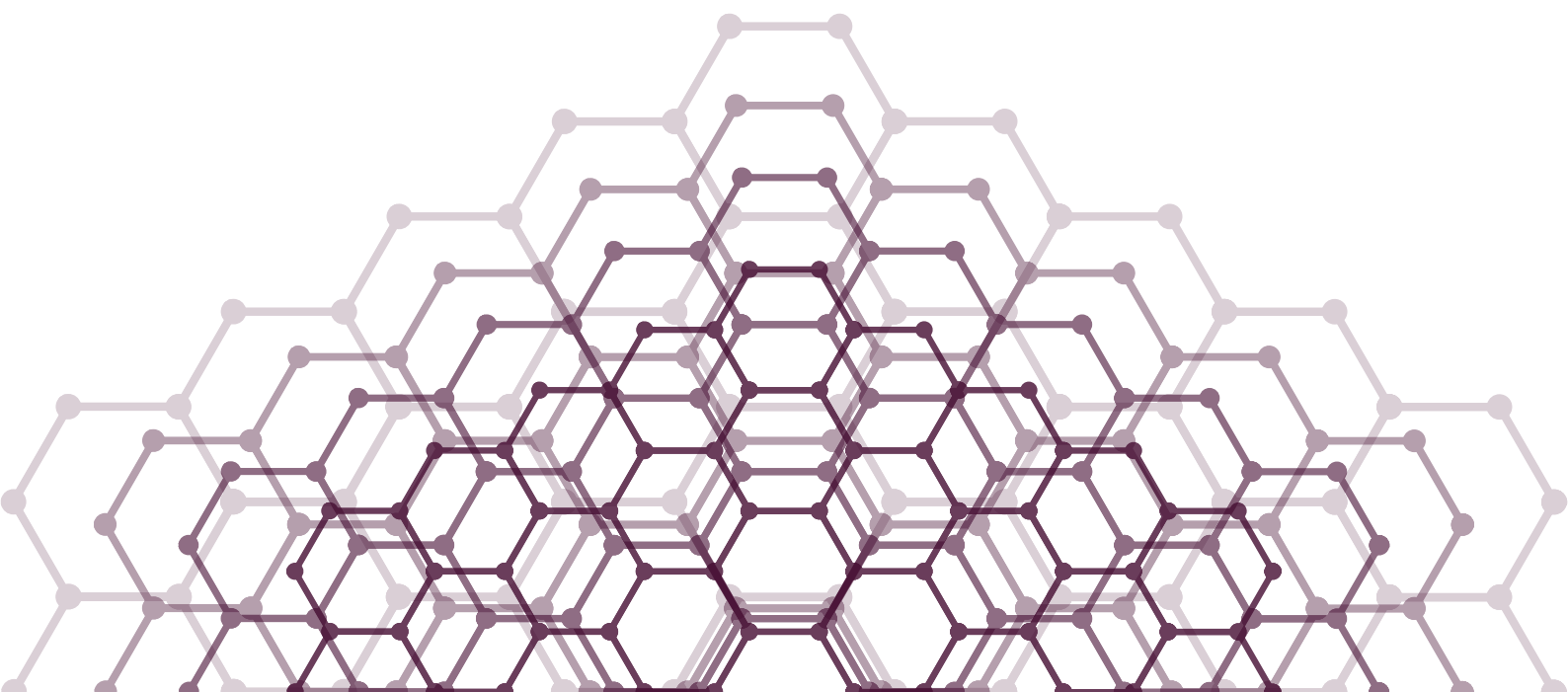
BJELIĆ ANA:	Lignin dimers hydrocracking: Kinetics of lignin typical bonds cleavage based on micro-kinetics of monomers	62
ŠKERJANC ANJA:	3D Printed Reconstruction of Plečnik's Monument.....	63
KUNC LORENA:	Dextran activated surface provides mild environment for cell attachment	64
KÖRGE KRISTI:	Interactions of active biopolymer packaging and fresh pasta during shelf life study	65
CVIKL JANINA GEA:	Comparison of three methods for DNA extraction from tissue samples and blood lymphocytes of breast cancer patients.....	66
IVANIŠ GORICA:	Experimental determination of vapor-liquid equilibrium for binary system CO ₂ +furfural.....	67
BOLJE ALJOŠA:	Polydentate pyridyl-mesoionic carbenes (Poly-MICs).....	68
KOREN ŠPELA:	Lipid droplets and autophagy cooperate to support the resistance of cancer cells to stress	69
ŠINIK ALEKSANDRA:	Managing the balance of sulfur in the refinery through the blending of crude oils.....	70
HOČEVAR JAN:	Functionalization of cellulose obtained from corn stover and wheat straw	71
VAUPOTIČ DOMEN:	Modelling of cell growth	72
ZAHIROVIĆ ABIDA:	Lactococcus lactis expressing fluorescent cytotoxic protein KillerRed for targeting, imaging, and destroying cancer cells	73
GABRIJELČIČ TOMC HELENA:	Reconstruction of antique city Petoviona from ground plans to 3D visualizations	74
HORVAT MONIKA:	Derivatives of emodine from invasive plant japanese knotweed as colorants for textile.....	75
VOZELJ ANŽE:	Analysis of functional interplay between orthocaspases and toxin-antitoxin systems in cyanobacteria.....	76
JUTERŠEK MOJCA:	Development of a TRAP-seq method, modified for study of hypersensitive response in PVY-infected cells of Solanum tuberosum	77
ARH NEJC:	Enhancing nanobodies as crystallization chaperones with engineered metal-binding sites.....	78
ŠOLN KATARINA:	Secret biochemical weapon of plants: allelopathy.....	79
ZUPANČIČ KLEMEN:	Assessing energy consumption of wastewater treatment plant.....	80
GRIČAR EMA:	Identification of volatile compounds in indigenous wines and musts' with headspace GC-MS analysis.....	81

PETEK NEJC:	Oxidation of substituted pyrazolidin-3-ones by photoredox catalysis	82
PRINČIČ GRIŠA GRIGORIJ:	Organic peroxides and their heteroatom derivatives stabilized with BODIPY scaffold.....	83
KLJUN JAKOB:	Organoruthenated nitroxoline inhibitors of cathepsin B with potent antimetastatic properties.....	84
POMEROY BRETT:	Synthesis of Nickel-Alumina Promoted Transition Metal Catalysts for Hydrodeoxygenation of Hydroxymethylfurfural.....	85
KLADNIK JERNEJA:	Synthesis and anticancer activity of methyl-substituted organoruthenium(II)-pyrithionato complexes	86
METARAPI DINO:	Nanoparticle Analysis in Biomaterials Using Laser Ablation–Single Particle–Inductively Coupled Plasma Mass Spectrometry.....	87
PODJED NINA:	Formation of ammonia during the synthesis of zinc quinaldinate complexes with alcoholamine ligands in autoclaves.....	88
STARC JURE:	Self-healing effect in bio-concrete	89
OBAHA ANA:	Characterization of succinimide amino acid derivatives as allosteric effectors of cathepsin L.....	90
TROBEC TOMAŽ:	Organoruthenium(II) complex with pyrithione is a potent inhibitor of cholinesterases and glutathione-S-transferase	91
CIRIKOVIĆ DAVID:	Study of stepped magnesium surface properties with density functional theory	92
PLEŠKO LEJA:	Determination of the toxicity of the waterborne epoxy coatings	93
RUPERT JAKOB:	Nothobranchius furzeri as a suitable model organism for TDP-43 proteinopathy studies	94
KISILAK MARIJA:	Effects of selected metal ions on activity of cathepsin K	95
NOVAK ROK:	Alkali carbonate reaction as a self-healing mechanism in concretes	96
MIHELAČ MATEJA:	Imine formation from acetylenes and anilines catalyzed by palladium complex	97
MARTEK BRUNO ALEKSANDER:	Simple and efficient flow chart diagram for azaindole core determination in new psychoactive substances: The case of 5F- MDMB-P7AICA	98
URLEP MATIČ:	Structural properties and Transformations of Pt(II) PCP Pincer Complexes	99
IVANČIČ ANŽE:	Synthesis of Haloalkynes	100
VIRANT MIHA:	Synthesis of triaryl substituted triazolium salts	101

GAZVODA MARTIN:	The mechanism of palladium catalyzed alkynylation, formal copper-free Sonogashira cross-coupling reaction	102
VIRANT GAŠPER:	Characterization of Solution's Physical Properties of Bio-based 2,5-Furandicarboxylic Acid (FDCA)	103
VIRANT URŠKA:	Antimicrobial activity of nitrosifying bacteria <i>Nitrosomonas eutropha</i>	104
BRAČIČ VERONIKA:	Superhydrophobic aluminium surface with excellent corrosion resistance, self-cleaning and anti-icing properties.....	105
LAVRIČ JURE:	Hybrid sol-gel coating to improve corrosion protection of AA2024-T3 in chloride media	106



POSTER PRESENTATIONS



The role of chemokine CCL5 and its receptor CCR5 in glioblastoma

Miha Koprivnikar Krajnc,^{1,2} Metka Novak,² Tamara Lah Turnšek^{1,2}

¹ Faculty of Chemistry and Chemical Technology, University of Ljubljana, Večna pot 113, SI-1000 Ljubljana, Slovenia

² National Institute of Biology, Večna pot 111, SI-1000 Ljubljana, Slovenia

Glioblastoma (GBM) is the most common of brain tumors, as well as the most malignant one, with the average survival period of 15 months;¹ this is the result of its resistance to therapy, as well as its ability to infiltrate healthy brain tissue, causing post-operative relapses in most cases. To improve the survival of GBM patients, a better understanding of the molecular processes is needed. That is why we investigated the expression and the biological role of ligand CCL5 and receptor CCR5 in human GBM samples. CCL5 is a chemokine, which binds to its chemokine receptor CCR5; this interaction is primarily responsible for leukocyte recruitment to the site of infection, i.e. immune activation, but has been often reported to play a role in many cancers, including GBM, but the precise role of CCR5 in the latter is poorly studied.^{2,3}

Using immunofluorescence and confocal microscopy we studied the expression pattern of CCL5 and CCR5 in GBM tissues; we found that CCR5 is expressed by macrophages and other cells, whereas CCL5 expression was restricted to cells in proximity to mesenchymal stem cells (MSC). Therefore, we analyzed the cell invasion ability of GBM cells in presence of MSC with or without the CCR5 antagonist Maraviroc (MRV). MSC increased GBM invasiveness, but when adding MRV the invasiveness was reduced dramatically. This confirms our hypothesis that CCR5-expressing MSC facilitate GBM invasion through the CCL5/CCR5 axis.

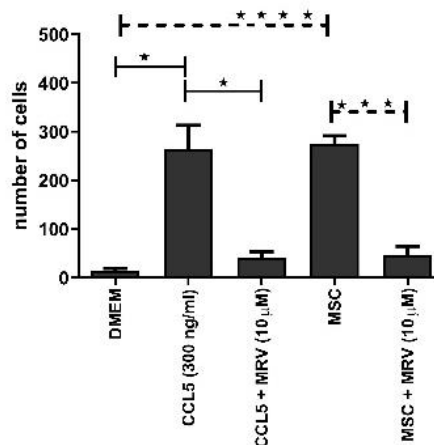


Figure 1: Different invasion assay conditions and their respective number of invading cells.

1. Y. Pan, L. J. Smithson, Y. Ma, D. Hambardzumyan, and D. H. Gutmann, “Ccl5 establishes an autocrine high-grade glioma growth regulatory circuit critical for mesenchymal glioblastoma survival,” *Oncotarget* **2017**, *8*, 32977–32989.
2. E. Laudati, D. Currò, P. Navarra, and L. Lisi, “Blockade of CCR5 receptor prevents M2 microglia phenotype in a microglia-glioma paradigm,” *Neurochem. Int.* **2017**, *108*, 100–108.
3. L. Zhao, Y. Wang, Y. Xue, W. Lv, Y. Zhang, and S. He, “Critical roles of chemokine receptor CCR5 in regulating glioblastoma proliferation and invasion,” *Acta Biochim. Biophys. Sin. (Shanghai)*, **2015**.

In situ simultaneous interpenetrating polymer networks as the precursors to porous polystyrene monoliths

Petra Utroša,¹ Ema Žagar,¹ Sebastijan Kovačič,^{*,1,2} David Pahovnik^{*,1}

¹ Department of Polymer Chemistry and Technology, National Institute of Chemistry, Hajdrihova 19, 1000 Ljubljana, sebastijan.kovacic@ki.si and david.pahovnik@ki.si

² Laboratory for Organic and Polymer Chemistry and Technology, Faculty of Chemistry and Chemical Engineering, University of Maribor, Smetanova 17, 2000 Maribor, Slovenia

Interpenetrating polymer networks (IPNs) consist of intertwined polymer networks that are not covalently bound to each other. The IPN morphology strongly depends on the synthetic conditions, affecting the phase separation process since miscibility of otherwise immiscible polymers depends on entanglement degree of polymer chains within the IPN. If IPN consists of non-degradable and degradable polymer constituents, the latter one can be selectively removed, resulting in a porous polymeric material.

In this work, semi-IPNs were prepared by *in situ* simultaneous orthogonal polymerizations, where the linear poly(ϵ -caprolactone) (PCL) was synthesized by ring-opening polymerization of ϵ -caprolactone using a diphenyl phosphate (DPP) organocatalyst, and the poly(styrene-*co*-divinylbenzene) (PS) network was formed by free-radical polymerization of styrene and divinylbenzene. The PCL domains were subsequently selectively removed by hydrolysis under basic conditions to obtain the porous PS frameworks (Fig. 1). By varying the amount of the DPP, the relative polymerization rate was tuned, which in turn played a fundamental role on the final morphology of the porous networks. Porous morphology of the PS frameworks was studied by SEM, whereas pore size distributions were determined by mercury intrusion porosimetry and BJH analyses of nitrogen sorption isotherms¹.

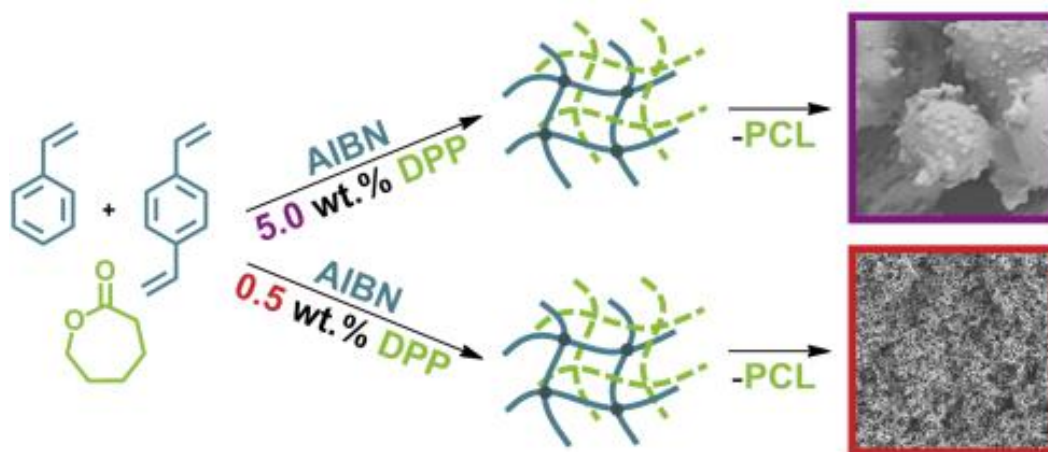


Figure 1: Preparation of *in situ* simultaneous semi-IPN of PCL and PS. After PCL removal, the porous PS framework is obtained.

1. Utroša, P., Žagar, E., Kovačič, S., Pahovnik, D., Porous Polystyrene Monoliths Prepared from *in Situ* Simultaneous Interpenetrating Polymer Networks: Modulation of Morphology by Polymerization Kinetics. *Macromolecules* **2019**, *52*, 819-826.

DARPin C4 mimics adenylyl cyclase 9 activation by $G\alpha_s$

Pia Lavriha,^{1,2} Chao Qi,^{1,2} Volodymyr M. Korkhov^{1,2} *

¹ Institute of Biochemistry, ETH Zürich, Otto-Stern-Weg 3, 8093 Zürich, Switzerland,
volodymyr.korkhov@bc.biol.ethz.ch

² Laboratory of Biomolecular Research, Paul Scherrer Institute

Mammalian membrane adenylyl cyclases (ACs) are enzymes, converting ATP to a key secondary messenger cAMP.¹ With the exception of activation by stimulatory $G\alpha$ ($G\alpha_s$) subunit of heterotrimeric G proteins and by a plant diterpene forskolin, the regulatory properties of the nine AC isoforms vary.^{1,2} The full-length structure of AC9 revealed a novel autoinhibitory mechanism where the C-terminal tail binds into the enzyme's active and allosteric sites.³ We explored the regulatory effect of DARPin C4 on the activity of AC9 and AC9₁₂₅₀, a truncated AC9, lacking the C-terminal inhibitory peptide. C4 activates both forms, causes conditional activation by forskolin and binds to the C2 domain of AC9, all in the same way as $G\alpha_s$. To assess if the activation mechanisms of AC9 by C4 and $G\alpha_s$ are similar, we obtained crystals of C4 in complex with AC9 C2 domain for X-ray diffraction crystallography. Additionally, we prepared sample grids of AC9₁₂₅₀ with MANT-GTP and DARPin C4 with a homogeneous particle distribution, suitable for data acquisition using cryo-electron microscopy for single particle structure determination. The results lead to the hypothesis that the C4 activation mechanism of AC9 is similar to activation by $G\alpha_s$. Thus, C4 could be used as an experimental tool for the studies of AC9 and potentially other AC isoforms, replacing $G\alpha_s$.

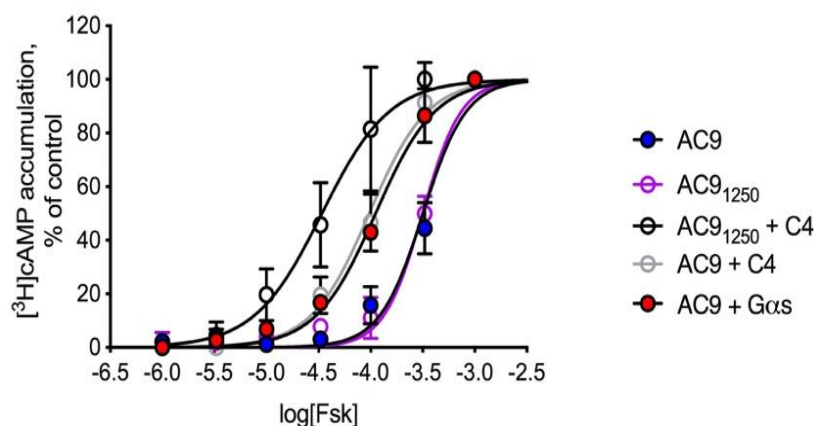


Figure 1: Effect of forskolin (Fsk) on activation of AC9 or AC9₁₂₅₀ alone, in complex with C4 and AC9 in complex with $G\alpha_s$. Fsk has an activating effect in all cases and the highest affinity for AC9₁₂₅₀, which lacks the inhibitory C-terminal peptide, in complex with C4.

1. Hurley, J. Structure, Mechanism, And Regulation Of Mammalian Adenylyl Cyclase. *J. Biol. Chem.* **1999**, *274*, 7599-7602.
2. Sadana, R.; Dessauer, C. Physiological Roles For G Protein-Regulated Adenylyl Cyclase Isoforms: Insights From Knockout And Overexpression Studies. *Neurosignals* **2009**, *17*, 5-22.
3. Qi, C.; Sorrentino, S.; Medalia, O.; Korkhov, V. The Structure Of A Membrane Adenylyl Cyclase Bound To An Activated Stimulatory G Protein. *Science* **2019**, *364*, 389-394.

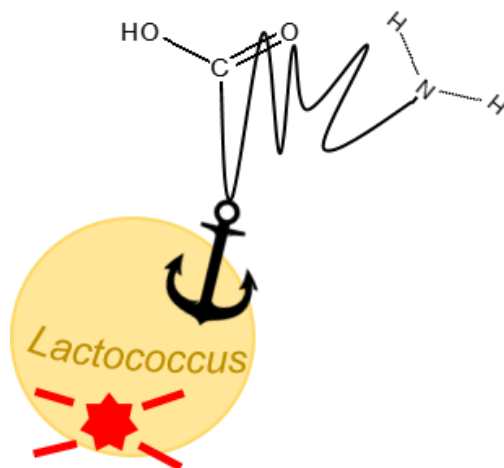
Tumor cell lines-targeting by Lactococcus lactis

Tina Vida Plavec,^{1,2} Milica Perišić Nanut,¹ Ana Mitrovič,¹ Borut Štrukelj,^{1,2} Janko Kos,^{1,2}
Aleš Berlec*^{1,2}

¹ Department of Biotechnology, Jožef Stefan Institute, Jamova 39, SI-1000 Ljubljana, Slovenia

² University of Ljubljana, Faculty of Pharmacy, Aškerčeva 7, SI-1000 Ljubljana, Slovenia, ales.berlec@ijs.si

Food-grade lactic acid bacterium (LAB) *Lactococcus lactis* is considered an attractive host for recombinant protein expression and a promising vector for *in vivo* delivery of bioactive proteins. LAB with surface-displayed recombinant proteins has already been exploited in therapy to display binding molecules directed against pro-inflammatory cytokines and to deliver antioxidant molecules in prevention of colorectal cancer¹. By surface-display of proteins targeting tumor antigens, directed binding of *L. lactis* to cancer cells could be achieved. In the present study, we focused on the development of a system for targeted binding of *L. lactis* to colorectal tumor cell lines. We designed targeting proteins with affinity for three tumor antigens, EpCAM, Her2 and Gb3, typically overexpressed in tumor cells of colorectal cancer. To enable concomitant imaging of bound bacteria, we simultaneously expressed infrared fluorescent protein (IRFP) in bacterial cytoplasm (Scheme 1), by using plasmid for double protein expression². Surface display of targeting proteins was confirmed by flow cytometry, while expression of IRFP fluorescent protein was determined by measuring fluorescence. Furthermore, we confirmed, with flow cytometry, binding of soluble tumor antigens, EpCAM and Her2, to bacteria displaying their respective targeting proteins. *L. lactis* with surface-displayed targeting proteins and IRFP were able to selectively recognize selected human tumor cell lines, indicating their promising targeting ability.



Scheme 1: Surface-displayed targeting protein and intracellularly expressed IRFP in *L. lactis*.

1. Del Carmen, S.; de Moreno de LeBlanc, A.; Levit, R.; Azevedo, V.; Langella, P.; Bermudez-Humaran, L. G.; LeBlanc, J. G., Anti-cancer effect of lactic acid bacteria expressing antioxidant enzymes or IL-10 in a colorectal cancer mouse model. *Int Immunopharmacol* **2017**, *42*, 122-129.
2. Berlec, A.; Skrllec, K.; Kocjan, J.; Olenic, M.; Strukelj, B., Single plasmid systems for inducible dual protein expression and for CRISPR-Cas9/CRISPRi gene regulation in lactic acid bacterium *Lactococcus lactis*. *Sci Rep* **2018**, *8*, 1009.

Transition of surface chemistry and morphology of laser-textured copper surfaces due to exposure to boiling critical heat flux

Matic Može,^{*,1} Matevž Zupančič,¹ Matej Hočevar,² Peter Gregorčič,¹ Iztok Golobič¹

¹ Faculty of Mechanical Engineering, University of Ljubljana, Aškerčeva 6, SI-1000 Ljubljana, Slovenia, matic.moze@fs.uni-lj.si

² Institute of Metals and Technology, Lepi pot 11, SI-1000 Ljubljana, Slovenia

Stability of functionalized surfaces is an often-neglected topic in phase-change heat transfer research. In this research, we examine the changes in chemical and morphological properties of laser-textured surfaces after the incipience of critical heat flux during saturated pool-boiling of water. Copper samples were laser textured via ablation using a nanosecond fiber laser under air or argon atmosphere. Multiscale microcavities, which serve as preferential nucleation sites^{1,2}, were produced on the samples, which exhibited significantly enhanced heat transfer performance in pool-boiling tests. A vapor film repeatedly formed during the incipience of the critical heat flux and was accompanied by temperatures of up to 320 °C. It was determined that Cu(II) oxide and hydroxide transform into Cu(I) oxide and Cu metal as a result of repeated low-temperature annealing of the surface due to the presence of a vapor film during the transition towards film boiling. A wettability transition from hydrophilic towards hydrophobic was also detected. Both effects importantly influence the solid-liquid-vapor interface during phase-change heat transfer with laser-textured surfaces exhibiting significantly enhanced stability.

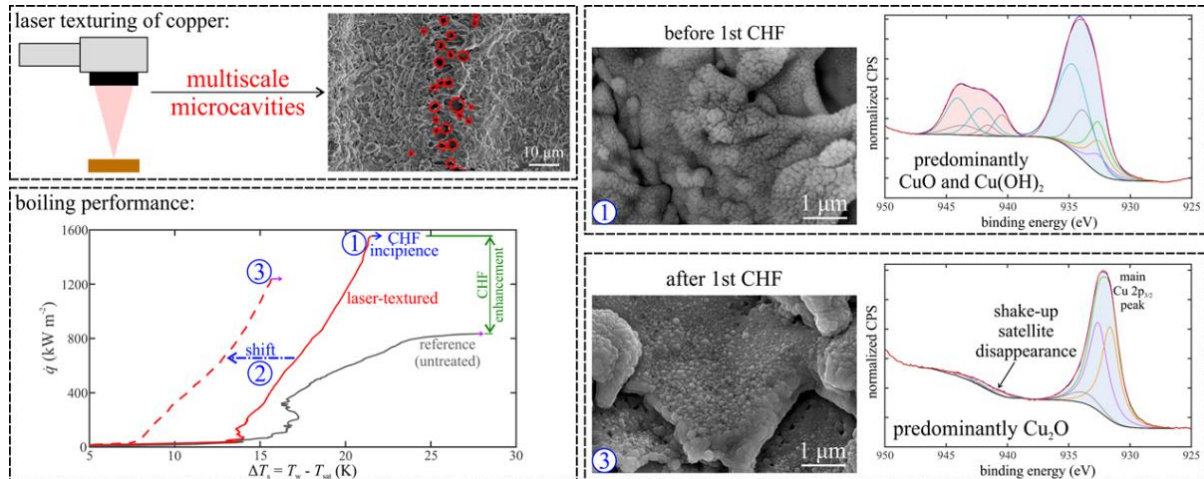


Figure 1: Summary of the research.

1. Gregorčič, P.; Zupančič, M.; Golobič, I., Scalable Surface Microstructuring by a Fiber Laser for Controlled Nucleate Boiling Performance of High- and Low-Surface-Tension Fluids. *Sci. Rep.* **2018**, *8*, 7461.
2. Zupančič, M.; Može, M.; Gregorčič, P.; Golobič, I., Nanosecond laser texturing of uniformly and non-uniformly wettable micro structured metal surfaces for enhanced boiling heat transfer. *Appl. Surf. Sci.* **2017**, *399*, 480–490.

Biodegradability study of chitosan-based films with added chestnut extract in an aqueous environment

Tina Ročnik,^{1,2} Uroš Novak,² Blaž Likozar,² Andreja Žgajnar Gotvajn,¹ Gabriela Kalčikova*¹

¹ Faculty of Chemistry and Chemical Technology, University of Ljubljana, Večna pot 113, SI-1000 Ljubljana, Slovenia, gabriela.kalcikova@fkkt.uni-lj.si

² National Institute of Chemistry, Hajdrihova 19, SI-1000 Ljubljana, Slovenia

In modern society, plastic waste is a serious environmental burden that presents a planetary boundary threat.¹ Bearing in mind the fact that single-use food packagings are one of the biggest sources of plastic waste, additional efforts should strive towards the utilization of alternative food packaging systems such as polymer-based films/coatings. Chitosan, a partly deacetylated derivative of biomass-based polymer chitin, can represent a very good alternative for the preparation of a broad palette of eco-friendly materials, including those intended for food packaging.¹ However, the fate of such biopolymers in the aquatic environment is mainly unknown.

In this context, the biodegradation of chitosan film with added chestnut extracts (CE 0%, 0.1%, 1%) used as antimicrobial agent was tested. The method of determination of the ultimate aerobic biodegradability in an aqueous medium by measuring the oxygen demand in a closed respirometer was applied. The activity of the microorganisms was checked with the reference compound (sodium acetate). In Figure 1, the maximal biodegradation for all tested chitosan films reached was up to 34 % in the first 5 days of experiment. Further, analysis of total phenolic content showed, that phenolic compounds were fully degraded already after one week. FT-IR analysis showed significant alternations in the film structures.

Although changes in composition of chitosan films were confirmed results indicated that they cannot be completely degraded under the common environmental conditions in the aquatic environment. Therefore, further research should involve determination of their composting potential, because composting could be a viable option for waste management of such waste bio-packaging.

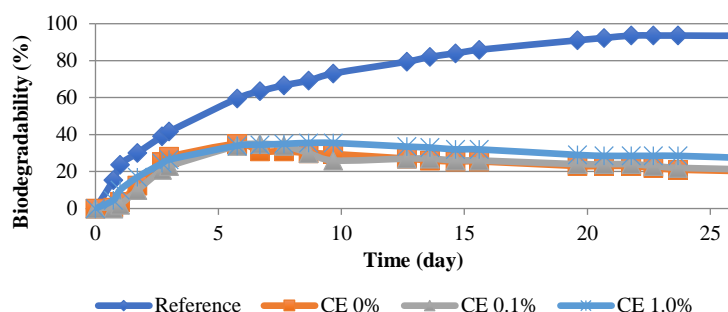


Figure 1: OxiTop® measurements of oxygen consumption.

1. Bajić, M.; Jalšovec, H.; Travan, A.; Novak, U.; Likozar, B., Chitosan-based films with incorporated supercritical CO₂ hop extract: Structural, physicochemical, and antibacterial properties. *Carbohydrate Polymers* **2019**, 219, 261-268.

Optimization of HFME for determination of benzotriazoles in environmental waters

Ariana Šuštarč¹, Ida Kraševc¹, Helena Prosen¹

¹ Faculty of Chemistry and Chemical Technology, University of Ljubljana, Večna pot 113, SI-1000 Ljubljana, Slovenia

Benzotriazole derivatives are toxic heterocyclic compounds which are nowadays indispensable for industry. Consequently, they have been found in environment, causing harmful effects on plants, aquatic organisms and humans.¹ Their determination usually includes extraction and preconcentration, coupled to sensitive analytical techniques, such as LC-MS/MS.² One of the existing microextraction techniques is hollow fiber microextraction (HFME), which was used in this work for extraction of 6 polar benzotriazoles from tap water and further from different river samples. Due to efficient preconcentration, this technique provides high enrichment factors and is a good substitution for classical techniques. In this technique, the acceptor phase is placed into the lumen of a polypropylene hollow fiber and organic solvent is immobilized into the pores of the fiber. Dipping the fiber in the aqueous solution enables analytes to be extracted.³ In this work, pH of the sample and concentration of EDTA as a ligand for metal ions in water were optimized. Enrichment factors (Fig. 1) for the analysed compounds in tap and river water were lower than in MQ water, except for OHBZ. Furthermore, matrix effects were considerable, which can be the consequence of other compounds present in the extract.²

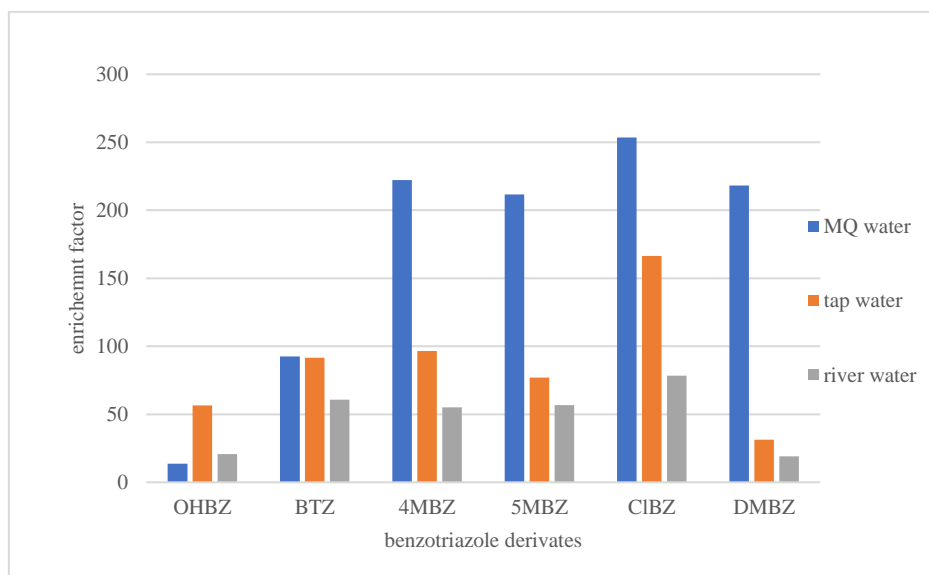


Figure 1: Comparison of enrichment factors for analysed compounds in different samples.

1. Kraševc, I., Prosen, H., Solid-Phase Extraction of Polar Benzotriazoles as Environmental Pollutants: A Review. *Molecules* **2018**, 23, 2501.
2. Kraševc, I., Prosen, H., Development of a Dispersive Liquid-Liquid Microextraction Followed by LC-MS/MS for Determination of Benzotriazoles in Environmental Waters. *Acta Chim. Slov.* **2019**, 66.
3. Ghambarian M., Yamini Y., Esrafil A., Developments in hollow fiber based liquid phase microextraction: principles and applications. *Microchim Acta* **2002**, 177, 271- 294.

Is transportin 1 involved in nuclear import of annexin A11?

Valentina Novak¹, Vera Župunski*¹

¹ Faculty of Chemistry and Chemical Technology, University of Ljubljana, Večna pot 113, SI-1000 Ljubljana, Slovenia, vera.zupunski@fkkt.uni-lj.si

Amyotrophic lateral sclerosis (ALS) is a fatal disease characterized by degeneration of motor neurons. Mutations in many genes have been associated with the disease, most recently mutations in *ANXA11* encoding a phospholipid binding protein annexin A11¹. Numerous cellular mechanisms were proposed to underlie ALS progression. Among them is defective nucleocytoplasmic transport that contributes to accumulation of toxic cytoplasmic protein aggregates². Transportin 1 is a member of karyopherin β family of nuclear transport proteins. Amino acid sequence of ANXA11 has been previously bioinformatically predicted to have a nuclear localization signal (NLS) that can be recognized by transportin 1. Predicted NLS is in the N-terminal structurally disordered part of annexin A11, has an overall positive charge and contains a consensus sequence R/K/H-X₍₂₋₅₎-P-Y (Fig. 1)³. We aimed to confirm the interaction between transportin 1 and annexin A11. Both proteins were expressed in *Escherichia coli*, strain BL21[DE3] pLysS and purified using glutathione S-transferase or nickel affinity chromatography. To investigate possible interaction, we performed GST-pulldown assay and protein-protein crosslinking. Our findings suggest that transportin 1 does not bind annexin A11. Further analysis of nuclear import of annexin A11 is needed to explain the underlying mechanism and possible implications in ALS progression.

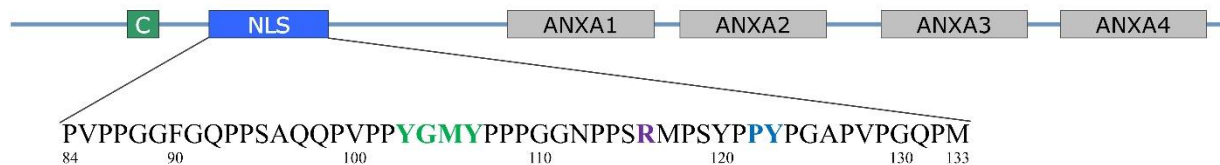


Figure 1: Schematic outline of annexin A11. ANXA – four annexin repeats that form an α -helical core of the protein structure; C – binding site of Ca^{2+} -binding protein calyculin; NLS – proposed nuclear localization sequence. Amino acid sequence of NLS is written out with colored parts possibly involved in binding of transportin 1^{1,3}.

1. Smith, B. N. *et al.* Mutations in the vesicular trafficking protein annexin A11 are associated with amyotrophic lateral sclerosis. *Sci. Transl. Med.* **2017**, *9*, eaad9157.
2. Prpar Mihevc, S. *et al.* Nuclear trafficking in amyotrophic lateral sclerosis and frontotemporal lobar degeneration. *Brain* **2016**, *140*, 13-26.
3. Lee, B. J. *et al.* Rules for nuclear localization sequence recognition by karyopherin β 2. *Cell* **2006**, *126*, 543-558.

Fractionation of shrimps shells biomass by choline chloride/lactic acid deep eutectic solvent

Bojana Bradić¹, Uroš Novak^{1*}, Blaž Likozar¹

¹ National institute of chemistry, Department of Catalysis and Chemical Reaction Engineering, Hajdrihova 19, 1000, Ljubljana, Slovenia, uroš.novak@ki.si

Globally fisheries and food industry produce between 6 million and 8 million tons of waste crab, shrimp and lobster shells. ¹ This type of waste material can be used as a source for extraction of valuable chemicals like, chitin, minerals and proteins, all which have market value. Biopolymer chitin (β -(1-4)-poly-N-acetyl-D-glucosamine) is widely distributed in nature and is the second most abundant polysaccharide after cellulose. ² Despite its huge availability, the utilization of chitin has been limited due to its insolubility in solvents. ³ This study provides a green fractionation process for recovery of α -chitin from shrimp shells by employing choline chloride/lactic acid deep eutectic solvents (DES). The fractionation of the shrimp shell biomass with DES was carried out in a stirred reactor batch reactor from 1-6 h at temperature range of 50-70°C. The process selectivity in dissolution was followed on-line using FBRM tracking probe submerged in DES. The process parameters; solid-liquid ratio (S/L ratio), temperature (T), and isolation time (t) were optimized to maximize chitin extraction yield. The results showed that choline chloride/lactic acid has excellent properties for extraction of chitin, wherein the yield of the resulting chitin is higher than 18% with purity of around 95%. Additionally the solvent was reused for chitin isolation several times.

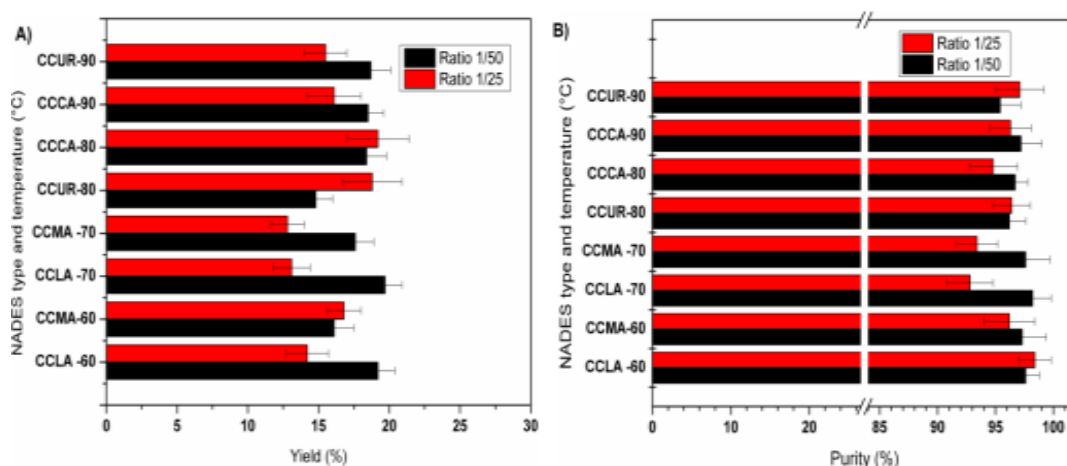


Figure 1. Obtained α -chitin A) yield and B) purity from the NADES based fractionation process for different NADES types at different temperatures.

1. Yan, N.; Chen, X. Sustainability, Don't waste shellfish waste. *Nature* **2015**, *524*, 155–157. <https://doi.org/10.1038/524155a>.
2. Younes, I.; Rinaudo, M. Chitin and chitosan preparation from marine sources. Structure, properties and applications. *Mar. Drugs* **2015**, *13*, 1133-1174. <https://doi.org/10.3390/md13031133>.
3. Cheung, R. C. F.; Ng, T. B.; Wong, J. H.; Chan, W. Y. Chitosan: An Update on Potential Biomedical and Pharmaceutical Applications.; *Mar. Drugs* **2015**, *13*, 5156-5183. <https://doi.org/10.3390/md13085156>.

A novel method for discovery of DNA-protein interaction partners

Andreja Habič¹, Vojč Kocman², Brigita Lenarčič¹, Janez Plavec^{1,2}, Miha Pavšič^{*,1}

¹ Faculty of Chemistry and Chemical Technology, University of Ljubljana, Večna pot 113, SI-1000 Ljubljana, Slovenia; Miha.Pavsic@fkkt.uni-lj.si

² Slovenian NMR Centre, National Institute of Chemistry, Hajdrihova 19, SI-1000 Ljubljana, Slovenia

Regulatory functions of certain DNA elements, be it linear or adopting higher-order structure like DNA-quadruplexes, are often achieved in concert with proteins that bind to them, either via stable or transient interactions. While there are numerous methods to detect stable interaction partners, transient interactors are often overlooked. To be able to detect them both we set on to develop a novel biotinylation-based method for DNA interaction partners discovery. In the initial phase of method development, we constructed a proof-of-concept system involving a known DNA-protein interaction pair, namely GADD(DNA)-p53(protein)¹. The system (Fig. 1) consists of a synthetic DNA with three specific sequences: GADD, *TerA* and UAS_{GAL}. Such DNA fragment is incubated with cell lysate plus two recombinant fusion proteins prepared separately: (1) Tus-TurboID, which binds to *TerA* and contains an active biotin ligase moiety, and (2) GAL4(1-147)-sfGFP, which binds to UAS_{GAL} and serves as an internal positive control. Binding of p53 to GADD results in its biotinylation and the biotin-labelled p53 is then identified by mass spectrometry. The modularity of the system allows the GADD region to be replaced by any other DNA element under study. The system can be used either *in vivo* together with cell extracts or *in cellula*; in the latter case the target DNA elements and fragments coding for the labelling machinery are located on a plasmid or integrated in cell genome.

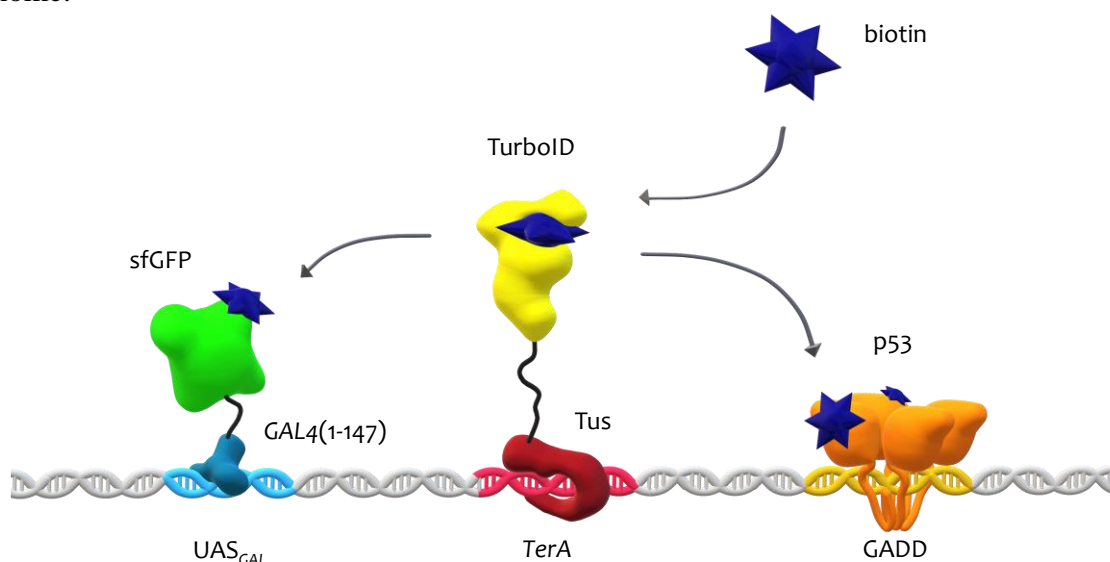


Figure 1: Control system of a novel method for DNA interaction partners discovery.

1. Bian, J.; Sun, Y. p53CP, a putative p53 competing protein that specifically binds to the consensus p53 DNA binding sites: A third member of the p53 family?. *Proc. Natl. Acad. Sci. U. S. A.* **1997**, *94*, 14753–14758.

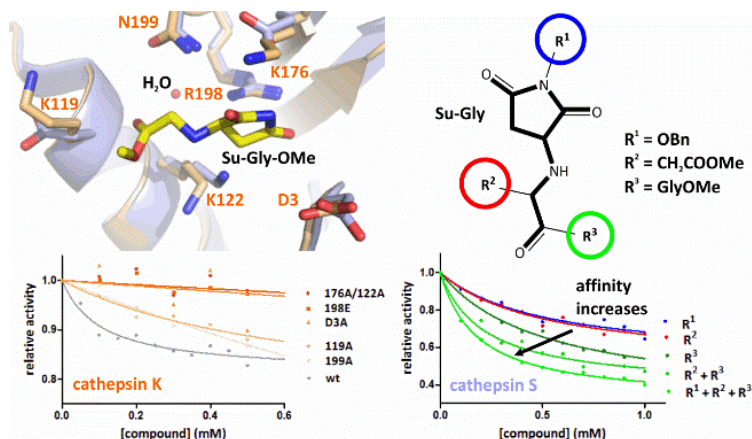
Development of allosteric modifiers of cathepsin S based on the scaffold of a cathepsin K effector

Tjaša Goričan,¹ Nejc Petek,¹ Jurij Svete,¹ Marko Novinec*¹

¹ Faculty of Chemistry and Chemical Technology, University of Ljubljana, Večna pot 113, SI-1000 Ljubljana, Slovenia, marko.novinec@fkkt.uni-lj.si

In the human body the activity of papain-like proteases must be carefully regulated since their dysregulation can lead to numerous diseases, including osteoporosis in the case of cathepsin K and rheumatoid arthritis in the cases of both cathepsins K and S. For this reason these two enzymes represent potential targets for drug development. Thus far cathepsin K is the only member known to be allosterically regulated.^{1,2}

We have recently identified and characterized a novel allosteric effector of cathepsin K Su-Gly-OMe (Scheme 1). By site-directed mutagenesis we also identified residues in the allosteric site critical for the binding of Su-Gly-OMe. We confirmed that the novel effector partially inhibits not only cathepsin K but also cathepsin S and we proposed that it binds to the same allosteric site on cathepsin S. Based on the scaffold of Su-Gly-OMe we prepared a library of compounds with three sites of diversity. By analyzing the structure-activity relationship of these compounds we identified substituents at each site that contribute towards their higher affinity and selectivity for each target cathepsin. By combining these substituents, we were able to develop the first selective allosteric modifiers of cathepsin S with optimized affinities in comparison to Su-Gly-OMe. In particular, measured IC₅₀ values for several compounds were more than five times lower compared to Su-Gly-OMe. The highest affinity was estimated to be about fifteen times higher in the case of the compound having benzyloxy group at R¹ site and CH₂COOMe at R² site.



Scheme 1: Optimization of allosteric modifiers of cathepsin S based on the Su-Gly scaffold.

1. Novinec, M.; Korenč, M.; Cafilisch, A.; Ranganathan, R.; Lenarčič, B.; Baici, A. A novel allosteric mechanism in the cysteine peptidase cathepsin K discovered by computational methods. *Nat. Commun.* **2014**, *5*, 1-10.
2. Novinec, M.; Rebernik, M.; and Lenarčič, B. An allosteric site enables fine-tuning of cathepsin K by diverse effectors. *FEBS Lett.* **2016**, *590*, 4507-4518.

EpCAM – A shift from cell-cell adhesion to signaling

Aljaž Gaber^{1,2}, Daria Latysheva, Uroš Prešern, Peter Škrinjar, Brigita Lenarčič^{*,1,2}

¹ Faculty of Chemistry and Chemical Technology, University of Ljubljana, Večna pot 113, SI-1000 Ljubljana, Slovenia, brigita.lenarcic@fkkt.uni-lj.si

² Department of Biochemistry, Molecular and Structural Biology, Institute Jožef Stefan, Jamova 39, SI-1000 Ljubljana, Slovenia

Epithelial Cell Adhesion/Activating Molecule (EpCAM) is one of the key molecules in epithelial development and the most commonly targeted tumor marker on the surface of epithelial cancer cells. Initially, it was described as a novel cell-cell adhesion molecule¹. However, our group and others have recently provided evidence that refutes its direct involvement in cell-cell adhesion, putting more emphasis on its role in outside-in signaling^{2,3}. Here we present our recent advances in an ongoing quest to elucidate the mechanism of EpCAM's involvement in two major signaling pathways: Regulated intramembrane proteolysis (RIP) and Epidermal Growth Factor Receptor (EGFR) signaling (Figure 1).

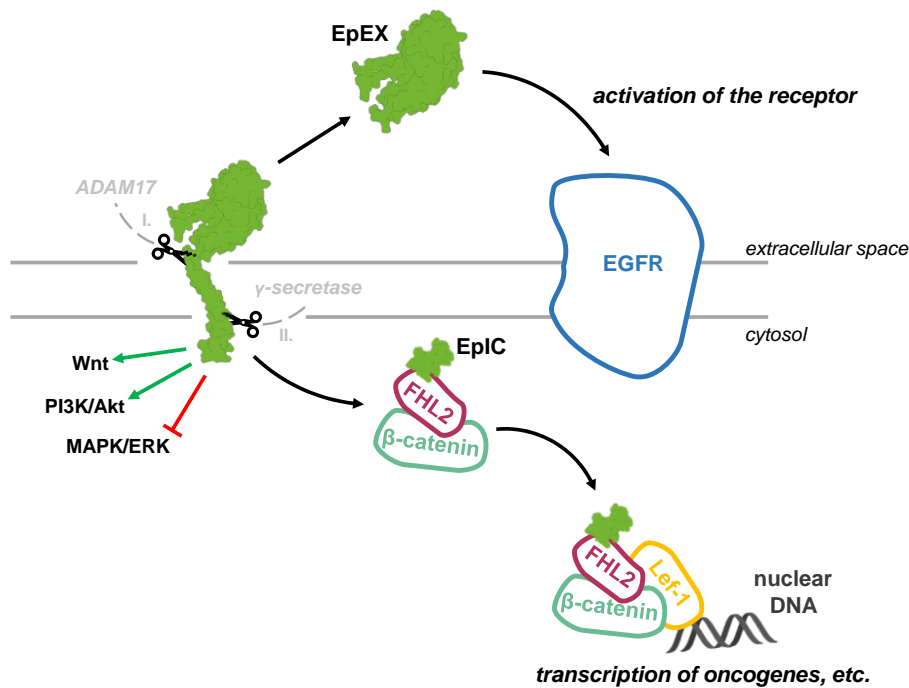


Figure 1: EpCAM as a signaling molecule. The figure describes key steps in two most prominent EpCAM-related signaling pathways and their biological outcomes.

1. Litvinov, S. V.; Balzar, M.; Winter, M. J.; Bakker, H. a.; Briaire-de Bruijn, I. H.; Prins, F.; Fleuren, G. J.; Warnaar, S. O. Epithelial Cell Adhesion Molecule (Ep-CAM) Modulates Cell-Cell Interactions Mediated by Classic Cadherins. *J. Cell Biol.* **1997**, *139*, 1337–1348.
2. Gaber, A.; Kim, S. J.; Kaake, R. M.; Benčina, M.; Krogan, N.; Šali, A.; Pavšič, M.; Lenarčič, B. EpCAM Homo-Oligomerization Is Not the Basis for Its Role in Cell-Cell Adhesion. *Sci. Rep.* **2018**, *8*.
3. Tsaktanis, T.; Kremling, H.; Pavšič, M.; von Stackelberg, R.; Mack, B.; Fukumori, A.; Steiner, H.; Vielmuth, F.; Spindler, V.; Huang, Z.; et al. Cleavage and Cell Adhesion Properties of Human Epithelial Cell Adhesion Molecule (HEPCAM). *J. Biol. Chem.* **2015**, *290*, 24574–24591

Physico-chemical and qualitative properties of Slovene honey

Jure Avsenik¹, Martin Rafael Gulin¹, Blaž Kozjan¹, Maša Legan¹, Nastja Marondini¹, Blagoj Mukaetov¹, Lara Eva Rudolf¹, Deja Zupancič,^{*,1} Helena Baša Česnik², Miha Lukšič¹, Barbara Hribar-Lee¹

¹ Faculty of Chemistry and Chemical Technology, University of Ljubljana, Večna pot 113, SI-1000 Ljubljana, Slovenia, deja.zupancic@gmail.com

² Agricultural Institute of Slovenia, Hacquetova ulica 17, SI-1000 Ljubljana, Slovenia

Honey is composed of sugars, small amount of water, and minor quantities of enzymes, acids, phenols, vitamins and minerals. In modern intense agriculture plant protection products are used to increase crop production, and their residues can be introduced into the honey by the bees, from contaminated blossoms. Safety of the honey depends on its pesticide residues content. Multiresidual GC-MS method for determining the pesticide residues in honey was developed by Agricultural Institute of Slovenia.

An alternative method to determine the concentration of pesticides in samples is spectrophotometry (Fig. 1). Using the UV-VIS spectrophotometry we have investigated the range of validity of Beer-Lambert linear relationship between concentration and absorbance for different pesticides. The results show that the range of linearity depends on the pesticide.

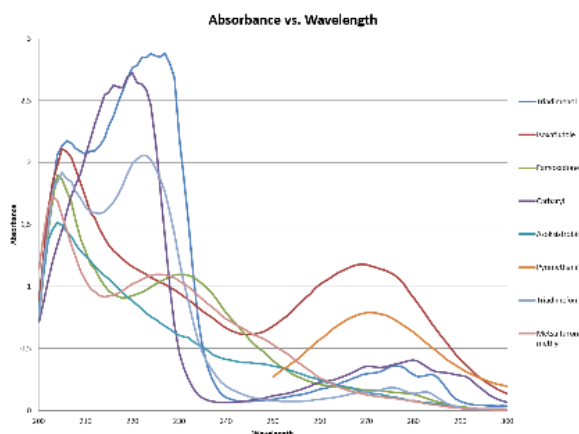


Figure 1: Absorption spectra for different pesticides.

Using the methods described in ¹ and ² we have investigated the viscosity, pH, colour intensity, and optical density of different Slovene honey samples. pH of the honey depends on the sugar fermentation, while the viscosity depends on its water content. The colour characteristics of the honey change with its mineral content, and the content of phenols and flavonoids, but they can also be influenced by the honey-maker through the honey processing. Our results show that all the properties studied depend not just on the sort of honey, but also on its origin.

1. El Sohaimy, S. A., Masry, S. H. D., Shehata, M. G., Physicochemical characteristics of honey from different origins. *Ann. Agricult. Sci.* **2015**, *60*, 279-287.
2. Gómez-Díaz, D., Navaza, J. M., Quintáns-Riveiro, L. C., Effect of temperature on the viscosity of honey. *Int. J. Food Properties* **2009**, *12*, 369-404.

Structure–dynamics relationship in aqueous tert-butanol solutions

Jure Cerar¹, Andrej Jamnik¹, Ildikó Pethes², László Pusztai^{2,3} and Matija Tomšič^{*,1}

¹ Faculty of Chemistry and Chemical Technology, University of Ljubljana, Večna pot 113, SI-1000 Ljubljana, Slovenia, Matija.Tomsic@fkkt.uni-lj.si

² Wigner Research Centre for Physics, Hungarian Academy of Sciences, Budapest, Konkoly Thege út 29-33., H-1121, Hungary

³ International Research Organization for Advanced Science and Technology (IROAST), Kumamoto University, 2-39-1 Kurokami, Chuo-ku, Kumamoto 860-8555, Japan

We investigated the structure–dynamics relationship in aqueous tert-butanol (TBA; 2-methylpropan-2-ol) solutions throughout the whole concentration regime. We effectively combined the experimental small- and wide-angle x-ray scattering (SWAXS) technique¹ and the molecular dynamics (MD) simulations supplemented by the ‘complemented system approach’ method². MD simulations were also used to calculate the viscosity of the systems, H-bond lifetimes, and molecular self-diffusion coefficients. While TBA/water mixtures appeared homogeneous on a mesoscopic scale, considerable heterogeneities could be observed in the structure on a microscopic scale. The appearance and properties of these heterogeneities strongly depend on the composition of the mixture, as is evident from the corresponding SWAXS and rheological results presented in Fig. 1. Such heterogeneities seem to have significant effect on the dynamical properties of the system. As the TBA/water mixtures are extensively used in various applications, *e.g.*, as reaction media, solvents in liquid extraction processes, mobile phase in high-pressure liquid chromatography, etc., the knowledge about their structure and connected rheological properties is crucial for designing and optimizing these media for different tasks.

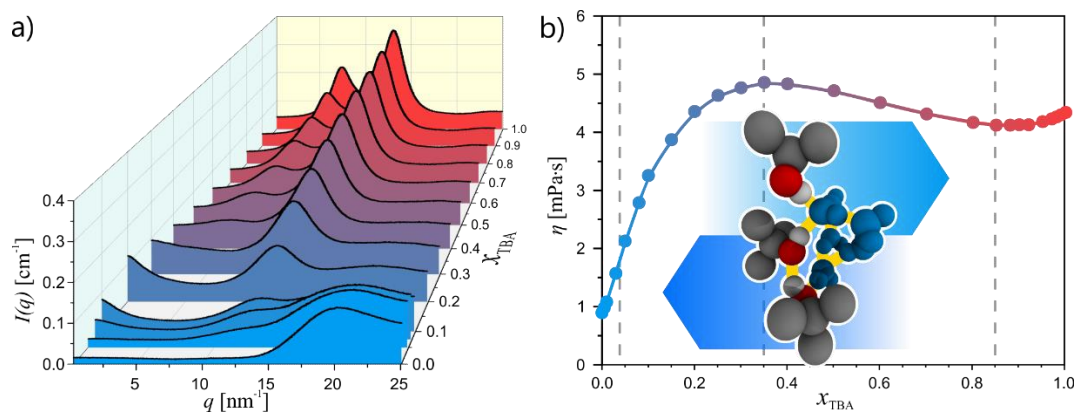


Figure 1: (a) The dependence of the experimental SWAXS intensity and (b) the experimental viscosity³ on the molar fraction of TBA in TBA/water system throughout the whole concentration regime.

1. (a) Cerar, J., Jamnik, A., Tomšič, M., *Journal of Molecular Liquids* 2019, 276, 307-317, (b) Tomšič, M., Jamnik, A., Fritz-Popovski, G., Glatter, O., Vlček, L., *J. Phys. Chem. B* **2007**, 111, 1738-1751.
2. Lajovic, A., Tomšič, M., Jamnik, A., *J. Chem. Phys.* **2010**, 133, 174123.
3. Kipkemboi, P. K., Eastal, A. J., *Canad. J. Chem.* **1994**, 72, 1937-1945.

Characterization of waste fungal biomass – an effective adsorbent for heavy metals

Ula Rozman^{*,1}, Andreja Žgajnar Gotvajn¹, Gregor Marolt¹, Andrej Gregori², Tina Skalar¹, Gabriela Kalčíkova¹

¹ University of Ljubljana, Faculty of Chemistry and Chemical Technology, Večna pot 113, SI-1000 Ljubljana, Slovenia, ula.rozman@gmail.com

² MycoMedica d.o.o., Podkoren 72, SI-4280 Kranjska Gora, Slovenia

Heavy metals can easily enter the environment and pose a serious threat to humans and environment. Adsorption is widely used for its removal due to cost-effectiveness ratio. In the last decade, different low-cost adsorbents have been investigated, especially bio-materials¹. In our study, waste fungal biomass with substrate (mixture of beech sawdust and rye bran) was used as adsorbent, which was obtained after production of *Ganoderma lucidum* fruiting bodies.

Characterization of investigated adsorbent was determined with three different techniques. Observation of the surface was performed by scanning electron microscopy (SEM) at an acceleration voltage of 1.00 kV after sputter-coating the sample with Au/Pd with thickness of 10 nm. Particles with two different surface shapes were seen, indicating one of them is fungal biomass (Fig. 1, left) and another is substrate residues (Fig. 1, right). The Braunauer-Emmett-Teller (BET) method was used to calculate the specific surface area, which was relatively small, 0.84 m² g⁻¹. Average particle size of the number and volume distribution was 73.73 μm and 265.8 μm, respectively.

Characterized waste fungal biomass was then used for removal of lead(II) (Pb(NO₃)₂) and cadmium(II) (Cd(NO₃)₂) from water medium. The adsorption of both metals was very fast, most of the metals was removed already after 5 min. The maximal removal efficiency was 88.7 % and 81.4 % for Pb(II) and Cd(II), respectively. Calculated rate constants are comparable to those obtained for activated carbon. Although the surface area of fungal waste biomass is small, it can be assumed that high removal efficiency is due to the chemical bonding of heavy metals to functional groups that are on the surface of the fungal biomass.

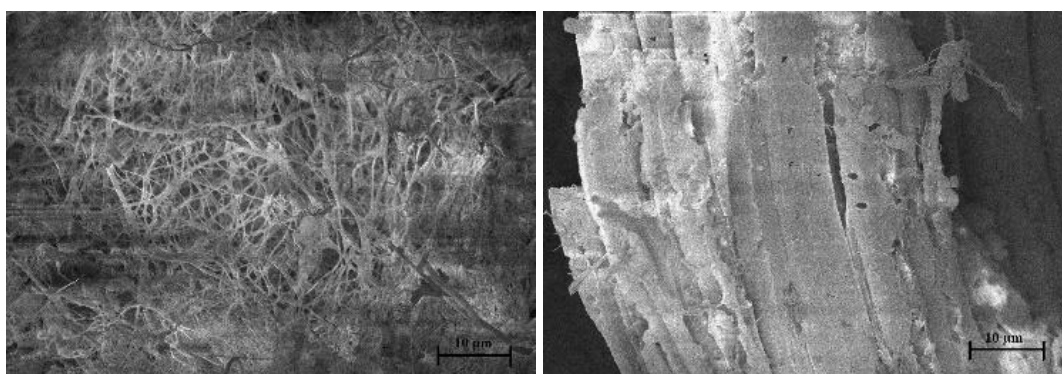


Figure 1: SEM micrographs of fungal biomass (left) and substrate residues (right).

1. Krowiak Witek, A., Szafran, R. G., Modelski, S., Biosorption of heavy metals from aqueous solutions onto peanut shell as a low-cost biosorbent. *Desalination*. **2011**, 265, 126-134.

Engineering fluorescent probiotic bacteria

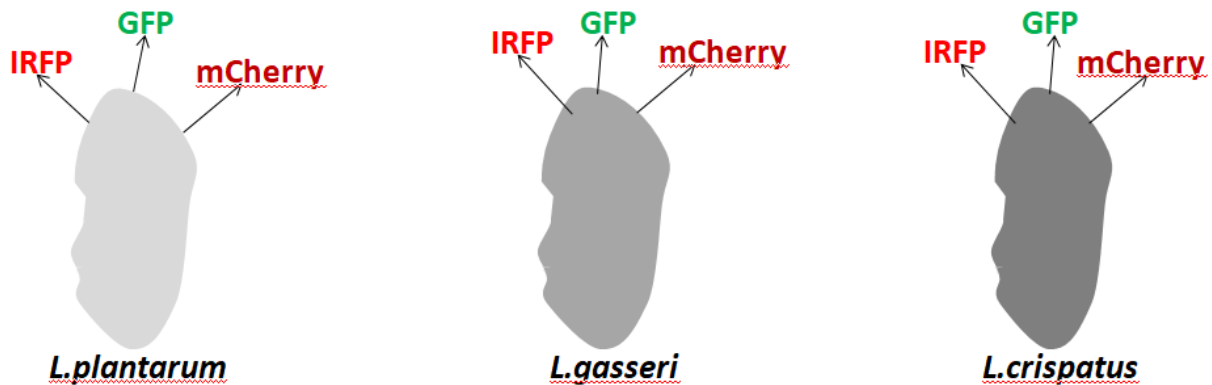
Spase Stojanov^{1,2}, Aleš Berlec*^{1,2}

¹ Department of Biotechnology, Jožef Stefan Institute, Jamovacesta39,1000 Ljubljana, Slovenia, ales.berlec@ijs.si

² Faculty of pharmacy, University of Ljubljana, Askerčeva cesta 7, 1000 Ljubljana, Slovenia

Probiotics are live microorganisms that can confer health benefits to the host when administered in adequate amounts. The beneficial effects of probiotics are related to gastrointestinal diseases, immunomodulation, intestinal and vaginal microbial balance and antimicrobial properties.

These positive impacts have increased the researcher's interest in human microbiome and its role in human health. In order to decipher the mechanism of action of probiotics it is important to track them inside the host. One of the ways to achieve this is through imaging the bacteria with fluorescent proteins. Our idea is to transform different plasmids (pMSP3545, pNZRK, pMEC, and pCD256) which express fluorescent proteins with different spectral properties (IRFP, GFP and mCherry) to *Lactobacillus gasseri*, *Lactobacillus plantarum* and *Lactobacillus crispatus* as important vaginal species. The use of *Lactobacillus* probiotic strains can prevent or treat bacterial vaginosis and vaginal infections¹. Their antibacterial properties are related to the production of hydrogen peroxide and lactic acid. *Lactobacillus gasseri* was successfully transformed² with all four plasmids, but only GFP showed high fluorescence. The GFP gene in pMEC plasmid was cloned under the control of the LDH promoter. Our goal is to insert the LDH promoter in other plasmids in order to enable the expression of IRFP and mCherry.



The engineered plasmids will then be transformed into bacteria by electroporation. The purpose is the engineering of lactobacilli to express different fluorescence proteins and observing the cell's viability. This will allow tracking of the bacteria *in vivo* and learning more about their effects and characteristics.

1. Cribby, S.; Taylor, M.; Reid G., Vaginal Microbiota and the Use of Probiotics. *Interdiscip. Perspect. Infect. Dis.* **2008**, 2008, 256490.
2. Allain, T.; Mansour, N. M.; Bahr, M.M.A.; Martin, R.; Florent I.; Langella, P.; Humaran, L.G.B., A new lactobacilli *in vivo* expression system for the production and delivery of heterologous proteins at mucosal surfaces. *FEMS Microbiol. Lett.* **2016**, 363, fnw117.

Degradation of antibiotics by ozone-based reactions.

Teja Antončič*¹, Martin Vrabel², Jan Derco², Andreja Žgajnar Gotvajn¹.

¹ University of Ljubljana, Faculty of Chemistry and Chemical Technology, Večna pot 113, SI-1000 Ljubljana, Slovenia, teja.ant@gmail.com

² Faculty of Chemical and Food Technology, Slovak University of Technology, Radlinského 9, 812 37, Bratislava.

The wide use of antibiotics nowadays is polluting environment and contaminating even natural water systems.¹ The most efficient method to degrade those compounds so far seem to be the advanced oxidation processes (AOPs).² Application of effective oxidants such as ozone can lead to decomposition of pollutants and reduction of their toxicity.³

The aim of the research was degradation of amoxicillin, levofloxacin and vancomycin in aqueous solutions. They are used as human or veterinary antibiotics to treat infections caused by bacteria such as pneumonia, tonsillitis and others⁴. The initial concentration of all investigated antibiotics was 400 mg.L⁻¹. All experiments lasted 120 min. They were carried out in a cylindrical glass reactor with volume of 300 mL and the nominal inflow of ozone into reactor was 3 g.h⁻¹. Different methods such as ozonation (O₃), ozonation in buffer solution with pH 9.5 (O₃/pH_{9.5}), ozonation with added hydrogen peroxide (O₃/H₂O₂), catalytic ozonation with Fe²⁺ (O₃/Fe²⁺), catalytic ozonation with Fe²⁺ and UV-A black light (O₃/Fe²⁺/UV) and photo-Fenton ozonation (O₃/Fe²⁺/H₂O₂/UV) were compared. The removal efficiency of each method was determined by total organic carbon (TOC) measurements. Results (Table 1) show that the most efficient removal of levofloxacin and vancomycin was achieved with O₃/Fe²⁺/H₂O₂/UV and in case of amoxicillin the most efficient method was O₃/Fe²⁺/UV. In the end, we can conclude that further research in that field is still needed.

Table 1: TOC removal efficiency [%] for different treatment methods.

	O ₃	O ₃ /pH _{9.5}	O ₃ /H ₂ O ₂	O ₃ /Fe ²⁺	O ₃ /Fe ²⁺ /UV	O ₃ /Fe ²⁺ /H ₂ O ₂ /UV
Amoxicillin	32.9	50.8	49.1	54.8	78.5	76.0
Levofloxacin	35.4	58.2	54.0	55.6	75.1	82.7
Vancomycin	26.4	42.3	45.7	47.4	74.2	89.8

1. Ay, F.; Kargi, F., Advanced Oxidation of Amoxicillin by Fenton's Reagent Treatment. *J. Hazard. Mat.* **2010**, 179, 622–627.
2. Chen, Y.; Xie, Y.; Yang, J.; Cao, H.; Zhang, Y., Reaction Mechanism and Metal Ion Transformation in Photocatalytic Ozonation of Phenol and Oxalic Acid with Ag+/TiO₂. *J. Environ. Sci.* **2014**, 26, 662–672.
3. Nawrocki, J.; Kasprzyk-Hordern, B., The Efficiency and Mechanisms of Catalytic Ozonation. *Appl. Cat. B: Environ.* **2010**, 99, 27–42.
4. Adelglass, J.; Deabate, C. A.; Mcelvaine, P.; Fowler, C. L.; Lococco, J.; Campbell, T., Comparison of the Effectiveness of Levofloxacin and Amoxicillin-Clavulanate for the Treatment of Acute Sinusitis in Adults. *Otolaryngol. Head Neck Surg.* **1999**, 120, 320–327.

New methods to reveal pathogenic viruses in food and water sources

Olivera Maksimović^{1, 2, 3, (current) *}, Maja Ravnikar³, Ion Gutierrez Aguirre³, Denis Kutnjak³, Martin D'Agostino¹

¹ Campden BRI, Chipping Campden, UK,

² KU Leuven, Gent, Belgium

³ Nacionalni Inštitut za Biologijo, Ljubljana, Slovenia, olivera.maksimovic@nib.si

The global water shortage is looming on the horizon, which is causing a rapidly growing interest in the field of water reuse for industrial and cropland applications. However, the commercial sewage wastewater treatment systems, such as ponds, do not accommodate for sufficiently efficient virus removal, especially with high influent loads¹. This means that both human, animal and plant pathogens can be recirculated in the area of effluent discharge or reuse.

Efficient concentration and precise diagnostic methods like digital droplet PCR method for specific detection of pathogens and high-throughput sequencing as a generic detection tool revolutionized diagnostic field especially for viruses. One such example is the base protocol for hepatitis E virus (HEV) detection in pork and other matrices developed in Campden BRI, UK (unpublished). HEV alongside other pathogenic viruses was reported in waste and surface water² thus emphasizing the necessity for a more complex research aimed at answering the composition and biological impact of the water virome. Our future research, which is a part of the MSCA-ITN INEXTVIR project (Fig. 1)³, will be aimed to give us better understanding of viral communities in water sources used in agriculture and in related crops.

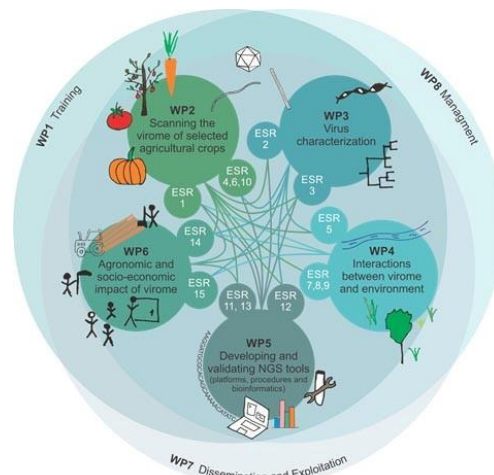


Figure 1: Overview of INEXTVIR project

1. Steyer, A.; Gutiérrez-Aguirre, I.; Rački, N.; Beigot Glaser, S.; Brajer Humar, B.; Stražar, M.; Škrjanc, I.; Poljšak-Prijatelj, M.; Ravnikar, M.; Rupnik, M. The Detection Rate of Enteric Viruses and Clostridium Difficile in a Waste Water Treatment Plant Effluent. *Food Environ. Virol.* **2015**, *7*, 164–172.
2. Ricci, A.; Allende, A.; Bolton, D.; Chemaly, M.; Davies, R.; Fernandez Escamez, P. S.; Herman, L.; Koutsoumanis, K.; Lindqvist, R.; Nørrung, B.; et al. Public Health Risks Associated with Hepatitis E Virus (HEV) as a Food-borne Pathogen. *EFSA J.* **2017**, *15*. <https://doi.org/10.2903/j.efsa.2017.4886>.
3. Innovative Network for Next Generation Training and Sequencing of Virome | INEXTVIR <https://inextvir.eu/> (accessed Jun 10, 2019).

Degradation of antibiotic mixture by ozone-based reactions.

Martin Vrabel*¹, Teja Antončič², Gabriela Kalčíková², Jan Derco¹, Andreja Žgajnar Gotvajn²

¹ Faculty of Chemical and Food Technology, Slovak University of Technology, Radlinského 9, 812 37, Bratislava, Slovakia, vrabel.martin13@gmail.com

² University of Ljubljana, Faculty of Chemistry and Chemical Technology, Večna pot 113, SI-1000 Ljubljana, Slovenia

The increasing use of human and veterinary antibiotics during the last decades has led to the occurrence of pharmaceutical active compounds in municipal wastewaters, natural waters and even drinking waters¹. Conventional methods applied in municipal wastewater treatment plants are not able to remove these pollutants. Therefore, advanced oxidation processes, which include ozonation based processes need to be applied in much greater scale in the near future².

The aim of the research was to determine the best ozone-based method for the degradation of mixture of three antibiotics - amoxicillin, levofloxacin and vancomycin. These drugs are used as human or veterinary antibiotics to treat infections caused by bacteria such as pneumonia, tonsillitis and others³. The initial concentration of each of the investigated antibiotics was 100 mg.L⁻¹. Experiments were performed in batch mode for 2 hours in a 300 mL cylindrical glass reactor and the nominal inflow of ozone into the reactor was 3 g.h⁻¹. Different methods such as ozonation (O₃), ozonation irradiated with the UV-A blacklight (O₃/UV), catalytic ozonation with Fe²⁺ (O₃/Fe²⁺), catalytic ozonation with Fe²⁺ and UV-A black light (O₃/Fe²⁺/UV) and photo-Fenton ozonation (O₃/Fe²⁺/H₂O₂/UV) were compared. The removal efficiency of each method was determined by total organic carbon (TOC) and chemical oxygen demand (COD) measurements. The initial TOC of mixture was 168.8 mg.L⁻¹. The highest removal efficiency was obtained with photo-Fenton ozonation – 85.8 %. It can be concluded that results are very promising and further research needs to be done in this area.

Table 2: TOC removal efficiency [%] for different treatment methods.

Process	O ₃	O ₃ /UV	O ₃ /Fe ²⁺	O ₃ /Fe ²⁺ /UV	O ₃ /Fe ²⁺ /H ₂ O ₂ /UV
Removal Efficiency [%]					
Mixture of ATBs	27.3	27.2	51.7	73.5	85.8

1. Gomes, J., Costa, R., Quinta-Ferreira, R.M., Martins, R.C., Application of ozonation for pharmaceuticals and personal care products removal from water. *Science of the Total Environment*, **2017**, 586, 265-283.
2. Stefan, M.I., Advanced Oxidation Processes for Water Treatment. *IWA publishing*, **2017**, ISBN: 9781780407197
3. Adelglass, J.; Deabate, C. A.; Mcelvaine, P.; Fowler, C. L.; Lococco, J.; Campbell, T., Comparison of the Effectiveness of Levofloxacin and Amoxicillin-Clavulanate for the Treatment of Acute Sinusitis in Adults. *Otolaryngol Head Neck Surg* **1999**, 120, 320–327.

In silico investigation of hen egg-white lysozyme self-association in aqueous solutions

Sandi Brudar,^{*,1} Jure Gujt,² Eckhard Spohr,³ Barbara Hribar-Lee¹

¹ Faculty of Chemistry and Chemical Technology, University of Ljubljana, Večna pot 113, SI-1000 Ljubljana, Slovenia, sandi.brudar@fkkt.uni-lj.si

² Faculty of Natural Sciences, University of Paderborn, Warburger Straße 100, Germany

³ Faculty of Chemistry, University of Duisburg-Essen, Universitätsstraße 5, Germany

Proteins are biological macromolecules that are involved in essential life processes. Aqueous protein solutions under certain conditions can undergo phase separation into solid and liquid or two distinct liquid phases. These solution changes can be described by a so-called thermodynamic phase diagram¹. Irrespective of whether phase stability changes are harmful or beneficial it is important to know the mechanisms under which they occur^{2,3}. Interparticle interactions govern protein phase stability, therefore knowledge about them is crucial for determining protein phase diagrams. Computer simulations, especially all-atom models, can provide detailed insight into protein interactions. In our study we have focused on phase stability of hen-egg white lysozyme (HEWL) solutions via atomistic molecular dynamics simulations. We were particularly interested in interparticle radial distribution functions that provide a clear insight into the microstructure of the solution, and this also allowed us to decipher the mechanism of HEWL self-association. With the calculation of HEWL density fluctuations we were able to visualize the phase stability of HEWL solutions. Radius of gyration, hydration number and diffusion properties were also calculated.

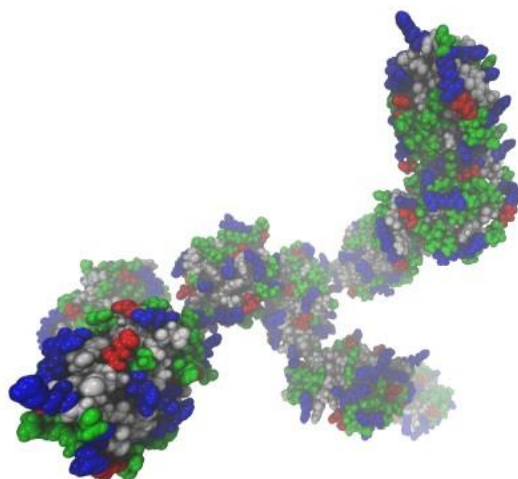


Figure 1: HEWL cluster formation at 92.7 mg/mL and 300 K.

1. Kastelic M., Kalyuzhnyi Y. V., Hribar-Lee B., Dill K. A., Vlachy V., Protein aggregation in salt solutions. *PNAS* **2015**, 112, 6766-6770.
2. Shin Y., Brangwynne, C. P., Liquid phase condensation in cell physiology and disease. *Science* **2017**, 357, 1-11.
3. Brudar S., Hribar-Lee B., The Role of Buffers in Wild-Type HEWL Amyloid Fibril Formation Mechanism. *Biomolecules* **2019**, 9, 1-18.

The effect of sucrose and sucralose on cloud point temperature of lysozyme solutions

Matjaž Simončič¹, Miha Lukšič^{*,1}

¹ Faculty of Chemistry and Chemical Technology, University of Ljubljana, Večna pot 113, SI-1000 Ljubljana, Slovenia, Miha.Luksic@fkkt.uni-lj.si

Sugars like sucrose or trehalose are known to lower the influence of physical stress in biological organisms¹ (elevated temperature, dehydration, cryogenic storage etc.). Man has mimicked this preservative function by including disaccharides in food, cosmetics and foremost in pharmaceutical formulations.

One example of the stabilization effect of disaccharides in protein solutions is the prevention of protein aggregation (phase separation). This can be evaluated by determining cloud-point temperature (UV-VIS spectroscopy) of solutions containing different concentrations of sugars. We examined the effect of added sucrose and sucralose (**Fig. 1**) on cloud-point temperature of lysozyme in aqueous buffer-salt solutions (NaBr, NaNO₃, NaI). The mechanism by which sugars stabilize protein solutions however still remains unclear, which is the reason why those two sugars were chosen as excipients as they differ in their water structuring capabilities through preferential exclusion from the protein-water interface².

We determined that both sugars lower the temperature of phase separation (cloud-point temperature) in a concentration dependent manner. Sucralose has a greater effect on lysozyme stability which we attributed to the interaction of sucralose molecules with the hydrophobic pockets on the protein³. Circular dichroism measurements showed no change in the secondary structure of lysozyme upon addition of either of the disaccharides.

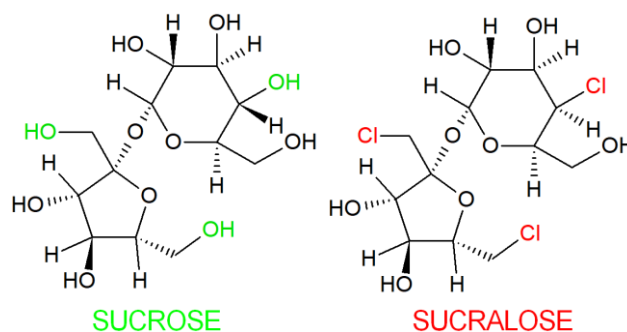


Figure 1: Added sugar excipients.

1. Storey, K. B. and Storey J. M., Frozen and Alive. *Sci. Am.* **1990**, 263, 92-97.
2. Jain, N. K. and Roy I., Effect of trehalose on protein structure. *Protein Sci.* **2009**, 18, 24-36.
3. Shukla, N. et al., Hydrophobic interactions of sucralose with protein structures. *Arch. Biochem. Biophys.* **2018**, 638, 38-43.

Degradation of antibiotic amoxicillin by hydrodynamic cavitation

Tanja Seme^{*1}, Martin Vrabel², Matevž Dular³, Andreja Žgajnar Gotvajn¹.

¹ University of Ljubljana, Faculty of Chemistry and Chemical Technology, Večna pot 113, SI-1000 Ljubljana, Slovenia, semetanja@gmail.com

² Faculty of Chemical and Food Technology, Slovak University of Technology, Radlinského 9, 812 37, Bratislava

³ University of Ljubljana, Faculty of Mechanical Engineering, Aškrčeva 6, SI-1000 Ljubljana, Slovenia

Pharmaceuticals such as antibiotics, anti-depressants, hormones are used in both veterinary and human medicine. These substances are bioactive and have low biodegradability¹. Therefore pharmaceutical water pollution is well recognized as a severe issue, causing long-term adverse impact on the ecosystem and human health². Antibiotics have low concentrations, ng/L to µg/L, which makes them difficult to detect. Amoxicillin is the member of beta-lactams group which have 65% of the total world market for antibiotics¹. Alternative non-biological treatments are being investigated such as advanced oxidation processes (AOPs), to prevent these compounds entering the aquatic environment via wastewater treatment plants due to the non-adequate treatment. One of them is cavitation³.

The aim of this study was to investigate efficiency of hydrodynamic cavitation in aqueous solution of amoxicillin. The initial concentration of antibiotic was 400 mg/L. Experiments were carried out in a pulse cavitation station with volume 1500 mL at pressure 7 bar for 90 minutes. The removal efficiency was determined by determination of chemical oxygen demand COD, biochemical oxygen demand (BOD₅) and total organic carbon (TOC). Results are shown in Table 1. The process was not efficient, only easily biodegradable components in terms of BOD₅ were removed (92%).

Table 1: COD, BOD₅ and TOC removal efficiency [%] for amoxicillin in cavitation experiment.

Amoxicillin	COD	BOD ₅	TOC
90 minutes	< 1	92	4

1. Demirezen D. A., Yıldız Y. S., Yılmaz D. D., Amoxicillin degradation using green synthesized iron oxide nanoparticles: Kinetics and mechanism analysis. *Environ. Nanotechnol. Monit. Manage.* **2019**, *11*, 100219.
2. Tao Y, Cai J., Huai X, Liu B, A novel antibiotic wastewater degradation technique combining cavitating jets impingement with multiple synergetic methods. *Ultrason. Sonochem.* **2018**, *44*, 36-44.
3. Zupanc M., Kosjek T., Petkovšek M., Dular M., Kompare B., Širok B., Stražar M., Heath E. Shear-induced hydrodynamic cavitation as a tool for pharmaceutical micropollutants removal from urban wastewater. *Ultrason. Sonochem.* **2014**, *21*, 1213-1221.

The use of electronic devices and musculoskeletal discomfort among university students at the Faculty of chemistry and chemical technology in Ljubljana

Maša Legan,¹ Klementina Zupan*¹

¹ Faculty of Chemistry and Chemical Technology, University of Ljubljana, Večna pot 113, SI-1000 Ljubljana, Slovenia, klementina.zupan@fkkt.uni-lj.si

One of the most common occupational diseases worldwide are musculoskeletal disorders (MSDs). MSDs that mainly resulting from the use of electronic devices are becoming increasingly frequent and will be or already constitute a significant problem for all users of electronic devices¹. Today, the largest group of mobile device users is represented by 18–29-year-olds, which is also the typical age of college attendees (students) Children, adolescents and students are facing the same musculoskeletal disorders as adults and the use of electronic devices even intensifies during the study period². Some older studies from Asia, Australia and USA revealed that more than half of college students reported having upper extremity symptoms while using the computer and other electronic devices (mobile phones, tablets, laptops) from 2 – 5 hours a day^{1, 3, 4}.

In this study we focused on musculoskeletal impact of the use of electronic devices on European student population at the Faculty of Chemistry and Chemical Technology, University of Ljubljana. Our results reveal the most common types of musculoskeletal discomforts which were back pain and shoulder pain, followed by neck pain and other (Table 1). As expected, the frequent use of different electronic devices was strongly related to musculoskeletal problems. Strong correlations were found between mobile phone use and neck pain.

Table 3: A comparison between the main findings about Asian and European student population

	Asian student population (503 participants)	European student population (535 participants)
Experience of MSDs	49.9%	39.6%
Doing sport (exercise)	33.2%	60.6%
Most common types of pain	Shoulder and neck pain	Back and shoulder pain

1. Woo, E. H. C.; White, P.; Lai, C. W. K., Musculoskeletal impact of the use of various types of electronic devices on university students in Hong Kong: An evaluation by means of self-reported questionnaire. *Manual Therapy*. **2016**, *26*, 47-53.
2. Albin, T. J., Computer Ergonomics: The State of the Art. *High Plains Engineering Service*. **2015**, *52*, 215-16.
3. James, D.; Drennan, J., Exploring Addictive Consumption of Mobile Phone Technology. *ANZMAC 2005 Conference: Electronic Marketing*, 87-96.
4. Katz, J. N.; Amick, B. C.; Carroll, B. B.; Hollis, C.; Fossel, A. H.; Coley, C. M., Prevalence of upper extremity musculoskeletal disorders. *The American Journal of Medicine*. **2000**, *109*, 586-88.

Caspase cleavage frequency at human protein exon junction sites

Lara Jerman,^{1,2,3} Matjaž Kukar,² Gregor Gunčar*¹

¹ Faculty of Chemistry and Chemical Technology, University of Ljubljana, Večna pot 113, SI-1000 Ljubljana, Slovenia, gregor.guncar@fkk.uni-lj.si

² Faculty of Computer and Information Science, University of Ljubljana, Večna pot 113, SI-1000 Ljubljana, Slovenia

³ Faculty of Mathematics and Physics, University of Ljubljana, Jadranska ulica 19, SI-1000, Ljubljana, Slovenia

Both exon junction and caspase cleavage sites are most frequently located on protein loops and between protein domains. We set out to find out whether the two types of sites coincide with a significant frequency, which might indicate a biological connection. Three different caspase cleavage datasets were analyzed – the experimental MerCASBA¹ as well as the predictive Cascleave 2.0² and CaspDB³. Data on exon junction sites were obtained from Ensembl⁴. The experimental caspase cleavage data was insufficient for any statistically supported conclusions. The calculations on theoretical data showed a 7-14 % increase in the empirical probabilities of both directions' coinciding frequencies (Tab. 1). Phase 1 exon junction sites coincide with the cleavage sites most clearly. This can be explained by known nucleotide preferences and does not necessarily indicate a novel connection. We could not eliminate the possibility of results reflecting the bias of the theoretical models of caspase cleavage sites.

Table 4: Empirical probabilities of one type of site coinciding with the other compared to those of random sites. Results are given for each of the predictive datasets.

Probability of coinciding with	For	CaspDB	Cascleave 2.0
An exon junction site	A random site	3,3 %	3,6 %
	A caspase cleavage site	3,7 %	3,8 %
A caspase cleavage site	A random site	7,3 %	2,6 %
	An exon junction site	8,3 %	2,8 %

1. Fridman, A.; Pak, I.; Butts, B. D.; Hoek, M.; Nicholson, D. W.; Mehmet, H. MerCASBA: an Updated and Refined Database of Caspase Substrates. *Apoptosis* **2013**, *18*, 369–371.
2. Wang, M.; Zhao, X.-M.; Tan, H.; Akutsu, T.; Whisstock, J. C.; Song, J. Cascleave 2.0, a New Approach for Predicting Caspase and Granzyme Cleavage Targets. *Bioinformatics* **2013**, *30*, 71–80.
3. Kumar, S.; Raam, B. J. V.; Salvesen, G. S.; Cieplak, P. Caspase Cleavage Sites in the Human Proteome: CaspDB, a Database of Predicted Substrates. *PLoS ONE* **2014**, *9*.
4. Aken, B. L.; Ayling, S.; Barrell, D.; Clarke, L.; Curwen, V.; Fairley, S.; Banet, J. F.; Billis, K.; Girón, C. G.; Hourlier, T.; Howe, K.; Kähäri, A.; Kokocinski, F.; Martin, F. J.; Murphy, D. N.; Nag, R.; Ruffier, M.; Schuster, M.; Tang, Y. A.; Vogel, J.-H.; White, S.; Zadissa, A.; Flicek, P.; Searle, S. M. J. The Ensembl Gene Annotation System. *Database* **2016**, *2016*, 1-19.

Corrosion testing and efficiency of benzotriazole based inhibitor on stainless steel and copper

Borislav Malinovic,¹ Tijana Djuricic,^{*1} Dusko Zoric²

¹ Faculty of Technology, University of Banja Luka, Stepe Stepanovica 73, 78000 Banja Luka, Bosnia and Herzegovina, tijana.malinovic@tf.unibl.org

² EFT Mine and Thermal Power Plant Stanari Ltd., Stanari, Bosnia and Herzegovina

The construction materials are necessary to protect against the impact of corrosion. Otherwise, this can lead to high maintenance costs, repairs or replacements and may cause a risk to people and environmental. Industrial equipment can be made of only one material, but a combination of two or more materials is often used. In that sense, a major challenge is finding a corrosion inhibitor that will effectively protect all parts of the equipment.

This paper presents the results of electrochemical testing (potentiodynamic polarization, linear polarization, Tafel extrapolation) the behavior of stainless steel EN 1.4301 and copper EN 13601 in hydrochloric acid (0.5 mol dm^{-3}) and efficiency testing of a multicomponent industrial corrosion inhibitor which contain benzotriazole (BTA)¹. Thiazole and triazole derivatives provide good corrosion protection, with much better inhibitory efficacy in less acidic and lower temperatures². The results indicate that tested inhibitor is effective in protecting both materials from corrosion. The higher protection efficiency was achieved on the copper, compared with stainless steel. The highest achieved efficiency for stainless steel was at inhibitor concentration of 0.16 mL/L ($E_p = 24.1\%$), while the highest efficacy for copper was achieved at the lowest tested concentration of inhibitor, 0.04 mL/L ($E_p = 74.2\%$).

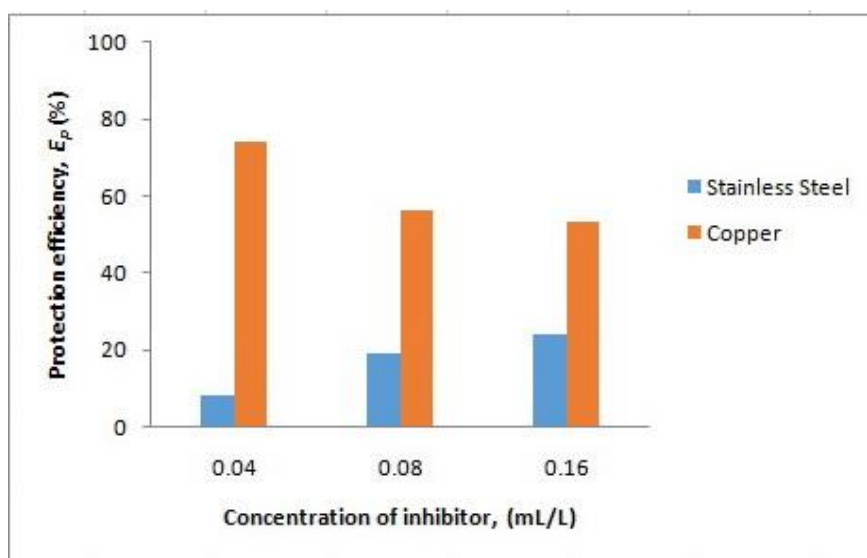


Figure 1: An overview of the achieved efficiency.

1. BWT France. (2016). Safety data sheet BWT CS -1006. Saint Deins Cedex.
2. Vašttag, Đ. & Nakomčić, J., Derivati tiazola i triazol kao inhibitori korozije metala, II deo. *Zaštita materijala* **2016**, 213-224.

The effect of the catalyst type and the reaction conditions on hydrodeoxygenation of aldaric acid

Brigita Hočevar¹, Miha Grilc*¹, Blaž Likozar¹

¹ Department of Catalysis and Chemical Reaction Engineering, National Institute of Chemistry, Hajdrihova 19, SI-1000 Ljubljana, Slovenia

Aldaric acids, linear compounds (length 5 or 6 carbon atoms) with carboxylic functional groups on terminal place and hydroxyl functional groups on secondary C atoms, are promising feedstock for producing many biobased chemicals, especially monomers for polymer industry, such as adipic acid. Our study was focused on hydrodeoxygenation of mucic acid over different metals supported on neutral or acidic supports in order to consider the most active catalyst for selective HDO (hydrodeoxygenation) of mucic acid. Experiments were performed in a batch three phase reactor, where solid reactant was dissolved in water and solid heterogeneous catalyst was added in the reaction mixture. Based on detected compounds in the liquid samples taken during the reaction time the reaction pathway network was developed. In the presence of a catalyst partially or completely deoxygenated compounds were formed. Tested heterogeneous catalysts (Ru, Pt, Rh, Ni, NiMo on C, SiO₂ and Al₂O₃) are active for reactions, such as decarboxylation, dehydroxylation, hydrogenation and C-C cleavage. Many of the detected compounds, such as tetrahydro-2-furfuryl alcohol, 2-hydroxy hexanoic acid, 2-hydroxypentanoic, levulinic acid, 2-furoic acid, adipic acid, etc., are industrially important chemicals.¹ Using cheaper NiMo catalyst under slightly higher temperature delivered better results compared to the more active noble metal catalysts at the lower temperature.

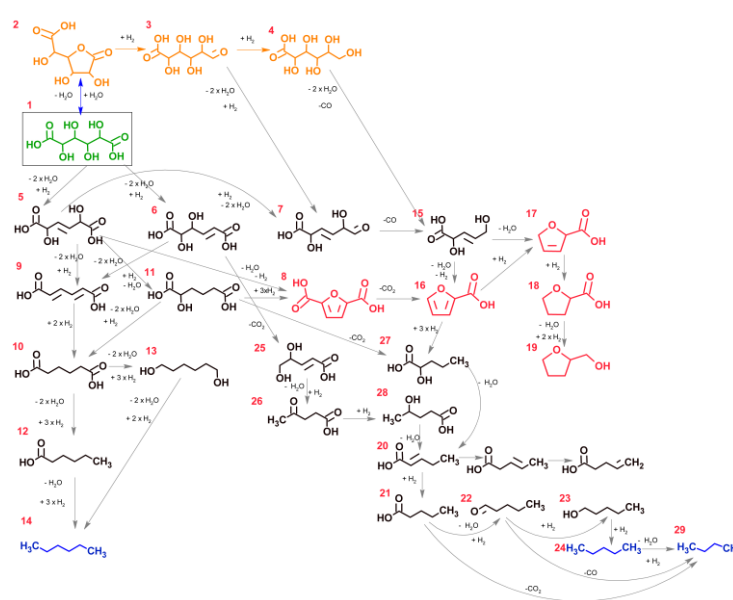


Figure 1: Reaction pathway of aldaric acid HDO.

- (1) Hočevar, B.; Grilc, M.; Likozar, B. Aqueous Dehydration, Hydrogenation, and Hydrodeoxygenation Reactions of Bio-Based Mucic Acid over Ni, NiMo, Pt, Rh, and Ru on Neutral or Acidic Catalyst Supports *Catalysts* **2019**, *9*, 286.

π -Conjugated polyHIPEs

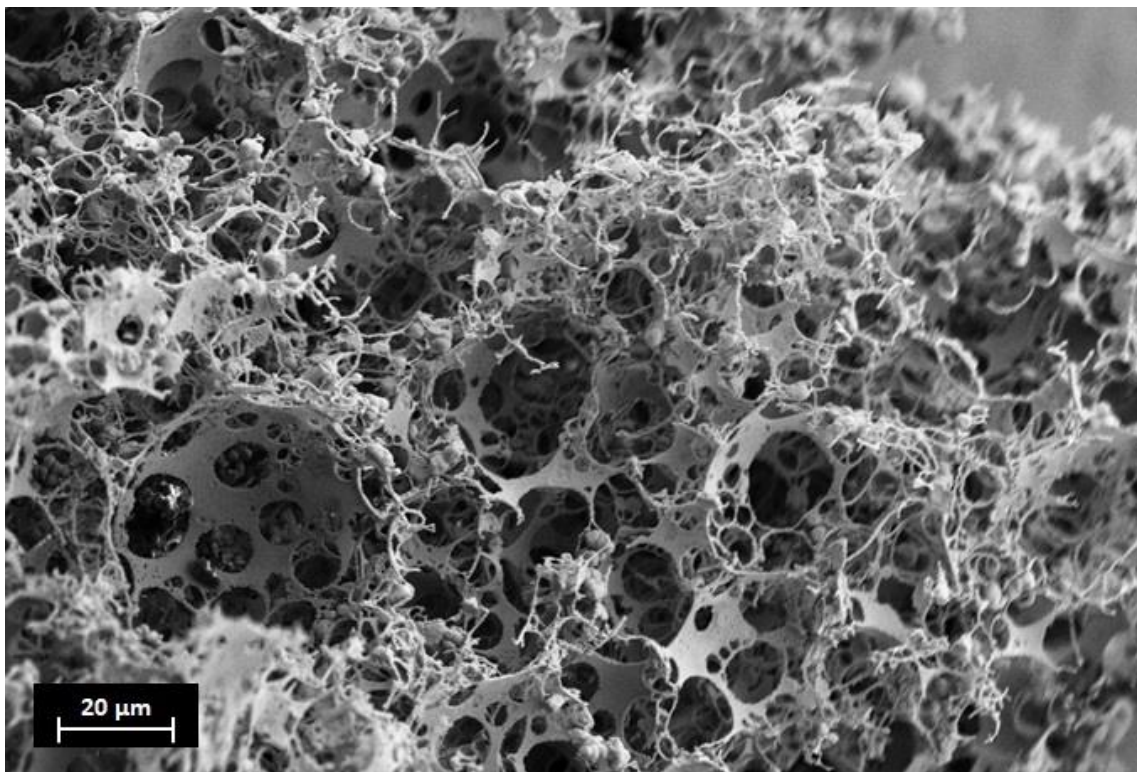
Sarah Jurjevec,¹ Ema Žagar,¹ Sebastijan Kovačič*^{1,2}

¹ National Institute of Chemistry, Department of Polymer Chemistry and Technology, Hajdrihova 19, SI-1001 Ljubljana, sebastijan.kovacic@ki.si

² Faculty of Chemistry and Chemical Engineering, Smetanova ulica 17, SI-2000 Maribor

PolyHIPEs are porous emulsion-templated polymers synthesized within the high internal phase emulsions (HIPEs). One way to polymerize HIPEs is to use the carbon-carbon (C-C) cross-coupling reaction. Recently, such synthetic approach has been successfully applied for polymer synthesis. As-obtained π -conjugated microporous polymers (CMPs) with high specific surface area have become particularly interesting and the subject of numerous studies.

Combining the macroporosity of the polyHIPEs with the polymer backbone based on the π -conjugated repeating units is particularly intriguing. Hence, the Sonogashira–Hagihara cross coupling reactions were used to couple iodinated benzene derivatives within the continuous phase of HIPEs. A series of hierarchically porous poly(*p*-dimethoxybenzene) and poly(*p*-nitrophenol)-based π -conjugated polyHIPE were successfully synthesized. Such π -conjugated hierarchically porous systems represent promising carriers for a plethora of applications.



Figure/Scheme 1: Morphological characterization of poly(*p*-nitrophenol) by SEM.

1. M. Silverstein, Recent advances in emulsion templated porous polymers, *Prog. Polym. Sci.*, **2014**, *39*, 199-234.
2. R. Dawson et al, Nanoporous organic polymer network, *Prog. Polym. Sci.*, **2012**, *37*, 530-563.

Expression of cystatin C in the PC12 cell model of Alzheimer's disease after exposure to amyloid beta peptide 25-35

Kity Požek*,¹ Bojan Doljak,²

¹ Faculty of Chemistry and Chemical Technology, University of Ljubljana, Večna pot 113, SI-1000 Ljubljana, Slovenia, kity.pozek@gmail.com

² Faculty of Pharmacy, University of Ljubljana, Aškerčeva cesta 7, SI-1000 Ljubljana, Slovenia

Alzheimer's disease (AD) is the most common cause of dementia in the elderly. Extracellular amyloid plaque deposition is one of the neuropathological hallmarks of AD. Amyloid plaques consist predominantly of amyloid beta ($A\beta$). Another important player in the onset and progression of AD is cystatin C (CysC), a cysteine protease inhibitor which localizes in amyloid plaques and exerts an anti-amyloidogenic function by binding to $A\beta$ and inhibiting the formation of its neurotoxic forms (fibrils and oligomers)^{1,2}. We studied CysC expression in rat PC12 pheochromocytoma cells by exposing them to $A\beta$ peptide 25-35 ($A\beta_{25-35}$)³. Being part of cell's defense against $A\beta$ neurotoxicity, we hypothesized that the CysC protein level in PC12 cell line would increase in the presence of $A\beta_{25-35}$ ^{1,2,4}. The total amount of CysC (intracellular and membrane-bound) in cell lysates was determined in $A\beta_{25-35}$ treated and control cells in time intervals of 12, 24, 36, 48, 60 and 72 hours by enzyme-linked immunosorbent assay (ELISA). We found that the level of CysC in PC12 cells in the first 12 hours of exposure to $A\beta_{25-35}$ increases by 77 % compared to the control. The level of CysC then slowly decreases and after 60 hours of exposure reaches the level of the control cells. Further research is currently under way to clarify the role of CysC in AD pathogenesis and evaluate it as a potential therapeutic target.

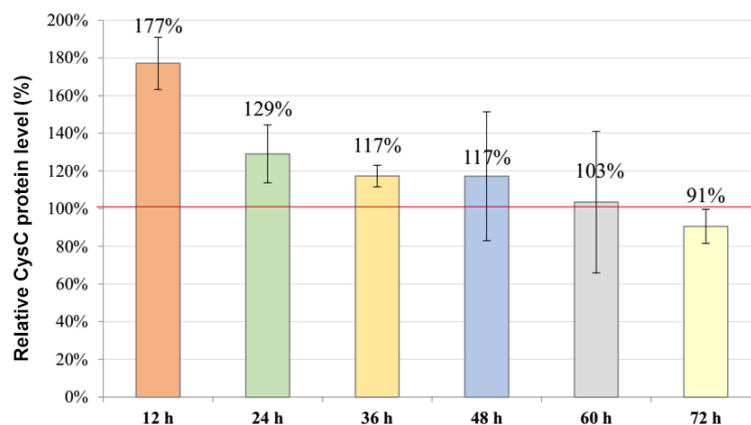


Figure 1: Total CysC protein level in PC12 cells exposed to $A\beta_{25-35}$ presented as a percentage of CysC level in control (untreated) cells at different time points.

1. Mathews, P.M.; Levy, E. *Ageing. Res. Rev.*, **2016**, 32, 38–50.
2. Tizon, B.; Ribe, E. M.; Mi, W.; Troy, C. M.; Levy, E. J. *Alzheimers. Dis.*, **2010**, 19, 885–94.
3. Millucci, L.; Ghezzi, L.; Bernardini, G.; Santucci, A. *Curr. Protein. Pept. Sci.*, **2010**, 11, 54–67.
4. Mi, W.; Pawlik, M.; Sastre, M.; Jung, S. S.; et al. *Nat. Genet.*, **2007**, 39, 1440–2.

Mechanical properties and curing kinetics of aromatic epoxides with aminomaleimide.

Žan Kovačič¹, Aleš Ručigaj*¹

¹ Faculty of Chemistry and Chemical Technology, University of Ljubljana, Večna pot 113, SI-1000 Ljubljana, Slovenia, ales.rucigaj@fkkt.uni-lj.si

Aminomaleimide was synthesized by an optimized procedure¹ and used in the curing process of epoxy resin. The effect of the amine functional group acting as a curing agent, and maleimide functional group acting as a hardener was studied. The research was performed by using aromatic and aliphatic epoxies with different molecular weights and numbers of epoxy functional groups. The curing kinetics² was performed by the means of differential scanning calorimetry (DSC) performing model-free kinetics. Samples showed typical autocatalytic behavior during the curing process. Excellent agreement between the experimental and calculated model data was achieved (Figure 1). Among that, each combination was prepared in three different ratios of aminomaleimide and epoxy (w/w) in order to understand and explain the curing mechanism. Besides the kinetic studies, the crosslinked materials were analyzed by dynamic mechanical analysis (DMA) with which mechanical properties and glass transition temperature T_g was determined. Also, thermal stability was determined by thermogravimetric analysis (TGA). To conclude, aminomaleimide proved to act as a curing agent and hardener improving the thermal stability and mechanical properties of the prepared samples due to the maleimide one-side functionality.³

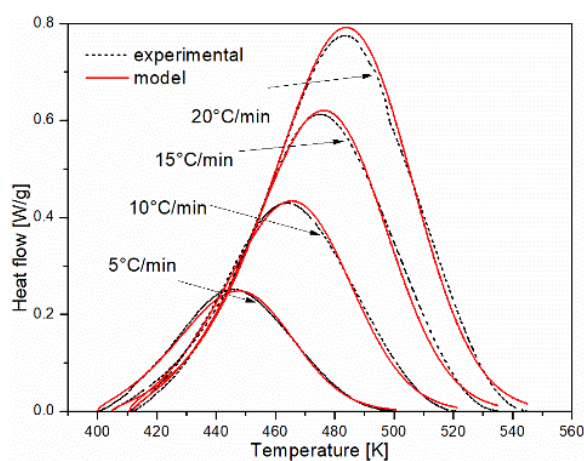


Figure 1: Comparison between experimental and fitting data for different heat rates for the Poly(Bisphenol A-co-epichlorohydrin), glycidyl end-capped Mn377/aminomaleimide system.

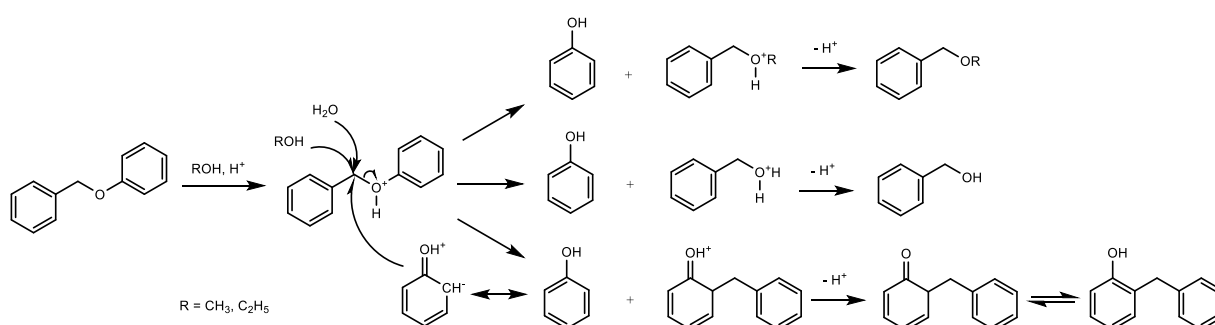
1. Stirn, Z., Rucigaj, A., Krajnc, M., Innovative approach using aminomaleimide for unlocking phenolic diversity in high-performance maleimidobenzoxazine resins. *Polymer* **2017**, *120*, 129-140.
2. Vyazovkin, S.; Burnham, A. K.; Criado, J. M.; Pérez-maqueda, L. A.; Popescu, C.; Sbirrazzuoli, N. ICTAC Kinetics Committee recommendations for performing kinetic computations on thermal analysis data. *Thermochim. Acta* **2011**, *520*, 1–19.
3. Wu, C.; Liu, Y.; Hsu, K. Maleimide-epoxy resins : preparation , thermal properties , and flame retardance. *Polymer* **2003**, *44*, 565–573.

Typical lignin bond cleavage in acidified aqueous and non-aqueous alcohols

Edita Jasiukaityte Grojzdek*, Ana Bjelić, Brigita Hočevnar, Miha Grilc, Blaž Likozar

Department of Catalysis and Chemical Reaction Engineering, National Institute of Chemistry, Hajdrihova 19, SI-1000 Ljubljana, Slovenia, edita.jasiukaityte@ki.si

Lignin conversion into the bio-based monoaromatics is a major challenge due to the complex lignin structure itself and additionally the macromolecule modification caused by the ether bond cleavage during the organosolv lignocellulosic (LC) biomass pulping in acidified aqueous ethanol¹⁻³. In this study the effect of solvent properties, acidity of the reaction media and temperature on the degree of typical lignin bond cleavage was determined. Specifically, acidolysis of benzyl phenyl ether (BPE), being an important α -O-4 linkage model compound, has been investigated in ethanol, methanol and in 75 % (v/v) ethanol/water with sulfuric acid as a catalyst. The determined product distribution in non-aqueous alcohols was strongly affected by the solvent acidity and polarity, and temperature. On the other side, acidity of the reaction media showed a less significant effect. Addition of water to ethanol had an advantageous effect on the typical ether bond cleavage, especially in terms of alkoxylation reactions. Thus, the effects of temperature and solvent polarity and acidity were confirmed to be key parameters for attaining the optimal ether bond cleavage extent.



Scheme 1: Proposed reaction mechanism of BPE acidolysis in aqueous and non-aqueous alcohol.

1. Schutyser, W., Renders, T., Van den Bosch, S., Koelewijn, S. F., Beckham, G. T., Sels, B. F., Chemicals from lignin: an interplay of lignocellulose fractionation, depolymerisation, and upgrading. *Chem. Soc. Rev.* **2018**, 47 (3), 852-908.
2. Bjelić, A., Grilc, M., Huš, M., Likozar, B., Hydrogenation and hydrodeoxygenation of aromatic lignin monomers over Cu/C, Ni/C, Pd/C, Pt/C, Rh/C and Ru/C catalysts: Mechanisms, reaction micro-kinetic modelling and quantitative structure-activity relationships. *Chem. Eng. J.* **2018**, 359, 305-320.
3. Bjelić, A.; Grilc, M.; Likozar, B., Catalytic hydrogenation and hydrodeoxygenation of lignin-derived model compound eugenol over Ru/C: Intrinsic microkinetics and transport phenomena. *Chem. Eng. J.* **2018**, 333, 240-259.

Antibodies glycan analysis using recombinant prokaryotic lectins

Metka Stantič,¹ Gregor Gunčar,*¹ Aleš Podgornik *¹

¹ Faculty of Chemistry and Chemical Technology, University of Ljubljana, Večna pot 113, SI-1000 Ljubljana, Slovenia, Ales.Podgornik@fkkt.uni-lj.si

Antibody glycosylation is a common post-translational modification and plays an important role in modulating antibody effector activity. IgG type antibodies have a single N-linked glycan attached at asparagine 297 of each heavy chain that are highly heterogeneous, because of the presence of different terminal sugars.¹ Oligosaccharides are normally hidden located within the folded structure of immunoglobulin G and to obtain freely accessible carbohydrate structures attached to the Fc region, the molecule should be partially unfolded. This can be achieved among other methods also by heating in the presence of reducing agent. To detect the glycosylation pattern we designed three different recombinant prokaryotic lectins that are capable of recognizing and binding reversibly to specific oligosaccharide structures and managed to produce them in large quantities using *E. coli* BL21[DE3]pLysS. The first two lectins are rPA-ILNmE6 and rPA-ILNmB10, both are mutated forms of PA-IL protein, the soluble lectin produced by the opportunistic pathogen *Pseudomonas aeruginosa*. Both lectins displayed strong binding to disaccharide Gal β 1-4GlcNAc and showed the capacity to bind even wider spectrum of other glycoproteins with lower affinity (Table 1)². The third is rhesus rotavirus sialic acid binding domain (VP8*), which specifically binds the glycans with terminal Neu5Ac and Neu5Gc³. Lectins were designed in a way that could be isolated with immobilized metal ion affinity chromatography and could further be immobilized to activated carriers through added tags for use as affinity chromatography ligands. To qualify lectin/antibody interactions as well as efficiency of antibody heat pretreatment, we used Bio-Layer Interferometry technique. We confirmed interactions between the reduced antibody and the two bacterial lectins.

Table 5: Glycoprotein specificity profile of lectins.

Lectin	Glycoprotein Specificity Profile
rPA-ILNmB10	LacNAc > Gal α 1-3 Gal = Gal β 1-3 Gal NAc > Gal α 1-2Gal = Man = Fuc > GalNAc = GlcNAc
rPA_ILNmE6	LacNAc >>> Gal α 1-3Gal = Gal β 1-3 GalNAc
VP8*	Neu5Ac α 2-6 LacNAc = Neu5Ac α 2-3 LacNAc > Neu5Gc

1. Raju S.T., Terminal sugars of Fc glycans influence antibody effector functions of IgGs. *Curr Opin Immunol* **2008**, 20, 471-478.
2. Keogh D., Thompson R., Larragy R., McMahon K., O'Connor B., Clarke P., Generating novel recombinant prokaryotic lectins with altered carbohydrate properties through mutagenesis of the PA-IL protein from *Pseudomonas aeruginosa*. *Biochim. Biophys Acta* **2014**, 1840, 2091-2104.
3. Dormitzer P.R., Sun Z.-Y. J., Wagner G., Harrison S. C. The rhesus rotavirus VP4 sialic acid binding domain with a novel carbohydrate binding site. *The EMBO Journal* **2002**, 21, 885-897.

Modelling water with rose functions

Martin Tušek,¹ Miha Lukšič*¹

¹ Faculty of Chemistry and Chemical Technology, University of Ljubljana, Večna pot 113, SI-1000 Ljubljana, Slovenia, miha.luksic@fkkt.uni-lj.si

Understanding how water's physico-chemical properties are encoded within its molecular structure and energies requires a combination of experimental data and modelling. Various models serve different purposes:¹ the so-called coarse-grained and reduced-dimensionality models of water are among the most simple ones. Nevertheless, such models are capable of providing simpler but concise information about the collective behaviour of the microscopic structure of the fluid.

In the present work, structure and thermodynamics of a two-dimensional single-point water model is explored by means of Monte Carlo computer simulations. A single angular degree of freedom, describing the hydrogen bonding between two water molecules, is accounted for through sinusoidal rose curves. A 3-petal rose potential of the general form $\sin(3\theta)$ was used and the model was therefore named rose water (Figure 1).² Compared to its analogue, i.e. a four-site 2D Mercedes Benz model,³ the rose water is computationally more efficient due to the resulting decrease in the number of pairwise interaction sites between neighbouring waters. Proper selection of model's potential parameters gives good agreement with the MB water model: it is structurally similar to MB water and exhibits same water-like anomalous behaviour. Evolution of the structure with temperature will be presented along with the changes in density, isothermal compressibility, coefficient of thermal expansion, and heat capacity.

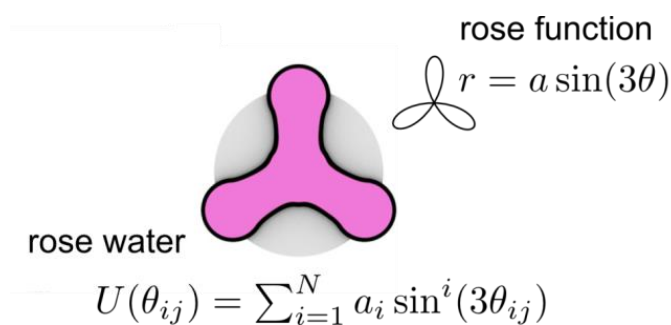


Figure 1: Parametric 3-petal rose function potential form of a rose water model

1. Brini, E.; Fennell, C. J.; Fernandez-Serra, M.; Hribar-Lee, B.; Lukšič, M.; Dill, K. A., How water's properties are encoded in its molecular structure and energies. *Chem. Rev.* **2017**, *117*, 12385-12414.
2. Williamson, C. H.; Hall, J. R.; Fennell, C. J., Two-dimensional molecular simulations using rose potentials. *J. Mol. Liq.* **2017**, *228*, 11-17.
3. Ben-Naim, A. Statistical mechanics of "waterlike" particles in two dimensions. I. Physical model and application of the Percus-Yevick equation. *J. Chem. Phys.* **1971**, *54*, 3682-3695.

Disinfection of wastewater – tertiary treatment in municipal wastewater treatment plant with peracetic acid

Anja Vehar^{1*}, Nadja Hvala², Marjetka Levstek⁴, Ana Kovačič^{2,3}, Ester Heath^{2,3}, Marjetka Stražar⁴, Andreja Žgajnar Gotvajn¹

¹ University of Ljubljana, Faculty of Chemistry and Chemical Technology, Večna pot 113, SI-1000 Ljubljana, Slovenia, anja.vehar15@gmail.com

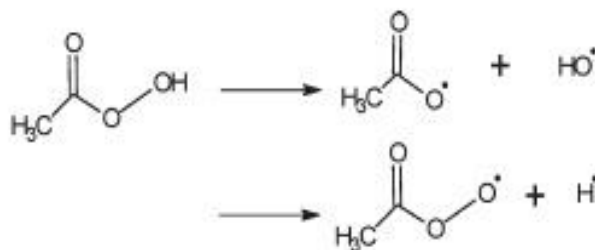
² Jožef Stefan Institute, Jamova cesta 39, SI-1000 Ljubljana, Slovenia

³ International Postgraduate School Jožef Stefan, Jamova cesta 39, SI-1000 Ljubljana, Slovenia

⁴ Javno Podjetje Centralna čistilna naprava Domžale-Kamnik d.o.o., Študljanska cesta 91, SI-1230, Domžale, Slovenia

Despite the considerable improvement in water quality as a result of modern wastewater treatment technologies there still exist areas for continued development. One is to disinfect the effluent, and the other one is to remove micropollutants. The bioindicator species, which show the pollution caused by municipal wastewater are *Enterococcus* and *Escherichia coli*. They can cause diseases and digestive problems, in the case of consumption of polluted water, and changes in the aquatic ecosystem. The efficiency of peracetic acid (PAA) in combination with hydrogen peroxide (H₂O₂) for disinfection has already been proven¹. PAA and H₂O₂ in water solution form nonselective and highly reactive peroxy and hydroxyl radicals², which have the potential not only to kill bacteria but also to remove persistent micropollutants.

In our work, we studied laboratory scale effluent disinfection with PersanTM (PAA and H₂O₂). The lowest concentration of Persan, which must be added to the effluent to remove 98% of *Enterococcus* and *Escherichia coli* was 5.7 mg L⁻¹. We also tested the ecotoxicity of the treated effluent with *Daphnia magna*, total organic carbon, and the removal of 12 bisphenols. Results are currently under evaluation.



Scheme 1: Peracetic acid and formation of highly reactive peroxy and hydroxyl radicals²

1. Koivunen, J., Heinonen-Tanski, H., Peracetic acid (PAA) disinfection of primary, secondary and tertiary treated municipal wastewaters. *Water Research* **2005**, 39, 4445–4453.
2. Kerkaert, B., Mestdagh, F., Cucu, T., Aedo, P. R., Ling, S. Y., Meulenaer, B. D., Hypochlorous and Peracetic acid Induces Oxidation of Dairy Proteins. *Journal of Agricultural and Food Chemistry* **2011**, 59, 907-914.

Development of an amperometric biosensor for the detection of biogenic amines

Tjaša Rijavec*,¹, Radovan Metelka²

¹ Faculty of Chemistry and Chemical Technology, University of Ljubljana, Večna pot 113, SI-1000 Ljubljana, Slovenia, rijavec.tjasa1@gmail.com

² Faculty of Chemical Technology, University of Pardubice, Studentská 573, CZ-53210 Pardubice, Czech Republic

The purpose of this work was to develop a biosensor based on the immobilization of the enzyme diamine oxidase (DAO, EC 1.4.3.22, ≥ 0.05 units/mg solid) on a screen-printed carbon electrode (SPCE), to selectively detect aliphatic diamines¹, such as putrescine, cadaverine, spermidine and spermine².

DAO is an enzyme that converts diamines to aldehydes in the presence of molecular oxygen as electron acceptor. It produces ammonia and hydrogen peroxide, which can be easily electrochemically detected. To provide better selectivity, the operational potential can be lowered by using mediators of electron transfer, such as RhO_2 , MnO_2 or RuO_2 . Working electrodes of commercial SPCEs were manually modified by three layers. First layer was made by drop casting the mediator RuO_2 suspended in 0.1 M phosphate buffer, then a second layer comprised DAO in glutaraldehyde and after cross-linking the enzyme a final layer of 1 % Nafion solution was added³. The biosensor was developed for use in flow injection analysis with amperometric detection. During the development, different flow rates and detection potentials were tested for four substrates (putrescine, cadaverine, spermidine and spermine) to determine the optimal experimental conditions and a flow rate of 0.6 ml/min at 0.4 V provided the highest current response. Analytical performance of developed biosensor was then evaluated within the concentration range of 0.05–1 mM for biogenic amines.

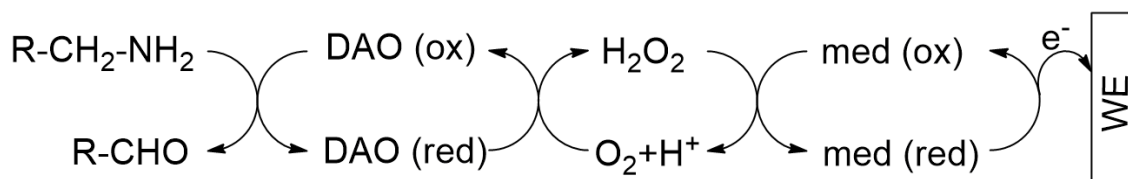


Figure 1: Schematic representation of the sensing mechanism. Mediator is noted as ‘med’.

1. Kalač, P.; Krausová, P. A Review of Dietary Polyamines: Formation, Implications for Growth and Health and Occurrence in Foods. *Food Chem.* **2005**, *90*, 219–230.
2. Boffi, A.; Favero, G.; Federico, R.; Macone, A.; Antiochia, R.; Tortolini, C.; Sanzó, G.; Mazzei, F. Amine Oxidase-Based Biosensors for Spermine and Spermidine Determination. *Anal. Bioanal. Chem.* **2015**, *407*, 1131–1137.
3. Telsnig, D.; Kalcher, K.; Leitner, A.; Ortner, A. Design of an Amperometric Biosensor for the Determination of Biogenic Amines Using Screen Printed Carbon Working Electrodes. *Electroanalysis* **2013**, *25*, 47–50.

The effect of ion size on the electrolyte distribution near a charged wall. A Poisson-Boltzmann and Monte Carlo study

Vid Ravnik,¹ Miha Lukšič,^{*,1}

¹ Faculty of Chemistry and Chemical Technology, University of Ljubljana, Večna pot 113, SI-1000 Ljubljana, Slovenia, miha.luksic@fkkt.uni-lj.si

Charged objects, e.g. membranes, macromolecules, metal surfaces in contact with an electrolyte solution form an electric double layer. Besides electrostatic interactions, the specific non-electrostatic interactions depend on the nature of the ions, solvent and interface.

A modified free energy functional, valid within the Poisson-Boltzmann (PB) theory, obtained using a lattice version of the ideal Coulomb gas for the electrolyte, was used to account for the size of the electrolyte ions in contact with an infinite charged wall. The modified PB equation (MPB)^{1,2} was solved numerically. The results were compared with Canonical Monte Carlo (MC) simulations where a primitive +1:-1 model electrolyte was used. The Coulomb interactions were accounted for with the charged sheet method.³

The electrostatic potential and concentration profile near the charged wall is dependent upon the size of the ions, the charge density of the wall, as well as the concentration of the electrolyte. Close to the wall, the disagreement between the MPB and MC results is magnified. This is attributed to differences in the models used in simulations and theory (primitive model vs. lattice Coulomb gas). For walls with high surface charge densities and for big ions, the concentration profile of the counterions obtained via MPB plateaus near the wall as it forms a saturated layer. The results of the MC simulations for similar cases sometimes show a second layer of ions one and a half radius away from the wall and a much higher maximum concentration in the first layer than predicted by the MPB.

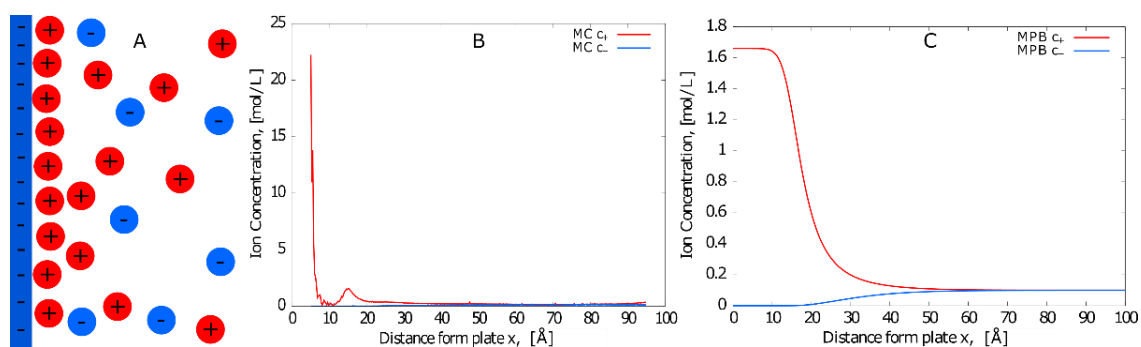


Figure 1: A) Schematic of an electric double layer B) Concentration profile from MC simulations and C) from the MPB equation.

1. Ben-Yaakov, D.; Andelman, D.; Podgornik, R. Beyond standard Poisson–Boltzmann theory: Ion-specific interactions in aqueous solutions. *J. Phys. Condens. Matter* **2009**, *21*, 424106.
2. Borukhov, I.; Andelman, D.; Orland, H. Adsorption of large ions from an electrolyte solution: A modified Poisson–Boltzmann equation. *Electrochim. Acta* **2000**, *46*, 221-229.
3. Boda, D.; Chan, K.; Henderson, D. Monte Carlo simulation of an ion-dipole mixture as a model of an electrical double layer. *J. Chem. Phys.* **1998**, *109*, 7362-7371.

The effect of drying conditions on mechanical properties of alginate-based films

Krista Lokar¹, Marijan Bajić¹, Uroš Novak^{1*}, Blaž Likozar¹

¹National Institute of Chemistry, Department of Catalysis and Chemical Reaction Engineering, Hajdrihova 19, Slovenia, uros.novak@ki.si

Biopolymers are materials made from renewable ingredients like polysaccharides, proteins and lipids. These biomaterials are known to degrade faster in the environment compared to the non-biodegradable petroleum-based polymers¹. Biopolymer alginate, a copolymer consisting of 1–4 linked β -D-mannuronate (M) and α -L-guluronate (G) units, can be easily collected from the natural resources². For the realistic application of the biodegradable films as a replacement for petroleum-based films, they should have good mechanical and barrier properties. Typically, films are produced using casting method, which requires long drying times³. In this study, the impact of drying conditions on mechanical properties was investigated. Prepared alginate-based films were dried at temperature range between 25 °C and 90 °C and ventilation speed between 40% and 60%. Elongation at break (*EB*) and tensile strength (*TS*) were evaluated. The obtained results have shown that the temperatures below 90 °C had no significant impact on *EB*, while the films prepared at ventilation speed of 60% exhibited higher values than their counterparts prepared at ventilation speed of 40% (Fig. 1-a). In addition, a 2² factorial design model was developed to study the effect of temperature and ventilation speed on the *TS* values of prepared alginate-based films. The results have revealed that *TS* is dependent on both temperature and ventilation speed. The highest *TS* of 46.9 MPa had the film sample prepared at the highest temperature (90 °C) and ventilation speed (60%) (Fig. 1-b).

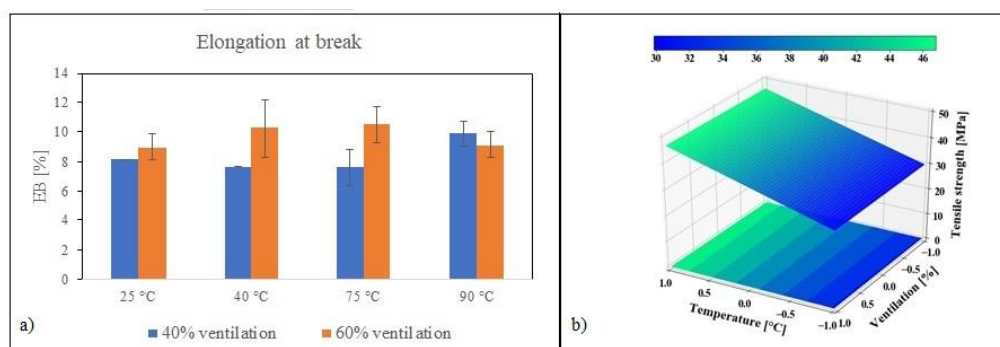


Figure 1: a) Elongation at break measured for alginate-based films prepared at different temperature and ventilation conditions, b) 3D surface plot showing a joint effect of temperature and ventilation speed on *TS* of alginate-based films.

1. Shit, S.C.; Shah, P.M., Review article: Edible polymers: Challenges and opportunities. *Journal of Polymers* **2014**, 427259/1–427259/13.
2. Stephen, A.M.; Phillips, G.O.; Williams, P.A., Food polysaccharides and their applications, 2nd ed.; *CRC Press, Taylor & Francis Group*, 2006.
3. Bagheri, F.; Radi, M.; Amiri, S., Drying conditions highly influence the characteristics of glycerol-plasticized alginate films. *Food Hydrocolloids*, **2018**, 90, 162–171.

Influence of molybdenum-oxides' oxidation state and morphology on furfural hydrodeoxygenation

Aleksa Kojčinović¹, Miha Grilc^{*1}, Blaž Likozar¹

¹ Department of Catalysis and Chemical Reaction Engineering, National Institute of Chemistry, Hajdrihova 19, 1000 Ljubljana, Slovenia

Furfural is a platform chemical derived from lignocellulosic biomass and represents a promising feedstock for sustainable production of biofuels and biochemicals. Due to its high functionalization, it can be converted to a wide array of value-added chemicals by various catalytic processes¹. One of the possible routes is by hydrodeoxygenation (HDO) over molybdenum-oxide catalysts. The activity and selectivity of MoO₃-NiO/Al₂O₃, MoO₂, and three different MoO₃ have been tested in 75 mL batch reactors after 5h at 175 °C and 50 bar H₂ pressure. Despite their relatively low specific surface areas (Table 1) compared to that of alumina-supported molybdenum, various unsupported molybdenum(VI)- and molybdenum(IV)-oxides have shown to be more active for liquid-phase HDO of furfural. Based on their GC-MS analyses (Shimadzu 2010 Ultra) a reaction pathway network has been proposed, suggesting hydrogenation reaction taking place without the catalyst and ring-opening to levulinic acid in presence of the catalyst. Obtained results suggested that there is no strictly defined correlation between the oxidation state and morphology to catalyst's activity, but rather congruence of both is preferred. Highest conversion of furfural (41.8%) and selectivity to levulinate-ethers have been observed for MoO₃ #2 catalyst which although has smallest particle size, still possesses some porosity. Similar conversion (37.0%) has been observed for MoO₂ which yet exhibited greater porosity and much larger particle size. Results presented at the conference will show deeper characterization of textural and structural properties of Mo-based catalysts and their influence on the activity and selectivity during the hydrotreatment of furfural.

Table 6: Pore volumes, particle sizes, and furfural conversions of molybdenum-oxide catalysts.

	MoO ₃ #1	MoO ₃ #2	MoO ₃ #3	MoO ₂	MoO ₃ -NiO/Al ₂ O ₃
V _P (cm ³ g ⁻¹)	0.013	0.002	< 0.001	0.014	0.520
d ₅₀ (μm)	80-100	2-4	10-15	60-80	NA
C _{FUR} (%)	25.7	41.8	27.8	37.0	20.8

V_P – pore volume; d₅₀ – mean particle size; C_{FUR} – conversion of furfural

Acknowledgments: Authors acknowledge financial support by the EU Framework Programme for Research and Innovation Horizon 2020 under Grant agreement no. 814416 (ReaxPro) and the ARRS (Programme P2-0152 and postdoctoral research project Z2-9200).

1. Li, X., Jia, P., Wang, T., Furfural: A Promising Platform Compound for Sustainable Production of C₄ and C₅ Chemicals. *ACS Catal.* **2016**, *6*, 7621-7640

Comparison of organic and ruthenium dyes in dye-sensitized solar cells

Eva Krejan¹, Lev Matoh¹, Urška Lavrenčič Štangar*¹

¹ Faculty of Chemistry and Chemical Technology, University of Ljubljana, Večna pot 113, SI-1000 Ljubljana, Slovenia, urska.lavrencic.stangar@fkk.uni-lj.si

Due to the increasing demand for electric energy, the development tends to seek alternative sources of energy which would substitute the usage of non-renewable energy sources. One of the many options is using dye-sensitized solar cells (DSSC)¹, since these solar cells are relatively cheap and simple to produce.

In this work, the focus was on the influence of the dye on the efficiency of the DSSC² (Fig. 1). The cells were prepared with commercial (ruthenium dye) and organic, natural dyes, which were extracted from fruits and vegetables: pomegranates, blueberries, blackberries, strawberries and beetroot. In addition, we observed the influence of different TiO₂ working electrodes on the efficiency of the DSSC.

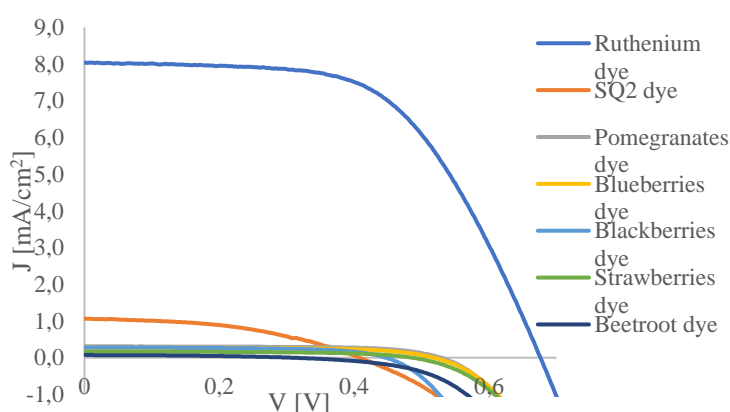


Figure 1: I-V characteristics of DSSC.

Dye	Efficiency [%]
Ruthenium dye	3,17
SQ ₂ dye	0,19
Pomegranates dye	0,11
Blueberries dye	0,09
Blackberries dye	0,08
Strawberries dye	0,05
Beetroot dye	0,01

Table 1: Efficiency of DSSC.

1. Ameta R., Benjamin S., Sharma S., Trivedi M.: *Dye-sensitized solar cells. Chapter 6: Solar energy conversion and storage*. Ameta S. C., Ameta R. (ur.), New York: CRC Press, Taylor & Francis Group, LLC, **2016**, 85–113.
2. Stathatos E., Lianos P., Lavrenčič Štangar U., Orel B.: A high-performance solid-state dye-sensitized photoelectrochemical cell employing a nanocomposite gel electrolyte made by the sol-gel route. *Adv. Mater.*, **2002**, *14*, 354–357.

Isolation and characterization of ANXA11 mutants D40G and dN1-118

Špela Supej¹ and Vera Župunski*¹

¹ Faculty of Chemistry and Chemical Technology, University of Ljubljana, Večna pot 113, SI-1000 Ljubljana, Slovenia, vera.zupunski@fkkt.uni-lj.si, spela.supej@gmail.com

Annexin A11 (ANXA11) is a Ca²⁺-regulated phospholipid-binding protein that belongs to a larger human annexin protein family of 12 members. It is composed of a conserved C-terminal region and a variable N-terminal domain. The ANXA11 N-terminal tail is the longest among 12 and plays an important role in nuclear location and degradation of ANXA11. It is composed of 219 amino acid residues that is rich in tyrosines, glycines and prolines¹. Mutations in the *ANXA11* gene have recently been associated with ALS,² which is a progressive neurodegenerative disorder that selectively impairs upper and lower motor neurons that dominate voluntary muscles³. We aimed to discover the structures of N-terminal mutations in ANXA11 as unstructured N-terminal tail contributes to the protein instability. We used LIC cloning in vector pMCSG7 to prepare N-terminally truncated forms ANXA11^{dS119} and ANXA11^{dN-ter}. To increase stability and solubility, we also prepared fusion of ANXA11^{dS119} with GST on the N-terminal end of annexin A11, which can be easily removed during protein purification using TEV protease. D40G mutant was prepared to characterize an ALS-associated mutation. Recombinant proteins were produced in *E. coli* strain BL21[DE3] pLysS and later isolated using Ni²⁺- or glutathione S-transferase affinity chromatography. The protein variants were further purified for future crystallisation experiments. Analysis based on the crystal structure of ANXA11 is needed to explain the changes of mutated forms in protein interactions and their functions.

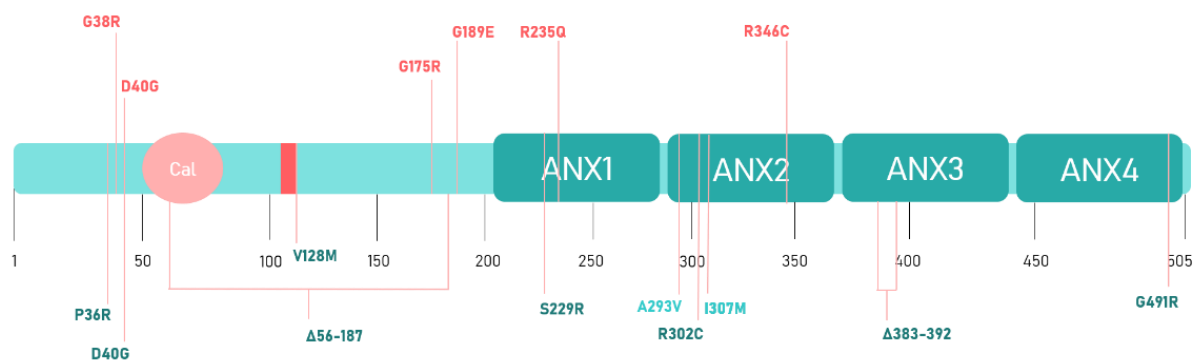


Figure 2: A model of ANXA11 with known mutations.

1. Wang, J.; Guo, C.; Liu, S.; Qi, H.; Yin, Y.; Liang, R.; Sun, M. Z.; Greenaway, F. T. Annexin A11 in Disease. *Clin. Chim. Acta* **2014**, *431*, 164–168.
2. Smith, B. N. et al. Mutations in the Vesicular Trafficking Protein Annexin A11 Are Associated with Amyotrophic Lateral Sclerosis. *Sci. Transl. Med.* **2017**, *9*, 1–16.
3. Kim, H. J.; Taylor, J. P. Lost in Transportation: Nucleocytoplasmic Transport Defects in ALS and Other Neurodegenerative Diseases. *Neuron* **2017**, *96*, 285–297.

Introduction of surface exposed thiol groups on filamentous virus like particles

Marija Srnko^{*, 1, 2}, Andreja Kežar¹, Luka Kavčič¹, Magda Tušek-Žnidarič³ and Marjetka Podobnik¹

¹ Department of Molecular Biology and Nanobiotechnology, National Institute of Chemistry, Hajdrihova ulica 19, SI-1000 Ljubljana, Slovenia, marija.srnko@gmail.com

² Faculty of Chemistry and Chemical Technology, University of Ljubljana, Večna pot 113, SI-1000 Ljubljana, Slovenia

³ Department of Biotechnology and Systems Biology, National Institute of Biology, Večna pot 111, SI-1000 Ljubljana, Slovenia

Virus like particles (VLPs) are assembled from thousands of copies of a coat protein (CP), which lack the viral genetic material and are therefore safer and more applicable for biotechnological use. Because of their modular design, they can be used as a scaffold for immobilization of different biomolecules (dyes, peptides, proteins, enzymes, antibodies, etc.) as well as metal deposition, as nanocontainers for targeted delivery of drugs, imaging agents or dyes, as vaccines or as building blocks for biosensors and complex nanomaterials¹. Potato virus Y (PVY) forms filamentous virions around 740 nm in length and 13 nm in diameter, composed of CPs in left-handed helical symmetry. Expression of CP in bacteria results in self-assembled filamentous VLPs with a unique structure². Based on the 3D structure of PVY VLP that possesses only one cysteine per copy of CP², pointing into the interior of the filament, we prepared mutants with new cysteine side chains exposed on the outer surface of the filament. The ability of these constructs to form filaments was confirmed by transmission electron microscopy, as well as the availability of novel cysteine side-chains for coupling with maleimide conjugated fluorescent dye (Fig. 1).

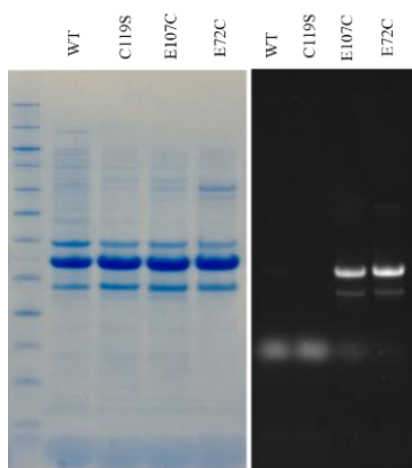


Figure 3: SDS-PAGE gel of control samples (WT, C119S – no cysteine control) and mutants with surface exposed cysteine (E107C, E72C) conjugated with fluorescent dye.

1. Ding, X.; Liu, D.; Booth, G.; Gao, W.; Lu, Y. Virus-Like Particle Engineering: From Rational Design to Versatile Applications. *Biotechnol. J.* **2018**, *13*, 1–7.
2. Kezar, A. *et al.* manuscript just accepted.

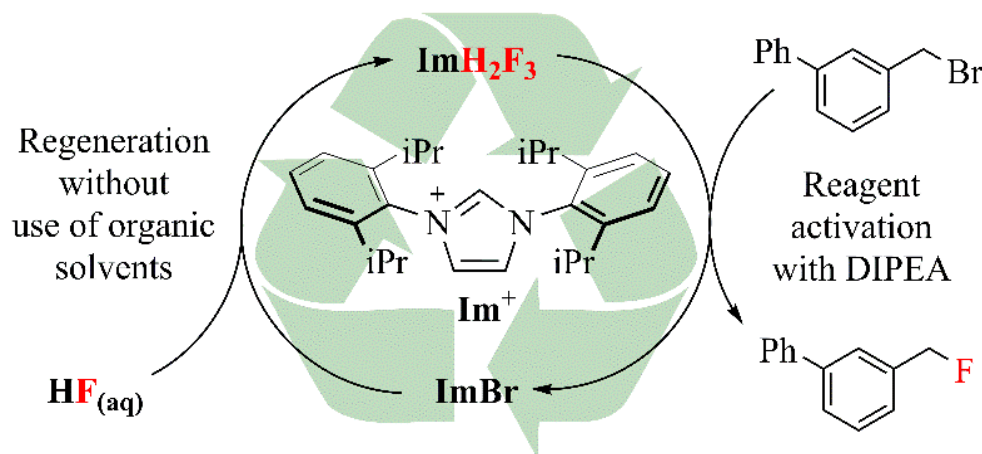
Can we recycle reagents for nucleophilic fluorination

Jan Petrovčič,¹ Blaž Alič,² Gašper Tavčar,² Jernej Iskra*¹

¹ Faculty of Chemistry and Chemical Technology, University of Ljubljana, Večna pot 113, SI-1000 Ljubljana, Slovenia, jerne.j.iskra@fktkt.uni-lj.si

² Jožef Stefan Institute, Jamova cesta 39, SI-1000 Ljubljana, Slovenia

Fluorinated organic compounds are conveniently used in agrochemistry, materials, medicine and diagnostics (e.g. positron emission tomography, PET). It has been estimated that **20 %** of all drugs available on the market contain fluorinated active ingredients¹. Introduction of fluorine atoms increases lipophilicity and metabolic stability of compounds while it decreases their pKa values². Considering the last ten years, the FDA set two new records in 2018. They approved **59** new drugs and **31 %** of them (**18**) contain fluorine atoms. It is therefore imperative to develop new methods and strategies for fluorination of organic compounds. In attempt to find new tools for late-stage nucleophilic fluorination we are investigating properties and reactivity of three new imidazolium fluoride-based reagents³. Our previously conducted research suggests that 1,3-bis(2,6-diisopropylphenyl)imidazolium dihydrogen trifluoride (**ImH₂F₃**) is the most promising candidate. We have successfully activated this reagent with *N,N'*-diisopropylethylamine to fluorinate α -bromoketones, benzylic and aliphatic substrates. Benzyl fluorides were isolated in good to excellent yields. The reagent can also be used for fluorodenitration of activated aromatic compounds, fluorination of acyl and sulfonyl chlorides and deprotection of silyl ethers. We are studying the possibility of regeneration of **ImH₂F₃**.



Scheme 1: Fluorination of 3-phenylbenzyl bromide with **ImH₂F₃** and its regeneration.

1. Champagne, P. A.; Desroches, J.; Hamel, J.-D.; Vandamme, M.; Paquin, J.-F. Monofluorination of Organic Compounds: 10 Years of Innovation. *Chem. Rev.* **2015**, *115*, 9073–9174.
2. Swallow, S. Fluorine in Medicinal Chemistry. *Prog. Med. Chem.* **2015**, *54*, 65–133.
3. Alič, B.; Tavčar, G. Reaction of N-Heterocyclic Carbene (NHC) with Different HF Sources and Ratios – A Free Fluoride Reagent Based on Imidazolium Fluoride. *J. Fluor. Chem.* **2016**, *192*, 141–146.

Effect of M33 nanobody on cell death caused by MLKL protein

Urška Černe,¹ Gregor Gunčar*¹

¹ Faculty of Chemistry and Chemical Technology, University of Ljubljana, Večna pot 113, SI-1000 Ljubljana, Slovenia, gregor.guncar@fkkt.uni-lj.si

The mixed lineage kinase domain-like (MLKL) pseudokinase is an essential molecular component of necroptosis, a form of programmed cell death with morphological characteristics of necrosis. Necroptosis has an important function in many human inflammatory diseases¹. To cause cell death, MLKL needs to oligomerize and translocate to the cell membrane². Nanobodies in fusion with fluorescent proteins are an important tool in tracking and visualization of almost any antigen within the living cell. They can interfere with the function of the target protein by binding the active site of enzymes or other proteins. Nanobodies against proteins involved in inflammation have been developed to modulate immune response³. In our study, we wanted to determine whether M33-mCherry and GFP-MLKLN-154 colocalize in HEK293T cells after transfection with both constructs. Nanobody M33-mCherry recognizes the N-terminal region of MLKL (MLKLN-154). Membrane translocation is crucial for necroptosis, so colocalization might be observed on the plasma membrane. MLKLN-154 localizes in the cytoplasm and cannot induce necroptosis, but mutant D144K, which mimics activated MLKL, causes cell death. We determined the time point when MLKLN-154 D144K is expressed, but cells are still alive and also confirmed the expression of the M33-mCherry fusion protein. However, we could not observe their colocalization. Further on, we wanted to estimate if nanobody M33-mCherry affects cell death caused by MLKLN-154 D144K. There was no difference in cell death level between samples with nanobody and without it, so we concluded that in this case, the nanobody M33-mCherry does not affect cell death.

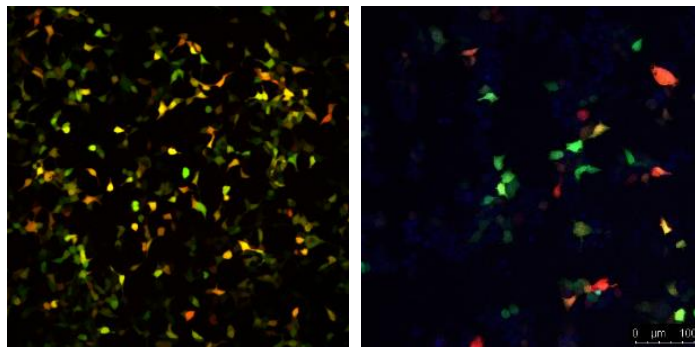


Figure 1: Cells HEK293T expressing M33-mCherry (red) and GFP-MLKLN-154 (green). Yellow cells express both proteins.

1. Pasparakis, M. in Vandenabeele, P., Necroptosis and its role in inflammation. *Nature*, **2015**, *517*, 311-320.
2. Chen, W. X. in sod., Translocation of mixed lineage kinase domain-like protein to plasma membrane leads to necrotic cell death. *Cell research*, **2014**, *24*, 105-21.
3. Rissiek, B., Koch-Nolte, F. in Magnus T., Nanobodies as modulators of inflammation: potential applications for acute brain injury. *Frontiers in Cellular Neuroscience*, **2014**, *8*, 1-7.

Extraction of flavonoids from lignocellulosic biomass as the first valorization step in a biorefinery

Lucija Hladnik¹, Brigita Hočevar¹, Ana Bjelić¹, Edita Jasiukaityte Grojzdek¹, Miha Grilc*¹, Blaž Likozar¹

¹ Department of Catalysis and Chemical Reaction Engineering, National Institute of Chemistry, Hajdrihova 19, SI-1000 Ljubljana, Slovenia, miha.grilc@ki.si

Lignocellulosic (LC) biomass is considered to be a sustainable and low-cost alternative resource that can be converted into fuels and chemicals on a large scale. In order to develop an efficient process, the lignocellulosic biomass needs to be firstly fractionated into its main constituents, e.g. lignin, cellulose, and hemicellulose. Another way of biomass treatment is their extraction to extractives – value added chemicals, due to antioxidant activity and beneficial health effects. Pretreatments and fractionation are essential steps in the overall conversion of LC biomass to biofuel or bio-based products, presented in Figure 1.¹²

Flavonoids are one of the extractives from lignocellulose biomass. They can be used in food and pharmaceutical industry, hence to their antioxidant activity. The multi-step process consists of efficient separation, isolation and purification methods. The main step, extraction, can be performed as a classic (water, organic solvent), green (supercritical, deep eutectic solvents) or physical-mechanical assisted (ultrasound, microwave) extraction.³

On the conference, extraction of flavonoids from biomass will be presented. The main focus will be on extraction mechanism, describing the use of different solvents, reaction conditions and analytical techniques, with the goal to obtain value added chemicals.

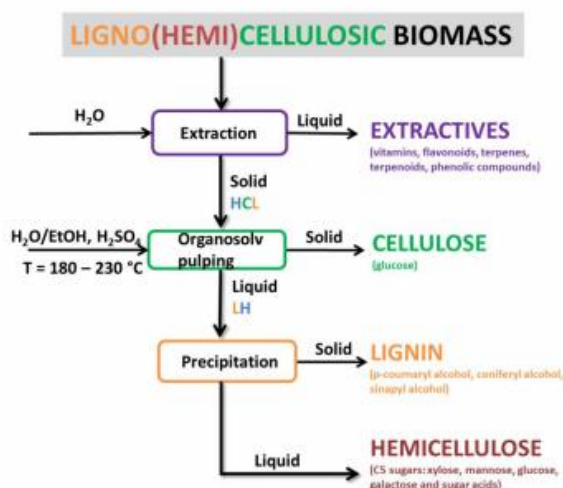


Figure 4: LC biomass fractionation.

- (1) Bjelić, A.; Grilc, M.; Likozar, B. *Chem. Eng. J.* **2018**, *333* (Supplement C), 240–259.
- (2) Mussatto, S. I.; Dragone, G. M. In *Biomass Fractionation Technologies for a Lignocellulosic Feedstock Based Biorefinery*; Mussatto, S. I., Ed.; Elsevier: Amsterdam, **2016**; pp 1–22.
- (3) Sordon, S.; Madej, A.; Popłoński, J.; Bartmańska, A.; Tronina, T.; Brzezowska, E.; Juszczak, P.; Huszcza, E. *J. Agric. Food Chem.* **2016**, *64*, 5525–5530.

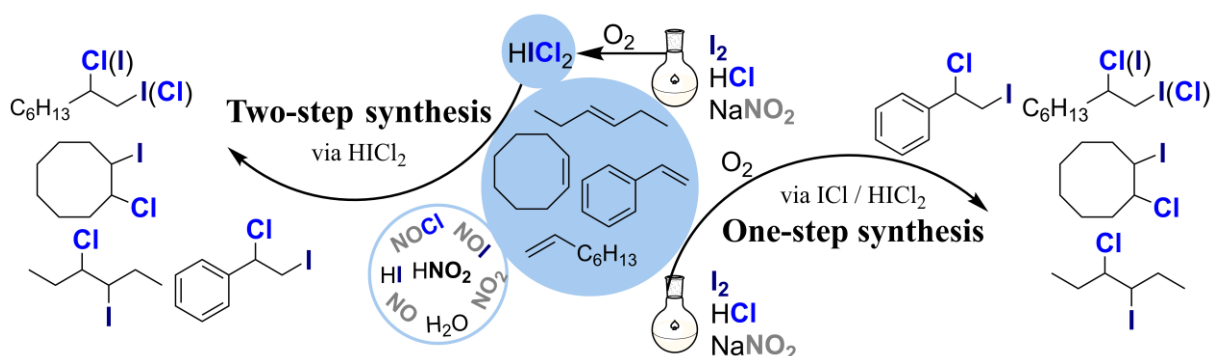
Aerobic iodochlorination of alkenes with iodine and hydrochloric acid catalysed by sodium nitrite

Aleksander Kravos¹, Jernej Iskra^{*,1}

¹ Faculty of Chemistry and Chemical Technology, University of Ljubljana, Večna pot 113, SI-1000 Ljubljana, Slovenia, jernej.iskra@fkkt.uni-lj.si

One of the preferences of modern organic synthesis is to replace conventional halogenation methods with more acceptable approaches. Significant breakthrough towards sustainable syntheses commenced by the introduction of oxidative halogenations using green oxidants¹. In general, oxidative chlorination is possible due to *in-situ* oxidation of HCl to Cl₂ by H₂O₂. Contrary, oxidative iodination is far the biggest challenge to achieve, particularly when using I₂. A possible solution to intensify its reactivity is to *in-situ* generate hypervalent iodine reagent (ICl, HICl₂) either oxidatively by I₂/HCl/H₂O₂² or aerobically by I₂/HCl/NaNO₂/O₂³ reaction system. Both methods were reported to be successful for iodination of arenes in acid-catalysed conditions^{2,3}. Therefore, the capability of the aerobic system to iodochlorinate alkenes was an interesting opportunity for us to research.

In our work we are going to present a general evaluation of the aerobic transformations on several types of alkenes using I₂/HCl/NaNO₂/O₂ system. In contrast to iodination of arenes, where HCl acts as catalyst, in addition reaction to alkenes stoichiometric amount of HCl was found to be essential. We focused the study to achieve high selectivity for iodochlorination of alkenes and understand its mechanism by applying different methods of synthesis (Scheme 1), reaction conditions and stoichiometric coefficients.



Scheme 1: Two- and one-step iodochlorination of alkenes with I₂/HCl/NaNO₂/O₂ aerobic system.

1. Podgoršek, A.; Zupan, M.; Iskra, J., Oxidative Halogenation with “Green” Oxidants: Oxygen and Hydrogen Peroxide. *Angew. Chem. Int. Ed.* **2009**, *48*, 8424-8450.
2. Bedrač, L.; Iskra, J., Iodine(I) reagents in hydrochloric acid-catalyzed oxidative iodination of aromatic compounds by hydrogen peroxide and iodine. *Adv. Synth. Catal.* **2013**, *355*, 1243-1248.
3. Iskra, J.; Murphree, S. S., Rapid aerobic iodination of arenes mediated by hypervalent iodine in fluorinated solvents. *Tetrahedron Lett.* **2017**, *58*, 645-648.

Biochar from beechwood: Preparation and characterization

Lucija Belingar¹, Špela Kapš¹, Matic Grojzdek^{*1}, Barbara Novosel¹, Janvit Golob¹,
Andreja Žgajnar Gotvajn¹

¹ University of Ljubljana, Faculty of Chemistry and Chemical Technology, Večna pot 113, SI-1000 Ljubljana, Slovenia, matic.grojzdek@fkkt.uni-lj.si

Biochar is a special kind of charcoal, which is obtained through pyrolysis, i.e. by thermal treatment of biomass in the absence of oxygen. It is mainly used in agriculture to increase soil fertility. Charcoal is classified as biochar when it meets the European Biochar Certificate¹ parameters that determine biochar suitability to be applied to the soil. The most important quality parameters include specific surface area, fixed carbon content and water-holding capacity. On the other hand, the parameters such as contents of heavy metals, polycyclic aromatic hydrocarbons and polychlorinated biphenyls are considered negative parameters.

In presented study biochar was prepared from 1 cm³ beech wood cubes. The pyrolysis was carried out in the thermal analysis apparatus at the heating rate of 20 K/min. The temperatures of pyrolysis were varied in the range of 450 - 800 °C and the time of isothermal stage was set constant (3 h). The pyrolysed samples were characterized by two methods. The first method² was carried out in a simultaneous thermal apparatus and was used to determine the biochar composition (the content of moisture, volatile components, fixed carbon (C-fix) and ash). The second method was accomplished to determine the specific surface area based on Brunauer-Emmett-Teller (BET) theory³.

Higher temperature of pyrolysis resulted in lower yield of obtained biochar, due to the mass loss at the expense of decomposition and evaporation of the volatile components (Table 1). The characterization of biochar composition showed the increase in C-fix content and decrease in volatile components content with higher temperature of pyrolysis. By analysing the specific surface area it was found that values increase with increasing temperature and reached the maximum value at 700 °C. Higher temperatures decrease the values of specific surface area. According to the results, the optimal temperature of pyrolysis for biochar preparation is 700°C resulting in biochar rich in C-fix content with the maximal specific surface area.

Table 7: The yield of biochar, C-fix content and specific surface in relation to the temperature.

Pyrolysis temperature [°C]	450	500	600	700	800
Yield of biochar [wt %, dry mass]	25.9	24.6	23.3	21.8	21.6
C-fix content [wt %, dry mass]	80.8	82.2	88.6	92.0	93.5
Specific surface area [m ² /g]	59.9	206.9	220.8	270.0	27.2

1. European Biochar certificate <http://www.european-biochar.org/en> (accessed 18. 6. 2019).
2. SIST-TP CEN/TR 15716:2008 Solid recovered fuels – Determination of combustion behaviour
3. ISO 9277:2010(E) Determination of specific surface area of solids by gas adsorption – BET method

Chitosan-based films with incorporated natural extracts

Ana Oberlintner¹, Marijan Bajić*¹, Uroš Novak¹, Blaž Likozar¹

¹ Department of Catalysis and Chemical Reaction engineering, National Institute of Chemistry, Hajdrihova 19, 1000 Ljubljana, Slovenia, marijan.bajic@ki.si

Chitosan-based films with separately incorporated natural extracts obtained from oak (*Quercus robur*), hops (*Humulus lupulus*), and brown algae (*Laminaria hyperborea*) were evaluated and mutually compared regarding structural, physicochemical, and antimicrobial properties¹. Processing of chitosan and extracted substances led to the blended films with a diverse physical appearance and physicochemical properties². Starting from the film containing oak extract and ending with the film containing algal extract, blended films shown ascending trend in moisture content (21.5% – 28.3%), total soluble matter (23.8% – 28.9%), and elongation at break (14.0% – 31.0%) as well as descending trend in tensile strength (12.7 MPa – 5.5 MPa), Young's modulus (230.8 MPa – 19.4 MPa), and total phenolic content (9.1 mg_{GAE} g_{film}⁻¹ – 1.0 mg_{GAE} g_{film}⁻¹). The films with oak and hop extracts had improved optical properties reflected in the ability to completely block the light transmittance at the wavelengths below ~330 nm. Moreover, the same films exhibited the appearance of inhibition zones implying the antimicrobial activity against *Bacillus subtilis*. Based on the results of this study, it can be concluded that chitosan-based films with incorporated oak extract have high potential to be used as food packaging³.

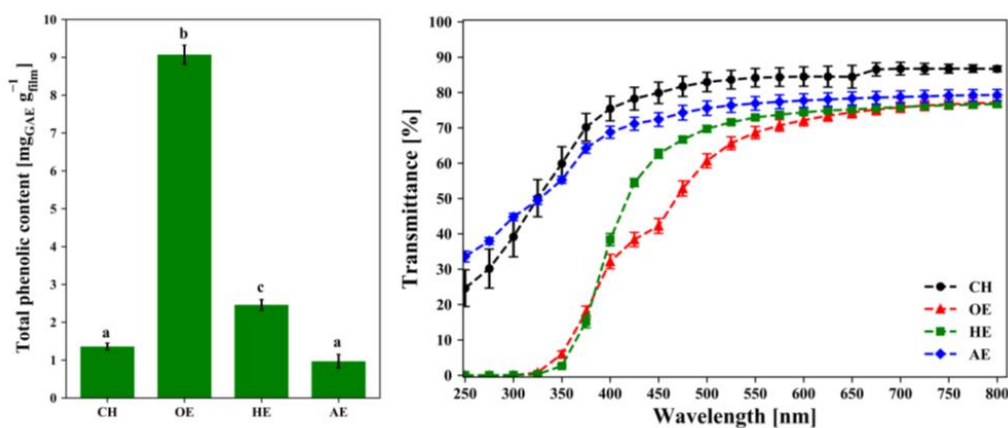


Figure 1: Total phenolic content in chitosan-based films (left) and the light transmittance of chitosan-based films in the UV-Vis light region (right).

1. Bajić, M.; Jalšovec, H.; Travan, A.; Novak, U.; Likozar, B., Chitosan-Based Films with Incorporated Supercritical CO₂ Hop Extract: Structural, Physicochemical, and Antibacterial Properties. *Carbohydr. Polym.* **2019**, *219*, 261–268.
2. Salgado, P. R.; Ortiz, C. M.; Musso, Y. S.; Giorgio, L. Di; Mauri, A. N., Edible Films and Coatings Containing Bioactives. *Curr. Opin. Food Sci.* **2015**, *5*, 586-592.
3. Van Den Broek, L. A. M.; Knoop, R. J. I.; Kappen, F. H. J.; Boeriu, C. G., Chitosan Films and Blends for Packaging Material. *Carbohydr. Polym.* **2015**, *116*, 237–242.

The influence of buffer identity on the hydrodynamic radius and zeta-potential of hen egg white lysozyme molecule

Matej Jaklin,^{*,1} Barbara Hribar-Lee¹

¹ Faculty of Chemistry and Chemical Technology, University of Ljubljana, Večna pot 113, SI-1000 Ljubljana, Slovenia, mj2544@student.uni-lj.si

Hen egg white lysozyme (HEWL) is a protein for which its structure, stability, and folding have been extensively studied under various conditions. HEWL consists of a single chain with 129 amino acid residues. It contains five alpha helical regions and five regions containing beta sheets (Figure 1). Its net surface charge is +18 at pH 3 and below, +8 at pH 4.5, and +7 at pH 7 and above¹.

The pH of the protein is maintained by an appropriate buffer. Only in the last couple of years it has been established that the role buffers is much broader than that; the buffer has an influence on the stability of the protein as well²

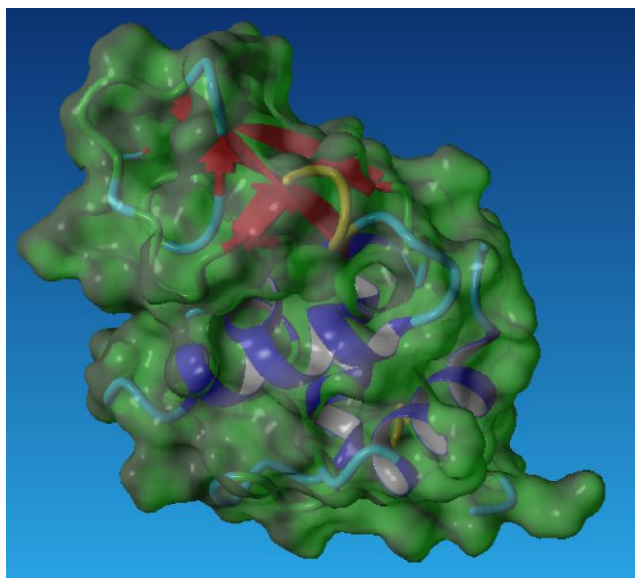


Figure 1: Structure and surface of the HEWL molecule.

In this work we have more closely examined the role of buffers on the size and surface charge (zeta-potential) of HEWL molecules at different pH and in different buffers. The results suggest that, as previously observed, the size, as well as the zeta potential of the protein depend on the buffer used, in agreement with the idea of binding the buffer molecules to the protein surface.

1. Brudar, S.; Hribar-Lee, B., The Role of Buffers in Wild-Type HEWL Amyloid Fibril Formation Mechanism. *Biomolecules* **2019**, *9*, 65.
2. Salis, A.; Monduzzi, M., Not only pH. Specific buffer effects in biological systems. *Curr. Opin. Colloid Interface Sci.* **2016**, *23*, 1–9.

Synthesis of stable diazonium salts

Ana Siljanovska,¹ Mateja Mihelač,¹ Martin Gazvoda,¹ Janez Košmrlj*,¹

¹ Faculty of Chemistry and Chemical Technology, University of Ljubljana, Večna pot 113, SI 1000 Ljubljana, Slovenia

Aromatic diazonium salts are important building blocks in organic chemistry and industry.¹ Recently, these compounds have been employed in palladium catalyzed C–C and C–Het coupling reactions, where their “superelectrophilicity” is used as an advantage over aryl halides.² Nitrogen coupling reactions result in the formation of triazenes, which are well known for antitubercular³ and antibacterial properties.⁴ An important industrial use of diazonium salts is the synthesis of azo dyes and pigments.⁵

Known for their high reactivity and instability, they are rarely isolated, but rather generated *in situ*. Recently, Filimonov et al. reported the synthesis of stable diazonium *p*-toluenesulfonates by employing polymer-based nitrosation agent,⁵ whereas Qiu et al. described the synthesis of stable diazonium 1,5-naphthalenedisulfonates.⁶



Scheme 1: Preparation of stable diazonium *p*-toluenesulfonates.

Herein, we report a novel, efficient and simple green procedure to diazonium *p*-toluenesulfonates (Scheme 1). The products are bench-stable over a longer period of time.

1. Mo, F.; Dong, G.; Zhang, Y.; Wang, J.: Recent applications of arene diazonium salts in organic synthesis. *Org. Biomol. Chem.* **2013**, *11*, 1582–1593.
2. Oger, N.; d’Halluin, M.; Le Grogneac, E.; Felpin, F.-X.: Using aryl diazonium salts in palladium-catalyzed reactions under safer conditions. *Org. Process Res. Dev.* **2014**, *18*, 1786–1801.
3. Torfs, E.; Vajs, J.; Bidart de Macedo, M.; Cools, F.; Vanhoutte, B.; Gorbanev, Y.; Bogaerts, A.; Verschaeve, L.; Caljon, G.; Maes, L.; Delputte, P.; Cos, P.; Košmrlj, J.; Cappoen, D.: Synthesis and in vitro investigation of halogenated 1,3-bis(4-nitrophenyl)triazene salts as antitubercular compounds. *Chem. Biol. Drug Des.* **2018**, *91*, 631–640.
4. Vajs, J.; Proud, C.; Brozovic, A.; Gazvoda, M.; Lloyd, A.; Roper, D. I.; Osmak, M.; Košmrlj, J.; Dowson, C. G.: Diaryltriazenes as antibacterial agents against methicillin resistant *Staphylococcus aureus* (MRSA) and *Mycobacterium smegmatis*. *Eur. J. Med. Chem.* **2017**, *127*, 223–234.
5. Qiu, J.; Tang, B.; Ju, B.; Xu, Y.; Zhang, S.: Stable diazonium salts of weakly basic amines—Convenient reagents for synthesis of disperse azo dyes. *Dyes Pigm.* **2017**, *136*, 63–69.
6. Filimonov, V. D. et al: Unusually stable, versatile, and pure arenediazonium tosylates: Their preparation, structures, and synthetic applicability. *Org. Lett.* **2008**, *10*, 3961–3964.

Characterisation of human retrotransposon L1 ORF1p clusters

Anamarija Habič¹, Vera Župunski*¹

¹ Faculty of Chemistry and Chemical Technology, University of Ljubljana, Večna pot 113, SI-1000 Ljubljana, Slovenia, vera.zupunski@fkkt.uni-lj.si

Long interspersed nuclear element 1 (L1) is the dominant and the only active autonomous retrotransposon in human, which has played an important role in genome evolution¹. Bicistronic L1 mRNA is translated into two proteins, ORF1p and ORF2p². Along with L1 mRNA they form ribonucleoproteins, which further interact with a series of other host proteins and form clusters³. The critical role of ORF1p in the process of L1 retrotransposition remains elusive. We aimed in the present study to determine ORF1p binding partners to better characterise ORF1p clusters. Immunocytochemical characterisation of ORF1p localisation in cell lines 2102Ep, nTERA2, HeLa and HEK293T revealed that endogenous as well as overexpressed ORF1p predominantly localises within cytoplasmic clusters and is only rarely found in nucleus. In some cells, a diffuse cytoplasmic signal is detected. In cell line 2102Ep exposed to sodium arsenite, which causes oxidative stress, endogenous ORF1p partially reorganizes into larger aggregates. To identify proteins in vicinity of the endogenous ORF1p in (un)stressed 2102Ep, we used a novel proximity-based labelling method called biotinylation by antibody recognition (Fig. 1). Identified binding partners will help characterise ORF1p clusters and, conceivably, enable a better understanding of the indispensable role of the protein in L1 retrotransposition.

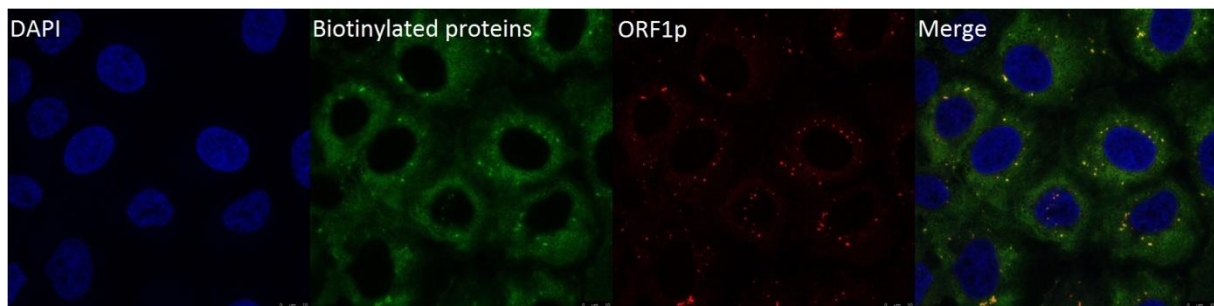


Figure 1: Immunocytochemical confirmation of colocalisation of ORF1p and biotinylated proteins after the BAR procedure in unstressed cell line 2102Ep.

1. Kazazian, H. H., Mobile elements: drivers of genome evolution. *Science* **2004**, *303*, 1626-32.
2. Khazina, E.; Truffault, V.; Büttner, R.; Schmidt, S.; Coles, M.; Weichenrieder, O., Trimeric structure and flexibility of the L1ORF1 protein in human L1 retrotransposition. *Nat Struct Mol Biol* **2011**, *18*, 1006-14.
3. Taylor, M. S.; Altukhov, I.; Molloy, K. R.; Mita, P.; Jiang, H.; Adney, E. M.; Wudzinska, A.; Badri, S.; Ischenko, D.; Eng, G.; Burns, K. H.; Fenyö, D.; Chait, B. T.; Alexeev, D.; Rout, M. P.; Boeke, J. D.; LaCava, J., Dissection of affinity captured LINE-1 macromolecular complexes. *Elife* **2018**, *7*.

Variation within ultraconserved elements in the human genome

Anamarija Habič,^{1,2} Tanja Kunej*¹

¹ Department of Animal Science, Biotechnical Faculty, University of Ljubljana, Groblje 3, SI-1230 Domžale, Slovenia, tanja.kunej@bf.uni-lj.si

² Faculty of Chemistry and Chemical Technology, University of Ljubljana, Večna pot 113, SI-1000 Ljubljana, Slovenia

13,736 ultraconserved elements (UCEs) of ≥ 100 bp in length are identical in at least three of five placental mammals (human, dog, cow, mouse, and rat)¹. Extreme conservation of these regions suggests that they are vitally important, but their roles still remain poorly understood. Several studies reported polymorphisms within UCEs^{2,3}. We aimed in our study to examine the extent of variation within UCEs and to check whether UCEs' polymorphisms have previously been associated with diseases or phenotypic traits. Firstly, we remapped genomic locations of 2189 UCEs ≥ 200 bp in length to the latest human genome assembly. Using the BioMart data mining tool, we identified 29983 dbSNP polymorphisms within analyzed UCEs (i.e. one polymorphism per 21 bps) (Fig. 1). However, these polymorphisms occur rarely – less than 6% exhibit minor allele frequencies of $> 0,01$. Among 29983 identified polymorphisms, 112 have annotated phenotype associations in the Ensembl genome browser. By literature review, we confirmed associations of 37 (out of the 112) polymorphisms with 25 phenotypic traits and diseases, including for example different types of muscular dystrophies, amyotrophic lateral sclerosis, some eye related diseases and cancer. Our results serve as a basis for further investigation of UCEs' functions.

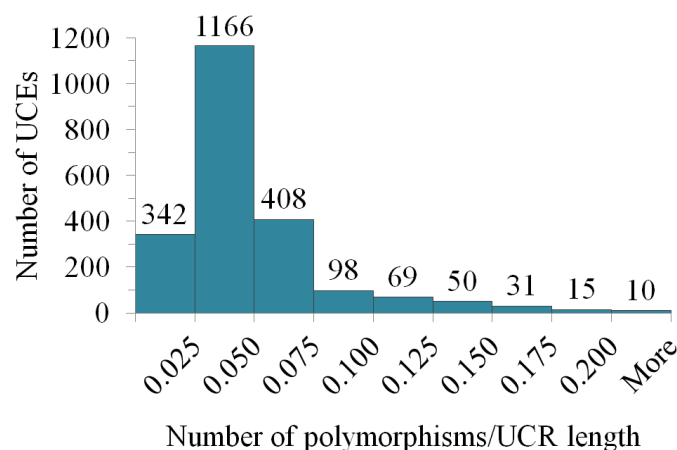


Figure 1: Distribution of UCEs according to polymorphisms density within them.

1. Stephen, S.; Pheasant, M.; Makunin, I. V.; Mattick, J. S., Large-scale appearance of ultraconserved elements in tetrapod genomes and slowdown of the molecular clock. *Molecular Biology and Evolution* **2008**, *25*, 402-408.
2. Bejerano, G.; Pheasant, M.; Makunin, I.; Stephen, S.; Kent, W. J.; Mattick, J. S.; Haussler, D., Ultraconserved elements in the human genome. *Science* **2004**, *304*, 1321-5.
3. Silla, T.; Kepp, K.; Tai, E. S.; Goh, L.; Davila, S.; Catela Ivkovic, T.; Calin, G. A.; Voorhoeve, P. M., Allele frequencies of variants in ultra conserved elements identify selective pressure on transcription factor binding. *PLoS One* **2014**, *9*, e110692.

Natural variants of human CYP51: a molecular dynamics study

Neli Sedej*¹, Franci Merzel², Tadeja Režen³, Damjana Rozman³

¹ Faculty of Chemistry and Chemical Technology, University of Ljubljana, Večna pot 113, SI-1000 Ljubljana, Slovenia, neli.sedej@gmail.com

² National Institute of Chemistry, Theory department, Hajdrihova 19, SI-1000 Ljubljana, Slovenia

³ Faculty of Medicine, Centre for Functional Genomics and Bio-Chips, Institute of Biochemistry, University of Ljubljana, Vrazov trg 2, SI-1000 Ljubljana, Slovenia

Sterol biosynthesis is an essential process in most eukaryotic organisms. Lanosterol 14- α -demethylase (CYP51) is one of the enzymes involved in this complex pathway. Homozygous deletion of CYP51 in mice has been shown to cause embryonal lethality and it is predicted that at least one functional allele is necessary for normal human development¹. Human CYP51 is highly conserved, however some rare variants have been associated with damaging phenotypes such as pediatric cataract, neonatal liver failure and premature labor. Furthermore, several mutations found in human population have been shown to result in dysfunctional protein *in vitro*². In present study, we selected three natural missense mutations (R277C, R277L and R431H), which have been previously shown as possibly damaging by *in vitro* expression² or genetic studies³. We investigated the effect of amino acid substitutions by molecular dynamics simulations. Simulations were performed at three different temperatures to assess the effect of mutations on protein stability. We show that mutation R277L causes significant destabilization, compared to wild type. Destabilization caused by a similar mutation R277C was less dramatic and no significant destabilization was observed by R431H. Our study suggests that mutation R277L yields less stable protein, which is less likely to fold and function correctly.

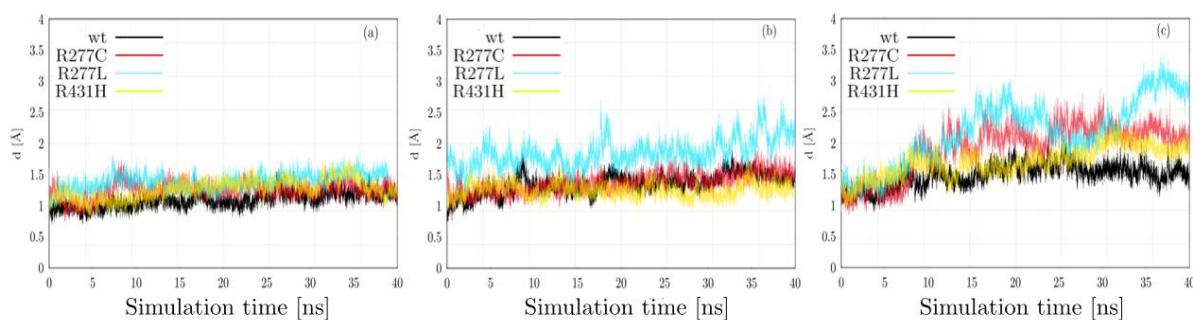


Figure 1: RMSD of C α atoms of wild-type and mutations during simulation at a) 300 K b) 330 K and c) 350 K.

1. Keber, R. et al. Mouse Knockout of the Cholesterogenic Cytochrome P450 Lanosterol 14 α -Demethylase (Cyp51) Resembles Antley-Bixler Syndrome. *J. Biol. Chem.* **2011**, 286, 29086–29097.
2. Režen, T. et al. Evaluation of Selected CYP51A1 Polymorphisms in View of Interactions with Substrate and Redox Partner. *Front. Pharmacol.* **2017**, 8, 417.
3. Aldahmesh, M. A. et al. Genomic Analysis of Pediatric Cataract in Saudi Arabia Reveals Novel Candidate Disease Genes. *Genet. Med.*, **2012**, 14, 955-962.

Designing hydrogels for controlled drug delivery

Tilen Kopač¹, Aleš Ručigaj¹, Matjaž Krajnc*¹

¹ Faculty of Chemistry and Chemical Technology, University of Ljubljana, Večna pot 113, SI-1000 Ljubljana, Slovenia, Matjaz.Krajnc@fkkt.uni-lj.si

Hydrogels have a great potential to be used in controlled drug release, since the high porosity of hydrogels makes the loading and releasing of the active substance easier¹. In present work we used modified natural biopolymers, sodium alginate (ALG) and TEMPO modified nanocellulose (TOCNF). Calcium chloride was used as a crosslinker, as calcium ions connect carboxyl functional groups of studied biopolymers. The investigations of composition and structure related rheological properties have been carried on. The rheological properties of hydrogels are an important factor in their ultimate biomedical application (mixing, injection), and provide an estimate to the theoretical mesh size. We used Maxwell-Wiechert model to describe the experimental data from oscillatory tests (frequency sweep). The sum of the Maxwell elastic elements and equilibrium modulus leads to the determination of the shear modulus². Shear modulus is used in Flory theory equation to calculate the average size of pores in hydrogels matrix. As shown in Fig. 1, higher crosslinker concentration reduces size of pores. It is evident that the alginate has smaller pores than nanocellulose. The mesh size has a significant impact on the rate of the drug release. With the mentioned work, it is easier to design suitable hydrogels according to the characteristics of the drug and the desired application³.

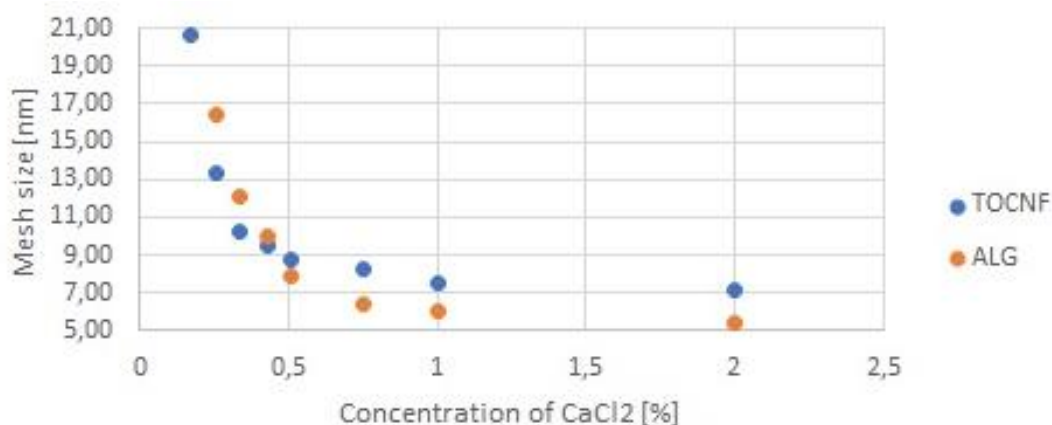


Figure 1: Effect of crosslinking agent (Ca^{2+}) concentration on the mesh size of hydrogels.

1. Kirchoff, S.; Abrami, M.; Messmann, V.; Hammer, N.; Goepferich, A. M.; Grassi, M.; Brandl, F. P. Diels–Alder hydrogels for controlled antibody release: correlation between mesh size and release rate. *Mol. Pharmaceutics*. **2015**, *12*, 3358-3368.
2. Lapasin, R.; Abrami, M.; Grassi, M.; Šebenik, U. Rheology of Laponite-scleroglucan hydrogels. *Carbohydr. Polym.* **2017**, *168*, 290-300.
3. Wong, R.; Ashton, M.; Dodou, K. Effect of crosslinking agent concentration on the properties of unmedicated hydrogels. *Pharmaceutics*. **2015**, *7*, 305-319.

Dyeing cotton with dyes obtained from invasive alien plants

Katja Brenčič, Marija Gorjanc*

Faculty of Natural Sciences and Engineering, department of textiles, graphic arts and design,
Snežniška ulica 5, SI-1000 Ljubljana, marija.gorjanc@ntf.uni-lj.si

Dyeing textiles using dyes extracted from a plant material is an ancient method of finishing textiles. Alien plant species have the tendency to spread to the degree that they cause damage predominantly to the economy. To take advantage of the potential offered by alien plant species, one of the objectives of the European project APPLAUSE is to use them for dye extraction and textile dyeing.

In this research the dyeing of cotton fabric with dyes extracted from the Japanese knotweed rhizome, Goldenrod flowers and Staghorn sumac¹ fruits was studied. The dye extracts were prepared at different pH values (neutral, acidic and alkaline) and in water of different hardness (soft, hard). Untreated cotton fabrics and fabrics pre-treated (mordanted) with copper and ferrous sulphate were dyed with prepared extracts.² The colour of dyed fabrics was measured using a reflectance spectrophotometer. Additionally, the samples were scanned. The results showed that all three plant species produce dyes that have affinity towards cellulosic textiles. With the Goldenrod dye, the yellow coloration of textiles is acquired, while the Staghorn sumac predominantly yields pink and violet.³ The dyeing with the dye obtained from the Japanese knotweed rhizome enables a wider spectrum of colours – from yellows, pinks, bordeaux to almost black. The hardness of water does not change the colour hue; however, it does influence the colour's lightness.

EXTRACTION TREATMET	pH					
	NEUTRAL		ALCAL		ACID	
	Hard H ₂ O	Soft H ₂ O	Hard H ₂ O	Soft H ₂ O	Hard H ₂ O	Soft H ₂ O
Mordant Fe						
Mordant Cu						
Without						

Scheme 1: Presentation of cotton samples dyed with Japanese knotweed rhizome.

1. Wang, S., Zhu, F. Chemical composition and biological activity of Staghorn sumac (*Rhus typhina*). *Food chemistry*, **2017**, 237, 431-443
2. Topič, T., Gorjanc, M., Kert, M. The influence of the treatment process on the dyeability of cotton fabric using goldenrod dye. *Tekstilec*, **2018**, 61, 192-200,
3. Leitner, P., Fitz-Binder, C., Mahmud-Ali, A., Bechtold, T. Production of a concentrated natural dye from Canadian Goldenrod (*Solidago canadensis*) extracts. *Dyes and pigments*, **2012**, 93, 1416-1421.

In situ phytosynthesis of silver nanoparticles on cellulose fibers with *Fallopia japonica* extract

Nina Čuk,¹ Martin Šala,² Marija Gorjanc*¹

¹ Faculty of Natural Sciences and Engineering, University of Ljubljana, Aškerčeva 12, SI-1000 Ljubljana, Slovenia, marija.gorjanc@ntf.uni-lj.si

² National Institute of Chemistry, Hajdrihova 19, SI-1000 Ljubljana, Slovenia

Silver nanoparticles (Ag-NPs) have been widely used for their unique properties¹. Phytosynthesis is one of the bottom-up synthesis where Ag-NPs are built up using plant extracts as reducing agent instead of toxic ones, i.e. sodium borohydride^{2,3}.

The aim of our research was to evaluate the capability of invasive alien plant species (IAPS) *Fallopia japonica* rhizome water extract as a reducing agent in phytosynthesis of Ag-NPs directly on cellulose fibers (*in situ*). The properties of cotton fabrics treated in extract alone and where *in situ* synthesis occurred are presented in Table 1. Besides newly formed nanoparticles (confirmed by scanning electron microscopy), in size 179 nm and silver content of 2412 mg/kg, the samples have higher color strength values, excellent protection against UV radiation and antibacterial properties against Gram positive (*Staphylococcus aureus*) and Gram negative (*Escherichia coli*) bacteria.

Table 1: Properties of cotton fabrics according to treatment

Treatment of cotton	Color strength (K/S values)	Size of nanoparticles (nm)	Silver (Ag) content (mg/kg)	UV protection factor	Antibacterial effectiveness as a bacterial reduction (%)	
					<i>Staphylococcus aureus</i>	<i>Escherichia coli</i>
Only extract	0.450	No nanoparticles detected	0	27.50	No reduction	No reduction
Ag-NP synthesis	2.687	179	2412	164.43	98	100

The research confirmed a great potential of *Fallopia japonica* rhizome water extract as a reducing agent in green synthesis of Ag-NPs directly on material for achieving multiprotective cellulose fibers.

1. Prabhu, S.; Poulouse, E. K., Silver nanoparticles: mechanism of antimicrobial action, synthesis, medical applications, and toxicity effects. *Int. Nano Lett.* **2012**, 2:32.
2. Khan, I.; Saeed, K.; Khan, I., Nanoparticles: Properties, applications and toxicities. *Arab. J. Chem.* **2017**, *in press*.
3. Chandrasekhara Reddy, M.; Sri Rama Murthy, K.; Srilakshmi, A.; Sambasiva Rao, K. R. S.; Pullaiah, T., Phytosynthesis of eco-friendly silver nanoparticles and biological applications – A novel concept in nanobiotechnology. *Afr. J. Biotechnol.* **2015**, 14, 222-247.

Calcium binding properties of α -actinin

David Titovšek,¹ Ajda Cafun,¹ Andrej Ivanovski,¹ Sara Drmota Prebil,^{*,1} Miha Pavšič,^{*,1}

¹ Faculty of Chemistry and Chemical Technology, University of Ljubljana, Večna pot 113, SI-1000 Ljubljana, Slovenia, sara.drmotaprebil@fkkt.uni-lj.si, miha.pavsic@fkkt.uni-lj.si

α -Actinin is a major actin filament cross-linking protein. It forms an anti-parallel dimer where one actin-binding domain is at each end (Fig. 1A), and links actin fibers in an anti-parallel orientation. The family of α -actinins can be divided into two classes: calcium insensitive muscle isoforms (2 and 3) and calcium sensitive non-muscle isoforms (1 and 4)¹.

We have focused on the calcium binding properties of non-muscle isoforms. In the first part, we prepared several constructs of α -actinins 1 and 4 (including a half-dimer; Fig. 1B) to determine their calcium binding affinities and other thermodynamic properties using isothermal titration calorimetry (ITC) (Table 1). Based on research on calmodulin-like domain (CaMD) of α -actinin-1, the model of regulation of actin binding activity of α -actinin-1 was proposed where CaMD in Ca²⁺-bound (holo) form interacts with the neck region connecting the actin-binding domain to the central rod region². However, due to limitations of NMR the structural changes have not yet been determined for the full-length protein. To tackle this problem, we set on to prepare segmentally labelled protein using ligation method, also called *protein trans-splicing*, where two separately expressed fragments are ligated by trans-splicing activity of split inteins³.



Figure 1: Schematic representation of full-length α -actinin (A) and half-dimer (B).

ABD – actin binding domain, SR – spectrin repeat, EF – EF-hand, NECK – NECK peptide.

Table 8: Calcium binding affinities, thermodynamic parameters and number of binding sites of α -actinin-1 constructs (CaMD – calmodulin-like domain, hd – half dimer of α -actinin).

	K_d [μ M]	N	ΔH [kcal/mol]	$-T\Delta S$ [kcal/mol]	ΔG [kcal/mol]
CaMD	127 ± 5	$1,03 \pm 0,01$	$2,22 \pm 0,03$	$-7,5$	$-5,3$
hd	$20,9 \pm 6,9$	$0,75 \pm 0,05$	$0,75 \pm 0,08$	$-7,1$	$-6,4$

1. Sjöblom, B.; Salmazo, A.; Djinović-Carugo, K., α -actinin structure and regulation. *Cell. Mol. Life Sci.* **2008**, *65*, 2688-2701.
2. Drmota Prebil, S.; Slapšak, U.; Pavšič, M.; Ilc, G.; Puž, V.; de Almeida Riberiro, E.; Hartl, A. M.; Backman, L.; Plavec, J.; Lenarčič, B.; Djinović-Carugo, K., Structure and calcium-binding studies of calmodulin-like domain of human non-muscle α -actinin-1. *Sci. Rep.* **2016**, *6*, 27383.
3. Mouna, M.; Sesilja Aranko, A.; Raulinaitis, V.; Iwai, H., Segmental isotopic labelling of multi-domain and fusion proteins by protein trans-splicing *in vivo* and *in vitro*. *Nat. Protoc.* **2010**, *5*, 574-586.

Intracellular responses of the model alga, Chlamydomonas reinhardtii, to oxidative and salt stress

Anže Jenko¹, Nika Goršek¹, Vida Štrancar¹, Marina Klemenčič*,¹

¹ Faculty of Chemistry and Chemical Technology, University of Ljubljana, Večna pot 113, SI-1000 Ljubljana, Slovenia, marina.klemencic@fkkt.uni-lj.si

Programmed cell death is crucial for plant development and for the interactions between plants and the environment. Plants know two ways of dying; vacuolar and necrotic. The vacuolar cell death plays a role in development and senescence. It manifests in various morphological features, for example, increased volume of lytic vacuoles at the cost of decreased volume of cytoplasm, DNA laddering and activation of different proteases. Necrosis is usually triggered by abiotic stress. It is identified by mitochondrial swelling and DNA shearing^{1,2}.

Interested in phenotype of programmed cellular death in unicellular green algae, *Chlamydomonas reinhardtii*, we treated its cell culture with two abiotic stressors, hydrogen peroxide and sodium chloride at different concentrations and time intervals. Upon both stressors most cells in the cultures died in 3-hour time. We also noticed a distinct time-dependent pattern of DNA in cultures, treated with hydrogen peroxide, also known as DNA laddering, which was absent in samples that were treated with sodium chloride (Figure 1). Protease activity of *C. reinhardtii* lysates against synthetic substrate Z-FR-AMC was shown to be increased after treating the cultures with 5 mM H₂O₂, but not when cultures were treated with 250 mM NaCl.

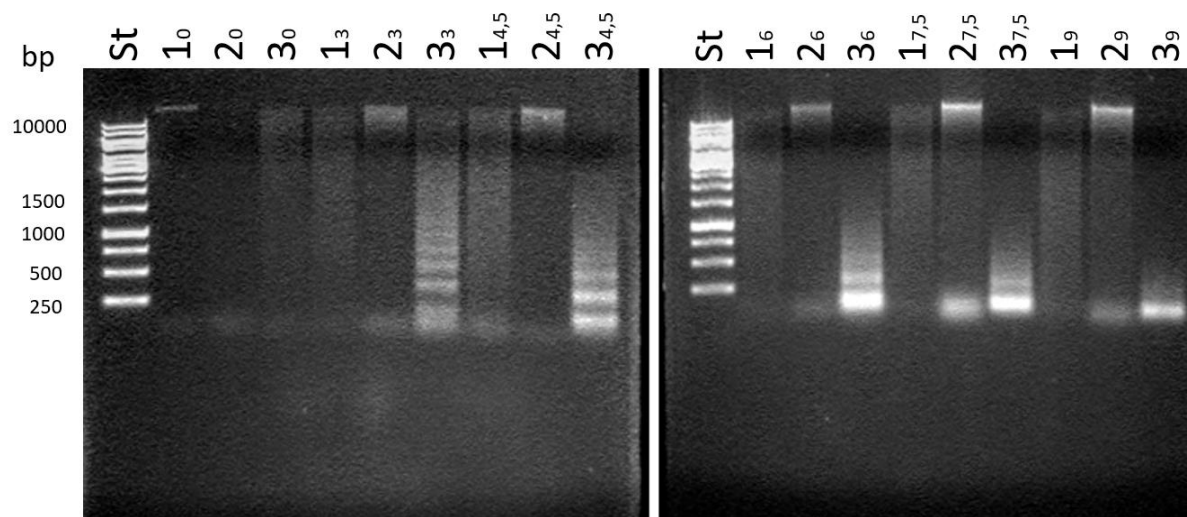


Figure 5: Effect on genomic DNA upon varying time exposure to 250 mM NaCl and 5 mM H₂O₂. With number 1 are marked lanes of genomic DNA of the untreated cells, whereas those from NaCl and H₂O₂ treated cells are marked with 2 and 3 respectively. Smaller numbers next to them indicate time of stressor treatment in hours.

1. Salvesen, G. S., Hempel, A. & Coll, N. S. Protease signaling in animal and plant-regulated cell death. *FEBS J.* **283**, 2577–2598 (2016).
2. Van Doorn, W. G. *et al.* Morphological classification of plant cell deaths. *Cell Death Differ.* **18**, 1241–1246 (2011).

The influence of physiological state of bacteria *Escherichia coli* in occurrence of hibernation mode in formation of bacteriophages

Ana Lisac*,¹ Aleš Podgornik*,¹, Katja Šivec¹

¹ Faculty of Chemistry and Chemical Technology, University of Ljubljana, Večna pot 113, SI-1000 Ljubljana, Slovenia, al1294@student.uni-lj.si

Due to an increasing antibiotic resistance among bacteria, bacteriophages represent potential substitution to antibiotics. A variety of bacterial physiological states can be found in human body, many times in limiting conditions causing latent and persistent infections. Under such conditions, efficacy of antibiotics is further diminished. To estimate efficiency of bacteriophages on such bacteria, we studied phage propagation by bacteria being in limiting conditions. This results in so called hibernation mode, a reversible dormant state of infected bacteria with low metabolic activity, what requires to determine whether phage therapy would be successful.^{2,3} As a model system, T4 phage and bacteria *E-coli* as a host was used. In various limiting physiological states of *E-coli* we determined bacteriophage parameters such as burst size and latent period. Bacteria were grown in a continuous system operating at low dilution rates between 0,024 and 0,24 h⁻¹. It was found that burst size increases exponentially from 3,7 to 25 PFU cell⁻¹ and that even in most limiting conditions an infection occurred but no phage multiplication was observed. As soon as certain amount of nutrients was added, bacteria produced bacteriophages causing bacteria lyses, therefore phage therapy seems to be feasible.

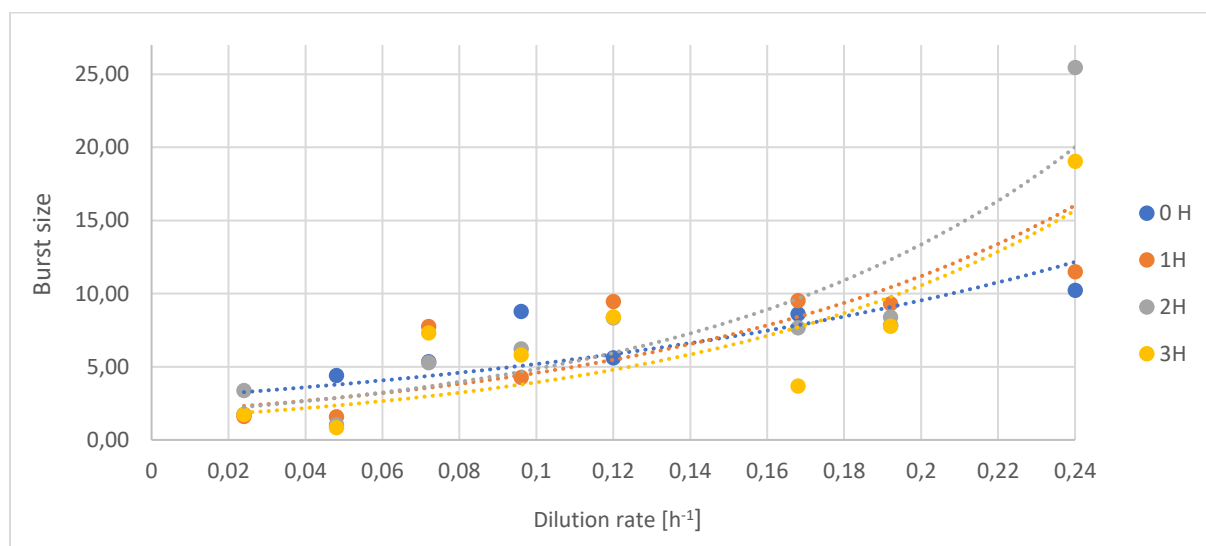


Figure 1: Phage growth parameter burst size (BS) as a function of dilution rate.

1. Bryan, D.; El-Shibiny, A.; Hobbs, Z.; Porter, J.; Kutter, E.M. Bacteriophage T4 Infection of stationary phase *E-coli*: Life after Log from a phage perspective. *Front. Microbiol.* **2016**, *12*, 1-12
2. Nabergoj, D.; Modic, P.; Podgornik, A. Effect of bacterial growth rate on bacteriophage population growth rate. *Microbiol. open* **2017**, *10*, e558
3. Mancuso, F.; Shi, J.; Malik, D.J. High throughput manufacturing of bacteriophages using continuous stirred tank bioreactors connected in series to ensure optimum host bacteria physiology for phage production. *Viruses* **2018**, *20*, 537

Novel inhibitors of the *Plasmodium falciparum* dihydroorotate dehydrogenase

Nika Strašek¹, Lara Lavrenčič¹, Andraž Oštrek¹, Dejan Slapšak¹, Uroš Grošelj¹, Marina Klemenčič¹, Helena Brodnik Žugelj¹, Jernej Waggener^{1,2}, Marko Novinec^{*,1}, Jurij Svete^{*,1}

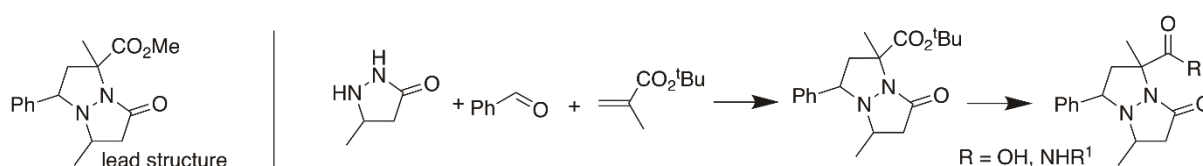
¹ Faculty of Chemistry and Chemical Technology, University of Ljubljana, Večna pot 113, SI-1000 Ljubljana, Slovenia, jurij.svete@fkkt.uni-lj.si, marko.novinec@fkkt.uni-lj.si

² Current address: Lek d.d., Novartis Anti-Infectives & Chemical Operations, Kolodvorska cesta 27, 1234 Mengeš, Slovenia

Malaria is a serious infectious disease impacting the global health with up to a million deaths every year. The emergence of drug-resistant parasite *Plasmodium falciparum* strains is demanding new drugs and therapies for malaria treatment¹.

Plasmodium falciparum dihydroorotate dehydrogenase (PfDHODH) has emerged as a promising target for new antimalarial drugs. It is a fourth and central enzyme in the *de novo* pyrimidine biosynthesis pathway. Studies have shown that inhibition of PfDHODH leads to parasite death, as this is the only source of pyrimidine production in *Plasmodium falciparum*; compared to humans where other pathways for pyrimidine synthesis exist².

The respective new tetrahydro-1*H*,5*H*-pyrazolo[1,2-*a*]pyrazole-1-carboxylates³, carboxylic acids and carboxamides were afforded by several synthetic methods from corresponding 5-substituted pyrazolidine-3-ones, aldehydes and methacrylates. The synthesized pyrazolo[1,2-*a*]pyrazoles were tested for enzymatic inhibition on *Plasmodium falciparum* and human dihydroorotate dehydrogenase (PfDHODH and HsDHODH respectively), and two of them showed promising activity at low μM range. Unfortunately, neither the carboxylic acids nor the carboxamides based on the lead structure showed any activity. Potency of the compounds was predicted with molecular docking into the active site of the PfDHODH.



Scheme 1: Lead structure, tetrahydro-1*H*,5*H*-pyrazolo[1,2-*a*]pyrazole-1-carboxylates and derivatives

1. Fidock, D. A., Antimalarial drug discovery: efficacy models for compound screening. *Nat. Rev. Drug Disc.* **2004**, *3*, 509–520.
2. Vyas, V. K., Recent Developments in the Medicinal Chemistry and Therapeutic Potential of Dihydroorotate Dehydrogenase (DHODH) Inhibitors. *Mini-Rev. Med. Chem.* **2011**, *11*, 1039–1055.
3. Grošelj, U.; Svete, J., Recent Advances in the Synthesis of Polysubstituted 3-Pyrazolidinones. *ARKIVOC* **2015**, *6*, 175–205.

In-vitro model for measurements of ionized calcium using ion-selective electrode

Lea Kastelec¹, Gregor Novljan^{2,3}, Mitja Kolar^{1*}

¹ Faculty of Chemistry and Chemical Technology, University of Ljubljana, Večna pot 113, SI-1000 Ljubljana, Slovenia (lea.kastelec@gmail.com, mitja.kolar@fkkt.uni-lj.si)

² Department of Pediatric Nephrology, Children's Hospital, University Medical Center Ljubljana, Ljubljana, Slovenia

³ Faculty of Medicine, University of Ljubljana, Ljubljana, Slovenia (gregor.novljan@mf.uni-lj.si)

Central venous catheters (CVC) are often used in young children undergoing chronic hemodialysis. A significant amount of citrate leaks from the catheter at the time of instillation, decreasing ionized calcium due to chelation. We aimed to evaluate the effect of citrate spilling on ionized calcium at the catheter tip. An in-vitro model was constructed to measure the citrate-induced change of calcium concentration at the tip of the CVC with an membrane calcium ion-selective electrode (ISE).¹ Two systems were compared: one system at room temperature and aerobic conditions, the other at 36.5 °C and anaerobic conditions as a simulation of conditions in the human body. Firstly, an electrode response to the addition of the locking solution into the mixture of isotonic saline and standard calcium solution, was measured, secondly human serum albumin was added into this mixture, whereby pH was additionally measured. Measurements were performed with 4% and 30% locking solutions, and the results were compared. A tenfold decrease of ionized calcium was observed when using 30% citrate as compared to 4% solutions in both systems/solutions. Additional studies are needed to define the safety of concentrated citrate in small children, which should include the time factor of low local calcium exposures.²

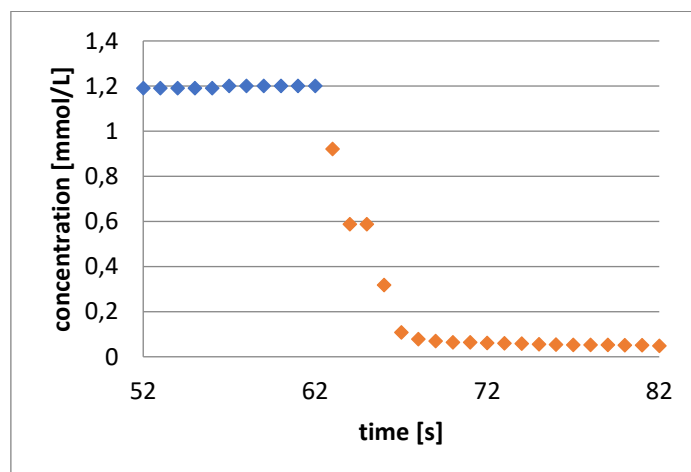


Figure 6: Addition 30 % locking solution into the mixture of isotonic saline and standard calcium solution in system with 36.5 °C.

1. Kastelec, L. Determination of calcium with an ion-selective electrode; Faculty of Chemistry and Chemical Technology: Ljubljana, **2017** (Diploma thesis).
2. Novljan, G.; Kolar, M.; Kastelec, L.; Battelino, N. Citrate-included local ionized calcium reduction in pediatric hemodialysis patients – in vitro study (In Press).

Compounds obtained by $K_3[Fe(C_2O_4)_3] \cdot 3H_2O$ and bis(3,5-dimethylpyrazol-1-yl)acetate

Matej Jarc Rydži,¹ Nives Kitanovski*¹

¹ Faculty of Chemistry and Chemical Technology, University of Ljubljana, Večna pot 113, SI-1000 Ljubljana, Slovenia, nives.kitanovski@fkkt.uni-lj.si.

Three compounds of iron(II) and bis(3,5-dimethylpyrazol-1-yl)acetate (later represented as L) were successfully synthesized from $K_3[Fe(C_2O_4)_3] \cdot 3H_2O$ and potassium salt of L, prepared from KOH and HL.¹ Different amounts of $K_2C_2O_4$ were also added. All isolated products are the complex with the basic formula $[FeL_2] \cdot xH_2O$ ($x = 3$ (**1**),² $x = 2$ (**2**, **3**)).

The ligand (L) forms three coordination bonds with the central ion, one via oxygen atom of the carboxylic group and the other two via nitrogen atoms of both pyrazole rings as is shown in the Figure 1. Water molecules form hydrogen bonds within the crystal lattice.

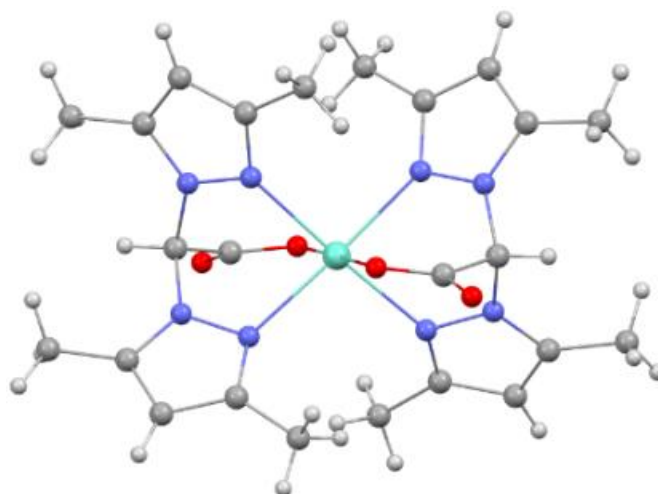


Figure 1: Molecular structure of $[FeL_2]$ in **1**.

Table 9: Unit cell dimensions in $[FeL_2] \cdot xH_2O$ compounds.

	1 ²	2	3
$a/\text{Å}$	16.1620(3)	7.7348(5)	11.4919(4)
$b/\text{Å}$	13.3097(2)	8.6005(6)	13.9073(4)
$c/\text{Å}$	13.9711(2)	11.2152(9)	17.6345(7)
$\alpha/\text{Å}$	90.00	112.477(7)	90.00
$\beta/\text{Å}$	109.089(2)	91.444(6)	106.286(4)
$\gamma/\text{Å}$	90.00	94.490(5)	90.00

1. Beck A.; Weibert B.; Burzlaff N., Monoanionic N,N,O-scorpionate ligands and their iron(II) and zinc(II) complexes: Models for mononuclear active sites of non-heme iron oxidases and zinc enzymes, *Eur. J. Inorg. Chem.* **2001**, 521-527.
2. Počkaj, M.; Kozlevčar, B.; Kitanovski, N., Stability of the compounds with the octahedral $[M^{II}(\kappa^3-L)_2]$ coordination building blocks of late 3d elements via solvate water supramolecular arrangement. *Acta Chim. Slov.* **2015**, 62, 272-280.

Lignin dimers hydrocracking: Kinetics of lignin typical bonds cleavage based on micro-kinetics of monomers

Ana Bjelić,¹ Edita Jasiukaityte Grojzdek,¹ Miha Grilc,^{*,1} Blaž Likozar¹

¹ Department of Catalysis and Chemical Reaction Engineering, National Institute of Chemistry, Hajdrihova 19, SI-1000 Ljubljana, Slovenia, miha.grilc@ki.si

We have applied a bottom-up approach in order to determine kinetics of lignin functionalities removal and cracking of typical links. Removal of functionalities has been investigated on a lignin monomer model compound eugenol.¹⁻³ Typical links cleavage has been investigated by using several dimer model compounds such as biphenyl, 2,2'-biphenol, 3-methoxy-biphenyl, benzyl phenyl ether and 2-phenoxy-1-phenylethanol. Kinetic data determined for eugenol were directly applied for dimers in terms of similar reactions. Figure 1 shows results for 2,2'-biphenol hydrodeoxygenation (HDO), whereas subplot *a* is referred to model results obtained with eugenol reaction rate constants, while subplot *b* to results obtained with optimised constants. Eugenol constants did not provide sufficient matching when dimers cleavage was not accomplished (representatives of C-C bond: biphenyl, 2,2'-biphenol, 3-methoxy-biphenyl). On the other side, when interrering bonds were cleaved (representatives of ether bond: benzyl phenyl ether and 2-phenoxy-1-phenylethanol) and thus monomers produced, eugenol constants were applied as such for monomers transformation, while reactions of dimers themselves needed to be optimised. Although eugenol constants could not be applied directly for similar reactions, nonetheless they provided a reasonably good matching. One may additionally say that applied strategy seems very promising in achieving the final goal of lignin depolymerisation kinetics determination.

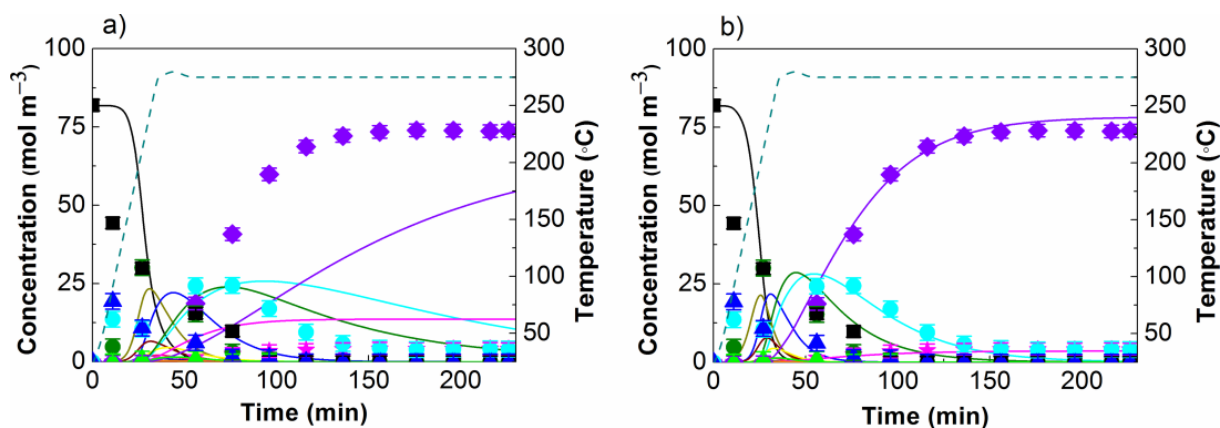


Figure 1: 2,2'-biphenol HDO over Pt/Al₂O₃ at 275 °C and 5 MPa of initial hydrogen pressure a) eugenol constants used directly b) reaction rate constants optimized. Black–2,2'-biphenol, blue–2,2'-bicyclohexanol, cyan–2-cyclohexylcyclohexanol, violet–bicyclohexyl.

1. Bjelić, A.; Grilc, M.; Gyergyek, S.; Kocjan, A.; Makovec, D.; Likozar, B., *Catalysts* **2018**, 8 (10), 425.
2. Bjelić, A.; Grilc, M.; Huš, M.; Likozar, B., *Chem Eng J.* **2018**, 359, 305-320.
3. Bjelić, A.; Grilc, M.; Likozar, B., *Chem Eng J.* **2018**, 333, 240-259.

3D Printed Reconstruction of Plečnik's Monument

Anja Škerjanc ^{*1}, Helena Gabrijelčič Tomc ¹, Tanja Nuša Kočevar ¹, Matej Pivar¹

¹ Faculty of Natural Sciences and Engineering, Department of Textiles, Graphic Arts and Design, University of Ljubljana, Snežniška 5, SI-1000 Ljubljana, Slovenia, anja.skerjanc123@gmail.com

Main contribution of the research includes the 3D-reconstruction of Jože Plečnik's monument to the Czech military leader Jan Žižka, based on multiple references, including his sketches, architectural plans and a photograph of the wooden model of the monument. These references provided insight into Plečnik's style which was used in the 3D-printed reconstruction.

The research includes all phases necessary for correct model interpretation and ultimately, reconstruction¹. The information obtained solely from Plečnik's references was insufficient for model reconstruction. That is why a thorough analysis of other sources was carried out to obtain additional information about Plečnik's style and the appearance of Hussite soldiers, especially Jan Žižka. Most attention was focused on Plečnik's way of depicting figures and details, clothing, horses, Hussite soldier props and facial and body features of Jan Žižka. Interpretation and 3D modelling of the monument followed. Figure bodies were designed in MakeHuman and then exported to Blender for modelling clothing and props. The architectural model was designed solely in Blender. The figures were then properly prepared for 3D-printing with stereolithography (SLA) technology. The architectural model was too large for printing, so it was separated into smaller parts and prepared for printing, using fuse deposition modeling (FDM). All elements were properly treated after printing and the entire 3D-reconstruction was prepared for exhibition (Fig. 1).



Figure 1: 3D printed reconstruction of Plečnik's monument (right).

1. Kočevar, T. N. (Ed.), Determining the framework for Žižka monument 3D reproduction. *Proceedings - The Ninth International Symposium GRID 2018*, **2018**, 389-395.

Dextran activated surface provides mild environment for cell attachment

Lorena Kunc¹, Aleš Podgornik¹

¹ Faculty of Chemistry and Chemical Technology, University of Ljubljana, Večna pot 113, SI-1000 Ljubljana, Slovenia, lorena.kunc@gmail.com

Dextran is a bacterial polysaccharide, mainly composed of linear α -1,6-linked D-glucopyranose residues with a low percentage of α -1,2-, α -1,3- or α -1,4-linked side chains. Nowadays, *Leuconostoc mesenteroids* (strain B-512) is responsible for the majority of the commercially available dextrans.

This polysaccharide is widely used for biomedical applications due to its excellent biocompatibility, low toxicity and it is potentially a desirable alternative to polyethylene glycol (PEG) as a low-protein base coating for surface immobilization of bioactive molecules. Furthermore, it is slowly degraded by human enzymes as compared to other polysaccharides. It has already been used clinically as a plasma volume expander, peripheral flow enhancer and antithrombolytic agent. Unlike other polysaccharides, which have many different functional groups (e.g., amine and amide), dextran only has hydroxyl groups, which do not support cell attachment.

Dextran-coated surface is activated with a catalysis-free aqueous method by the periodate ion which attacks vicinal diols promoting C-C bond breaking and creating aldehyde groups. The bicinchoninic acid (BCA) method, developed for measuring total protein concentration, may also be used to quantify the degree of oxidation of oxidized dextran (Table 1). As the degree of oxidation can deeply affect the final physico-chemical characteristics and its correct determination will be fundamental for the quantification of immobilized cells.

Table 10: Number of available binding sites dependent on degree of oxidation (DO) of dextran.

DO (%)	25	50	50	75	100
Num. of available binding sites	9,8 x 10 ⁸	1,56 x 10 ⁹	1,17 x 10 ⁹	1,14 x 10 ⁹	2,23 x 10 ⁹

1. Maia, J.; Evangelista, M., B.; Gil, H.; Ferreira, L., Dextran-based materials for biomedical applications. *Carbohydrates Applications in Medicine*: **2014**, 31-53
2. Massia, S., P.; Stark, J., Immobilized RGD peptides on surface-grafted dextran promote biospecific cell attachment. *John Wiley and Sons* **2001**, 390-399
3. Maia, J.; Carvalho, R., A.; Coelho, J., F., J.; Simões, P., N.; Gil, M., H., Insight on the periodate oxidation of dextran and its structural vicissitudes. *Polymer* **2011**, 52: 258-265
4. Massia, S., P.; Stark, J.; Letbetter, D., S.; Surface-immobilized dextran limits cell adhesion and spreading. *Biomaterials* **2000**, 21: 2253-2261

Interactions of active biopolymer packaging and fresh pasta during shelf life study

Kristi Kõrge^{1,2}, Uroš Novak^{*,1}, Marijan Bajić¹

¹ Department of Catalysis and Chemical Reaction Engineering, National Institute of Chemistry, Hajdrihova 19, SI-1000 Ljubljana, Slovenia, uros.novak@ki.si

² Department of Chemistry and Biotechnology, Tallinn University of Technology, Akadeemia tee 15, 12618, Tallinn, Estonia

Food in biodegradable packaging is an important research gap in need of filling next to biopackaging materials development itself¹. For the new age in demand packaging materials, marine biopolymer chitosan, compositioned with other nanoparticles has been recognized as tangible^{2,3}. In this study, we investigate the shelf life of spinach filled fresh pasta packaged in active chitosan-chestnut extract (CH-CE) biodegradable sachets. Pasteurized pasta aging evolved in conventional refrigerated no light storage conditions of 8 °C with relative humidity 60±2% during 60 days. The moisture mobility and total polyphenol release relation, evolution of microbiology, microstructure changes are observed and analyzed. We show rapid moisture mobility between a starchy food and CH-CE during the first 9 days of storage wherein fresh pasta started to develop retrogradated texture. Total phenolic content (TPC) show dependency in moisture throughout the shelf life (Figure 1). Packaging microcomponents do not migrate to food surface and it prevents microbial growth during 60 days. The material performed mechanically sustainable sachets for fresh pasta although further developments are required regarding vapour permeability.

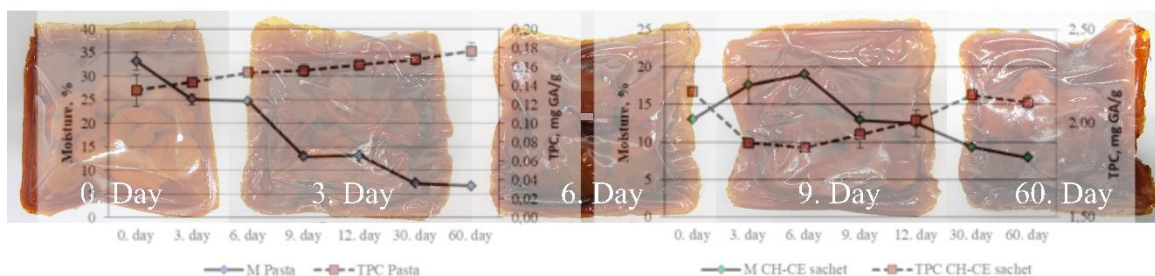


Figure 1: Fresh pasta in CH-CE sachet and TPC dependency in moisture during shelf life.

1. Moustafa H., Youssef A.M., Darwish N. A., Abou-Kandil A. I. Eco-friendly polymer composites for green packaging: Future vision and challenges. *Composites Part B* **2019**, 172, 16-25.
2. Rodríguez-Rojas A., Arango Ospina A., Rodríguez-Vélez P., Arana-Florez R. ¿What is the new about food packaging material? A bibliometric review during 1996–2016. *Trends Food Sci. Technol.* **2019**, 85, 252-261.
3. Bajić M., Jalšovec H., Travan A., Novak U., Likozar B. Chitosan-based films with incorporated supercritical CO₂ hop extract: Structural, physicochemical, and antibacterial properties, *Carbohydrate Polymers* **2019**, <https://doi.org/10.1016/j.carbpol.2019.05.003>

Comparison of three methods for DNA extraction from tissue samples and blood lymphocytes of breast cancer patients

Janina Gea Cvikl¹, Katja Repnik^{1,2}, Iztok Takač³, Uroš Potočnik^{1,2*}

¹ Faculty of Chemistry and Chemical Technology, University of Maribor, Smetanova ulica 17, SI-2000 Maribor, Slovenia, janinagea.cvikl@student.um.si

² Faculty of Medicine, University of Maribor, Taborska ulica 8, SI-2000 Maribor, Slovenia,

³ University Medical Centre Maribor, Ljubljanska ulica 5, 2000, SI-Maribor, Slovenia

The key to performing successful genotyping analysis is the isolation of genetic material. Isolated DNA must have a high enough quality, yield, purity and integrity to be considered appropriate for further analysis¹. We decided to compare and evaluate three different methods for DNA extraction from FFPE and fresh-frozen tissue samples as well as blood lymphocytes of breast cancer patients in order to determine the most suitable one. To isolate DNA from whole blood samples we used the standard TRI reagent method (Sigma-Aldrich); from fresh tissues, the TRI reagent method with previous homogenization and tissue preparation; and from formalin-fixed paraffin embedded tissues the BiOstic© FFPE DNA isolation kit (MO BIO Laboratories, Inc.). In addition, we evaluated cost, time and intensity of labor for each of these methods. We isolated DNA from a total number of 128 samples.

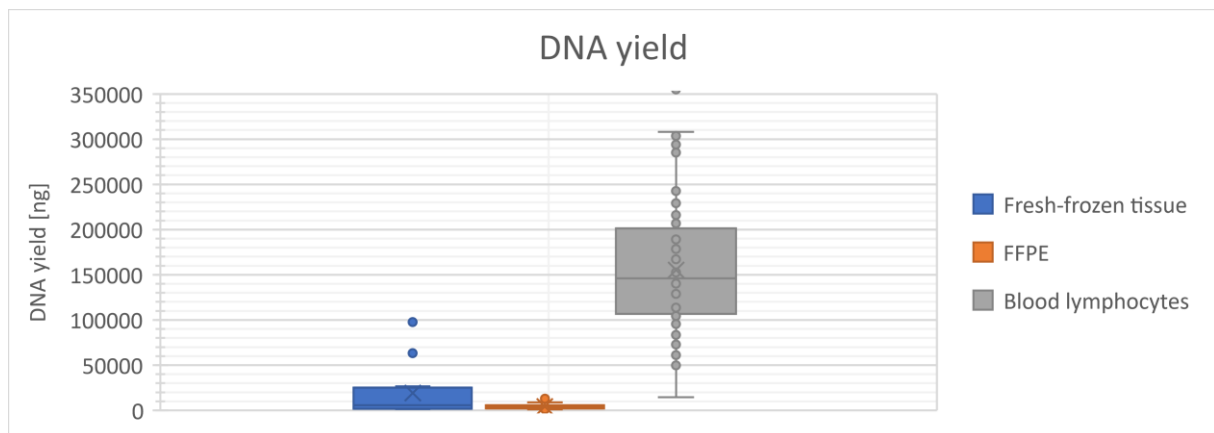


Figure 1: Comparison of DNA yield for different types of DNA isolation.

Results show that DNA obtained from whole blood samples had the highest concentration and yield, followed by DNA isolated from fresh tissues. Formalin-fixed paraffin embedded tissues represented the biggest challenge, with the lowest concentrations of obtained DNA. They did however prove to produce DNA with the highest purity. We obtained non-fragmented DNA of high molecular weight using all three methods.

1. a) Psifidi A et al. Comparison of Eleven Methods for Genomic DNA Extraction Suitable for Large-Scale Whole-Genome Genotyping and Long-Term DNA Banking Using Blood Samples. *PLoS ONE*. **2015**. 10(1): e0115960. b) Mirmomeni MH et al. Comparison of the Three Methods for DNA Extraction from Paraffin-Embedded Tissues. *Journal of Biological Sciences*. **2010**; 10: 261-266.

Experimental determination of vapor-liquid equilibrium for binary system CO₂+furfural

Gorica Ivaniš,¹ Ljudmila Fele Žilnik,¹ Blaž Likozar,¹ Miha Grilc*¹

¹ Department of Catalysis and Chemical Reaction Engineering, National Institute of Chemistry, Hajdrihova 19, Ljubljana, Slovenia, miha.grilc@ki.si

Lignocellulose and oils obtained from it are not equivalent to conventional energy sources because of their high oxygen content (various oxygenated functionalities) that can be reduced by various defunctionalisation processes, such as hydrogenation, dehydration, decarboxylation or hydrodeoxygenation. The design and optimization of these processes require accurate kinetic models that take into account the solubility of various gases in bio-based chemicals present in process¹. The analytical method for experimental determination of vapor-liquid equilibria at wide ranges of temperature and pressure (Fig. 1)² was tested on binary system CO₂+furfural. The obtained solubility data were compared with values found in literature³, showing good agreement, and modeled using several equations of state in order to get interaction parameters valuable for prediction of phase equilibria behavior of the studied system.



Figure 1: The apparatus for vapor-liquid equilibria measurements.

Acknowledgement: This research was funded by the Slovenian Research Agency (research core funding P2-0152 and basic postdoctoral research project Z2-9200).

1. Grilc, M.; Likozar, B.; Levec, J., Hydrodeoxygenation and hydrocracking of solvolysed lignocellulosic biomass by oxide, reduced and sulphide form of NiMo, Ni, Mo and Pd catalysts. *Appl. Catal. B: Environ.* **2014**, *150-151*, 275-287.
2. Fele Žilnik, L.; Grilc, M.; Levec, J.; Peper, S.; Dohrn, R., Phase-equilibrium measurements with a novel multi-purpose high-pressure view cell: CO₂+n-decane and CO₂+toluene. *Fluid Phase Equilib.* **2016**, *419*, 31-38
3. Sako, T.; Sugeta, T.; Nakazawa, N.; Otake, K.; Sato, M.; Ishihara, K.; Kato, M., High pressure vapor-liquid and vapor-liquid-liquid equilibria for systems containing supercritical carbon dioxide, water and furfural. *Fluid Phase Equilib.* **1995**, *108*, 293-303.

Polydentate pyridyl-mesoionic carbenes (Poly-MICs)

Aljoša Bolje,^{*1,2} Matej Huš,² Ema Žagar,² Biprajit Sarkar³

¹ Faculty of Pharmacy, University of Ljubljana, Aškerčeva cesta 7, SI-1000 Ljubljana, Slovenia, aljosa.bolje@ffa.uni-lj.si

² National Institute of Chemistry, Hajdrihova ulica 19, SI-1000 Ljubljana, Slovenia

³ Institut für Chemie und Biochemie, Anorganische Chemie, Freie Universität Berlin, Fabeckstraße 34-36, D-14195 Berlin, Germany

Cyclic and acyclic click triazoles having two pyridine and two triazolyledene donors were designed and prepared starting from click partners, i.e. azides and acetylenes, exploring several different reaction conditions.¹ The formation of cyclic vs. acyclic click triazole structures was studied in details with NMR spectroscopy and mass spectrometry. The studies are supported also by DFT calculations of the click reactions.² Triazoles were subsequently transformed into salts,³ which can act as precursors for mesoionic carbenes offering polydentate ligation towards several transition metals.² Our plan is to form iron(II) complexes and use them in polymerization reactions for a more sustainable way of catalysis.⁴

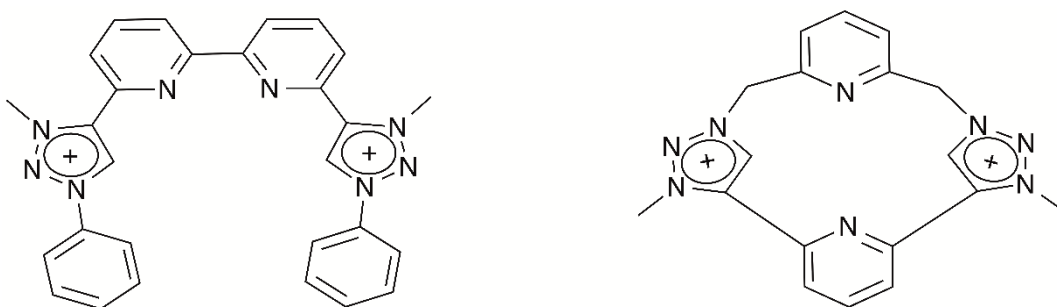


Figure 1: Acyclic(left) and cyclic(right) polydentate MICs with two pyridine and two triazolyledene donors.

1. a) Banert, K., Wutke, J., Rüffer, T., Land, H. Reactions of Unsaturated Azides; Part 22:¹ The Alkyne Azide Click Chemistry as a Synthetic Tool for the Generation of Cage-Like Triazole Compounds. *Synthesis* **2008**, *16*, 2603-2609. b) Li, Y., Flood, A. H. *J. Am. Chem. Soc.* **2008**, *130*, 12111-12122.
2. Bolje, A., Huš, M., Žagar, E., Sarkar, B. *Manuscript in preparation*.
3. Bolje, A., Košmrlj, J. A Selective Approach to Pyridine Appended 1,2,3-Triazolium Salts. *Org. Lett.* **2013**, *15*, 5084-5087.
4. Bolje, A., Žagar, E.; Sarkar, B. *Manuscript in preparation*.

Lipid droplets and autophagy cooperate to support the resistance of cancer cells to stress

Špela Koren¹, Eva Jarc^{1,2}, Ana Kump^{1,2}, Maida Jusović^{1,2}, Pia Starič¹, Toni Petan^{1,*}

¹ Department of Molecular and Biomedical Sciences, Jožef Stefan Institute, Jamova 39, SI-1000 Ljubljana, Slovenia

² Jožef Stefan International Postgraduate School, Jamova 39, SI-1000 Ljubljana, Slovenia

Lipid droplets (LDs) are dynamic fat storage organelles present in most eukaryotic cells from yeast to human. They are composed of a neutral lipid core covered by a phospholipid monolayer, in which numerous proteins are embedded¹. LD biogenesis is often induced in cells exposed to an excess of nutrients or lipids and is characteristic of many diseases, such as obesity and diabetes. Paradoxically, their formation occurs also in cells deprived of oxygen and nutrients, such as rapidly proliferating tumour cells that have poor access to the vasculature, suggesting that LDs are crucial for the cellular stress response². LDs are also involved in a complex but still poorly understood relationship with autophagy – the major cellular recycling machinery and stress response pathway. Autophagy is activated under various conditions of nutrient deprivation and it may participate in both LD biogenesis and LD breakdown³. We aim to discover the principal ways in which LDs and autophagy cooperate to promote the resistance of cancer cells to stress. Using genetic and pharmacological approaches that target major LD metabolism enzymes and the autophagy pathway, we will test several hypotheses, including 1) the possibility that autophagy drives LD biogenesis by providing lipids recycled from other membranous organelles and 2) that autophagic breakdown of LDs, i.e., lipophagy, provides lipids for the survival of starving breast cancer cells. Our study will provide new clues for the understanding of cancer stress resistance and may reveal new targets for cancer prevention and therapy.

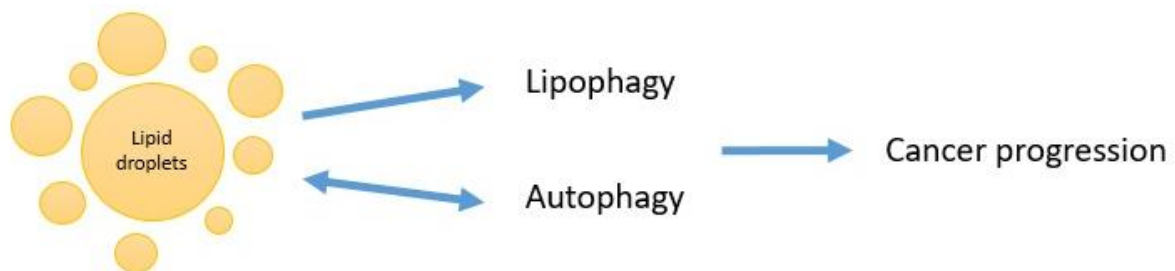


Figure 7: Crosstalk between autophagy and lipid droplets. Autophagy provides fatty acids for lipid droplet biogenesis in starved cells, but it may also participate in lipid droplet breakdown through lipophagy². All these processes may be important for cancer cell survival during stress and tumour progression.

1. Farese, R. V.; Walther, T. C. *Cell* **2009**, 139, 855–860.
2. Petan, T.; Jarc, E.; Jusović, M. *Molecules* **2018**, 23: 1941.
3. Rambold, A. S.; Cohen, S.; Lippincott-Schwartz, J. *Dev. Cell* **2015**, 32, 678–692.

Managing the balance of sulfur in the refinery through the blending of crude oils

Pero Dugic,¹ Tatjana Botic,¹ Aleksandra Sinik,^{*1}

¹ Faculty of Technology, University of Banja Luka, Stepe Stepanovica 73, 78000 Banja Luka, Bosnia and Herzegovina, aleksandra.sinik@tf.unibl.org

Environmental regulations are becoming more stringent in terms of emission limit values for pollutants. Therefore, the quality of liquid petroleum fuels, primarily gasoline and diesel fuels, is changing rapidly, and the sulfur content in them is limited to values below 10 mg/kg. In order to reduce the emissions of sulfur compounds, as one of the main actors in pollution of atmosphere, it is necessary to remove sulfur compounds from crude oil or in some other way to reduce its concentration in crude oil, and therefore in petroleum products. Given that today's raw materials for refineries are mainly heavy crude oils, rich in sulfur content, engineers are faced with the problem of better management of the sulfur balance. In this paper, the basic physicochemical characteristics of two crude oil of different origin are determined. As the sulfur content is greater than 1%, both crude oils are considered as sour. On the basis of these tests one of the ways of managing the sulfur balance is shown. The results of the test show that the optimum ratio of these two oil is 2,82:1.

Table 1. Physicochemical characteristics of crude oils			
Parameter	Unit	KIRKUK crude oil	REB crude oil
Density (15°C)	kg/m ³	867,6	871,2
°API (15°C)	°	31,59	30,92
Cloud point	°C	-30	-9
Pour point	°C	-33	-12
Total sulphur	% (m/m)	2,54	1,61
NaCl	mg/kg	13,13	114,42
Water	% (v/v)	0,075	0,25
Sediment	% (v/v)	0,05	0,05
Water and sediment	% (v/v)	0,125	0,30
Content of water by destilation	% (v/v)	0,10	0,400
Kinematics viscosity (20°C)	mm ² s ⁻¹	12,80	18,22
Kinematics viscosity (50°C)	mm ² s ⁻¹	5,391	7,130

1. Dugić, P. Botić, T. & Petrović. Z, Tehnologija prerade nafte, **2017**, 15-16.

Functionalization of cellulose obtained from corn stover and wheat straw

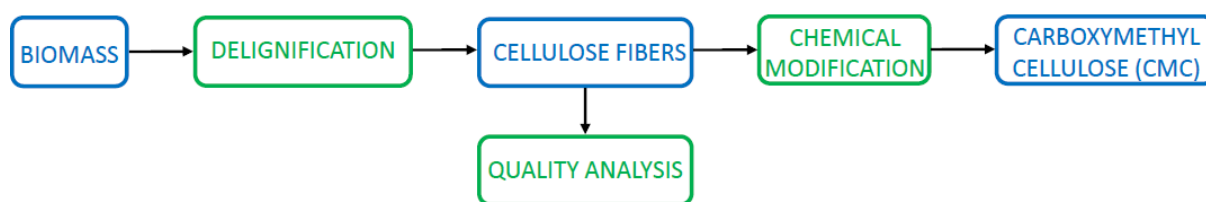
Jan Hočevar¹, Janja Zule², Primož Titan³, Jernej Iskra^{*,1,3}

¹ Faculty of Chemistry and Chemical Technology, University of Ljubljana, Večna pot 113, SI-1000 Ljubljana, Slovenia, jernej.iskra@fkk.uni-lj.si

² Pulp and Paper Institute, Bogišičeva 8, SI-1000 Ljubljana, Slovenia

³ RGA Ltd., Brodarska ul. 27, Krog, SI-9000 Murska Sobota, Slovenia

The increasing environmental concerns caused by modern industry have led researchers to obtain useful industrial materials and chemicals from biomass. Among other things, part of the residue streams from food production, such as corn stover and wheat straw could be used in chemical industry. The plant biomass is interesting source and consists largely of cellulose, hemicellulose and lignin. Cellulose is a linear and high molecular weight macromolecule in which glucose monosaccharide units are linked by β -1,4-glucosidic bonds. It is the most common organic compound on Earth. Moreover, it is non-toxic and biodegradable material. On average, plant biomass contains about 30-40% cellulose, while wood species contain 41-45% cellulose¹. It can be chemically modified to useful chemical feedstock, such as cellulose ethers and esters. Due to close packing by the intrachain and interchain hydrogen bonding between hydroxyl groups, cellulose neither melts nor dissolves in common organic solvents which limits its modification. CMC is the most widely used cellulose ether today with applications in the textile, food, paper and pharmaceutical industries. CMC is a linear, long-chain, water-soluble polysaccharide with really high viscosity and great polyelectrolyte character². We will present our study on the chemical delignification process to isolate cellulose fibers from corn stover and wheat straw and subsequent determination of their mechanical, morphological and other properties. We further studied conversion of cellulose into the CMC through Williamson ether synthesis in various solvents and under different reaction conditions³ (Scheme 1).



Scheme 1: Path from biomass to carboxymethyl cellulose.

1. Hon, D. N.-S.; Shiraishi, N., *Wood and cellulosic chemistry*. 2nd ed., revised and expanded; Marcel Dekker, Inc.: New York, Basel, **2001**.
2. Singh, R. K.; Singh, A. K., Optimization of Reaction Conditions for Preparing Carboxymethyl Cellulose from Corn Cob Agricultural Waste. *Waste Biomass Valorization* **2013**, 4, 129-137.
3. Ambjörnsson, H. A.; Schenzel, K.; Germgård, U., Carboxymethyl Cellulose Produced at Different Mercerization Conditions and Characterized by NIR FT Raman Spectroscopy in Combination with Multivariate Analytical Methods. *BioResources* **2013**, 8(2), 1918-1932.

Modelling of cell growth

Domen Vaupotič*,¹ Miha Lukšič¹

¹ Faculty of Chemistry and Chemical Technology, University of Ljubljana, Večna pot 113, SI-1000 Ljubljana, Slovenia, domenvaupotic@gmail.com

In order to maintain growth and maximize the utility of available nutrition, bacterial cell must precisely regulate the allocation of available energy into different metabolic compartments. The exact target of evolutionary pressure in a development of a bacterial cell remains unknown. We examined a simple coarse-grained model (Fig. 1) of bacterial cell (*E. coli*) undergoing moderate growth, which was developed by Maitra and Dill^{1,2}. The central energy value in the model is represented by ATP, which is produced by the catabolic machinery of the cell and is afterwards distributed to the synthesis of ribosomes and proteins. The model successfully recreates some of the basic growth laws and predicts that the evolution targets the maximization of energy efficiency of fast-growing cells. By using more experimental data and fitting it to the model we exposed some inconsistencies and proposed a modified model.

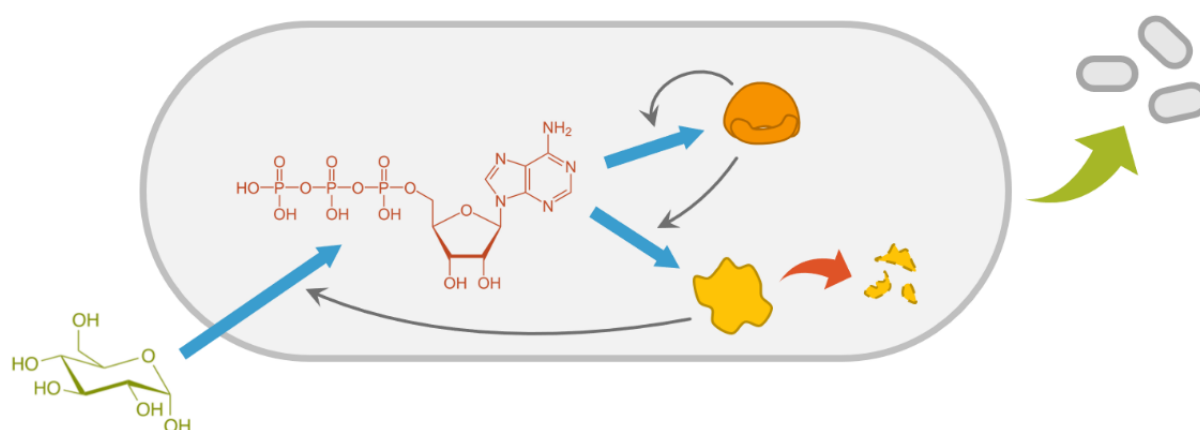


Figure 1: Bacterial growth model with ATP as a central energy molecule, which is spent in producing either ribosomes (orange) or proteins (yellow). Proteins are degraded (red arrow) and the cell undergoes growth (green arrow). Metabolic fluxes (blue arrows) are regulated by nonlinear feedback loops (gray arrows).

1. Maitra, A.; Dill, K. A. Bacterial Growth Laws Reflect the Evolutionary Importance of Energy Efficiency. *Proceedings of the National Academy of Sciences* **2014**, *112*, 406–411.
2. Maitra, A.; Dill, K. A. Modeling the Overproduction of Ribosomes When Antibacterial Drugs Act on Cells. *Biophysical Journal* **2016**, *110*, 743–748.

Lactococcus lactis expressing fluorescent cytotoxic protein KillerRed for targeting, imaging, and destroying cancer cells

Abida Zahirović^{1*}, Petra Zadravec¹, Aleš Berlec¹

¹ Department of Biotechnology, Jožef Stefan Institute, Jamova 39, SI-1000, Ljubljana, Slovenia, Abida.Zahirovic@ijs.si

Probiotic lactic acid bacterium, *Lactococcus lactis*, is being increasingly recognized as a host bacterium for expression of heterologous proteins. It has been used for delivery of immunomodulatory cytokine interleukin 10, antioxidant peptide BPC-157¹, and for display of proteins capable of binding proinflammatory cytokines² or chemokines³. In this study we engineered *L. lactis* to express KillerRed protein and explore its potential in photodynamic therapy. Photodynamic therapy involves the application of a photosensitive compound and its subsequent activation by light to achieve selective killing of cancerous cells by generation of reactive oxygen species (Figure 1). KillerRed, a red fluorescent protein, is the first genetically-encoded photosensitizer. It has 1000-fold more intense photo-induced cytotoxicity than other fluorescent proteins and can therefore be utilized to destroy cancer cell (photodynamic therapy) as well as to localize the tumor position using fluorescence imaging.

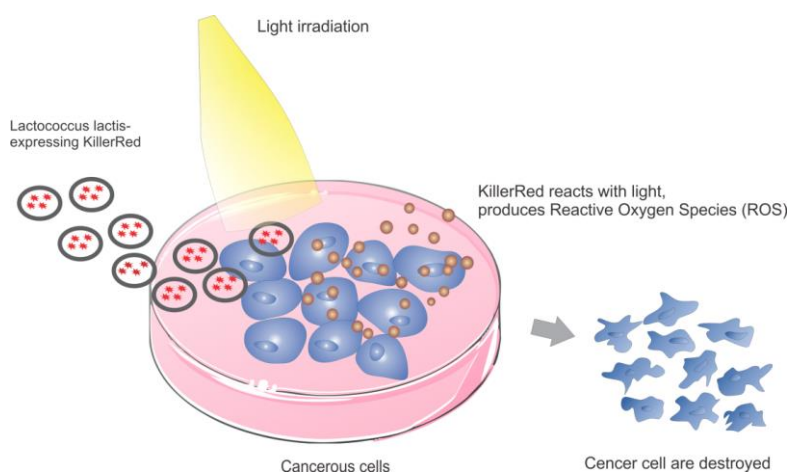


Figure 1: The principle of photodynamic therapy.

KillerRed-encoding gene was successfully expressed in *L. lactis*. Phototoxicity of KillerRed on bacteria-producer cells was determined using DropPlate method. The amount of generated reactive oxygen species was quantified using nitroblue tetrazolium assay. KillerRed-expressing *L. lactis* will be tested on cancer cell lines to assess whether a reactive oxygen species produced by the bacteria can kill cancer cells.

1. Škrlec, K., Engineering recombinant *Lactococcus lactis* as a delivery vehicle for BPC-157 peptide with antioxidant activities. *Appl. Microbiol. Biotechnol.* **2018**, *102*, 10103-10117.
2. Plavec, T., Engineered *Lactococcus lactis* Secreting IL-23 Receptor-Targeted REX Protein Blockers for Modulation of IL-23/Th17-Mediated Inflammation. *Microorganisms* **2019**, 152.
3. Škrlec, K., Evasin-displaying lactic acid bacteria bind different chemokines and neutralize CXCL8 production in Caco-2 cells. *Microb. Biotechnol.* **2017**, 1732-1743.

Reconstruction of antique city Petoviona from ground plans to 3D visualizations

Petra Žvab Rožič¹, Jerneja Sotlar², Ferdi Jajaj², Anja Štamcar², Maruša Možina², Lucija Slapnik¹, Špela Vučak³, Nuša Videc³, Špela Košir², Aleksandra Nestorović⁴, Helena Gabrijelčič Tomc*

¹ Department of geology, Faculty of Natural Sciences and Engineering, University of Ljubljana, Ljubljana, Slovenia,

² Department of Textiles, Graphic Arts and Design, Faculty of Natural Sciences and Engineering, Chair of Information and Graphic Arts Technology, University of Ljubljana, Ljubljana, Slovenia, helena.gabrijelcic@ntf.uni-lj.si,

³ Department of archeology, Faculty of Arts, University of Ljubljana, Ljubljana, Slovenia, ⁴ Provincial Museum of Ptuj – Ormož, Ptuj, Slovenia

3D technology are the most prosperous technologies that are used in cultural heritage (CH) for documentation, interpretation and presentation purposes. The main advantage of 3D technologies is the interchangeability between digital and physical that when it is implemented in the CH reconstruction workflow it benefits the framework and its results with accuracy, non-invasiveness, reliability, sustainability, attractiveness and interactivity. In the contribution an interdisciplinary research is presented with a result of 3D reconstruction of a part of ancient city Petoviona – Ptuj. On a basis of an extensive archeological research^{1,2} 3D models of buildings in the representative part of Petoviona (i.e. four sectors of Panorama) were constructed, textured and rendered (Fig. 1). Besides, geological study was performed, and typical materials used in ancient times were determined, analyzed and stylized as bitmaps images. Images were used as texture information on buildings and reconstructions were visualized enabling the experiencing of the ancient city in a totally new perspective.

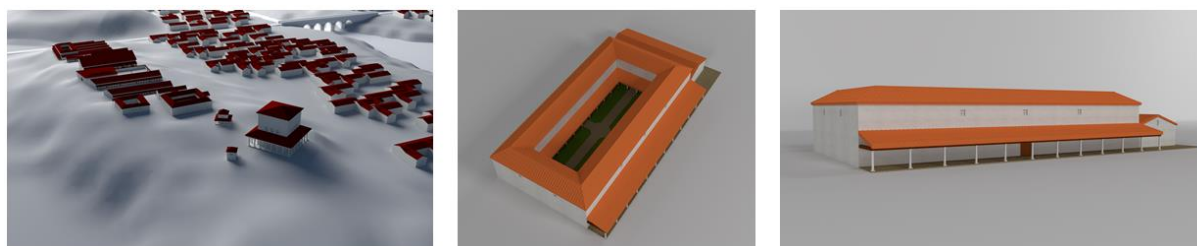


Figure 1: Reconstruction of the Panorama (ancient Petoviona) and of Domus I.

The research was supported by Social Benefit by Public Scholarship, Development, Disability and Maintenance Fund of the Republic of Slovenia and financed by Ministry of Education, Science and Sport (Republic of Slovenia) and European Social Fund.

1. Horvat, J., Dolenc Vičič, A. *Arheološka najdišča Ptuja / Archaeological Sites of Ptuj*. ZRC SAZU, Opera Instituti Archaeologici Sloveniae, **2010**, 216 p.
2. Golvin, J.C., Coulon, G. *Voyage en Gaule romaine*. Editions Errance, **2016**, 201 p.

Derivatives of emodine from invasive plant japanese knotweed as colorants for textile

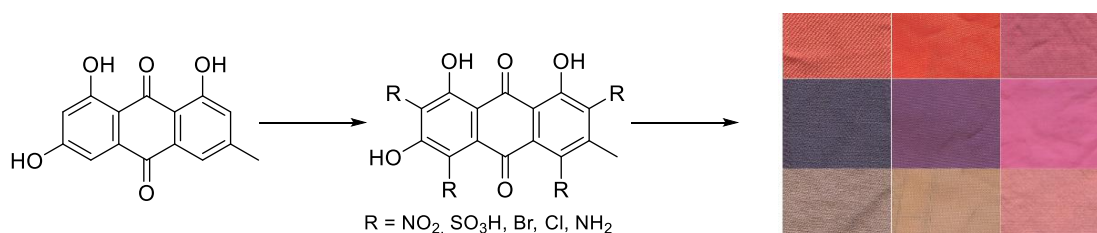
Monika Horvat,^a Marija Gorjanc,^b Jernej Iskra^{a*}

¹ Faculty of Chemistry and Chemical Technology, University of Ljubljana, Večna pot 113, SI-1000 Ljubljana, Slovenia, jernej.iskra@fkkt.uni-lj.si

² Department of Textiles, Graphic Arts and Design, University of Ljubljana, Faculty of Natural Sciences and Engineering, Aškerčeva 12, 1000 Ljubljana, Slovenia.

Japanese Knotweed is one of the most invasive alien species and represents a big ecological problem in Europe. It is also a rich source of anthraquinone derivative emodin, a potent bioactive molecule that could be also found in various plants¹. Pharmacological studies have demonstrated that emodin is a tumor cell-growth inhibitor and has anti-inflammatory, diuretic, antimicrobial, vasorelaxant and anticancer activities. It has antitumor effects in different types of cancers such as leukemia, breast cancer, colon cancer and others². Emodin is also anthraquinone dye and in its simplest form has yellow color³. Natural pigments and dyes are gaining important role because of their health benefits. They are eco-friendly dyes, biodegradable, easily and safely accessible from various part of the plants. They can be used in many applications such as cosmetic industry, food processing and in pharmaceutical industry⁴.

We will show comparison of dyeing properties of naturally extracted emodin from rhizome of Japanese Knotweed with chemically modified derivatives of emodin for dyeing of various textiles. Yellow colored emodin was extracted from rhizome with organic solvents. Aromatic rings of emodin offers entry point for introduction of various functional groups and we studied nitration, sulfonation, chlorination and bromination. With the use of emodin and its derivatives differently colored textiles (from yellow, orange, violet, red to brown-black) were obtained.



Scheme 1: Introduction of various functional groups to emodin and colored textile material.

1. Izhaki, I., Emodin – a secondary metabolite with multiple ecological functions in higher plants. *New Phytologist* **2002**, *155*, 205-217.
2. Sanders, B.; Woolger, J. M.; Lewis, J. E., Anti-cancer effects of aloe-emodin: a systematic review. *Journal of clinical and translational research* **2017**, *3*, 283-296.
3. Bechtold Thomas, M. R., *Handbook of Natural Colorants*. Wiley: 2009.
4. Shahid, M.; Shahid ul, I.; Mohammad, F., Recent advancements in natural dye applications: a review. *Journal of Cleaner Production* **2013**, *53*, 310-331.

Analysis of functional interplay between orthocaspases and toxin-antitoxin systems in cyanobacteria

Anže Vozelj^{1,2}, Ana Halužan Vasle¹, Aleksandra Uzar¹, Marina Klemenčič¹, Marko Dolinar*¹

¹ Faculty of Chemistry and Chemical Technology, University of Ljubljana, Večna pot 113, SI-1000 Ljubljana, Slovenia, marko.dolinar@fkkt.uni-lj.si,

² Biotechnical Faculty, University of Ljubljana, Večna pot 113, SI-1000 Ljubljana, Slovenia

Caspases are among the best characterized proteases, known to be involved in processes of regulated cell death in animals. Genes coding for structurally homologous proteins can also be found in bacteria and are especially abundant in cyanobacteria. We have been the first to biochemically characterize these proteins and have – due to their catalytic properties and evolutionary early emergence – termed them orthocaspases¹.

Analyzing the genome of the bloom-forming cyanobacterium *Microcystis aeruginosa*, strain PCC 7806, we observed that orthocaspase MaOC1 is encoded next to two putative toxin-antitoxin systems, which belong to superfamilies ParE/RelE and VapB/VapC, respectively (Fig. 1)². Moreover, we observed that the first antitoxin downstream of the orthocaspase gene contains several Arg-Arg motives, which are preferred cleavage sites for MaOC1. We expressed the two antitoxins and were able to show that MaOC1 specifically cleaves one of them.

We are currently constructing vectors, which would enable differential expression of either (or both) an orthocaspase gene and/or the toxin/antitoxin gene under control of two different inducible promoters for assesment of the functional interplay of orthocaspases and toxin-antitoxin proteins *in vivo*.

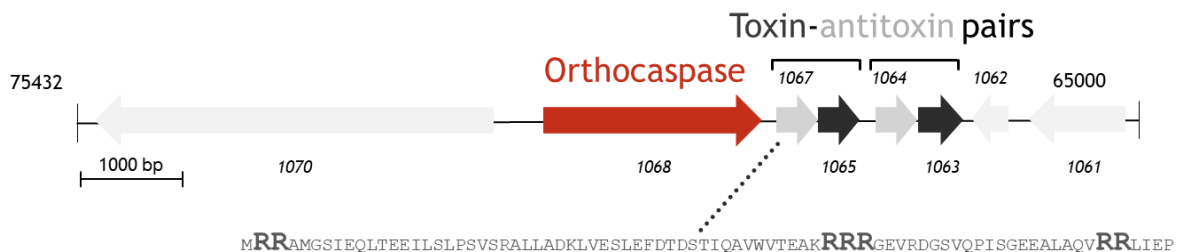


Figure 1: In the cyanobacterium *Microcystis aeruginosa* PCC 7806, orthocaspase *MaOC1* gene is followed by two toxin-antitoxin loci. MaOC1 orthocaspase specifically cleaves antitoxin 1067, encoded by a gene that directly follows the orthocaspase gene.

1. Klemenčič, M.; Novinec, M.; Dolinar, M. Orthocaspases Are Proteolytically Active Prokaryotic Caspase Homologues: The Case of *Microcystis Aeruginosa*. *Mol. Microbiol.* **2015**, *98*, 142–150. <https://doi.org/10.1111/mmi.13110>.
2. Klemenčič, M.; Dolinar, M. Orthocaspase and Toxin-Antitoxin Loci Rubbing Shoulders in the Genome of *Microcystis Aeruginosa* PCC 7806. *Curr. Genet.* **2016**, *62*, 669–675. <https://doi.org/10.1007/s00294-016-0582-6>.

Development of a TRAP-seq method, modified for study of hypersensitive response in PVY-infected cells of *Solanum tuberosum*

Mojca Juteršek*, Kristina Gruden, Špela Baebler

Department of Systems Biology and Biotechnology, National Institute of Biology, Večna pot 111, SI-1000 Ljubljana, Slovenia, mojca.jutersek@nib.si

Potato virus Y (PVY) is economically most devastating viral potato (*Solanum tuberosum*) pathogen. The severity of disease symptoms in PVY-infected potato plants depends on many factors and is the result of different plant-virus interactions. The latter range from compatible or susceptible, where virus can successfully replicate and invade the plant, to incompatible or resistant, where virus replication is limited to initially infected cells (extreme resistance - ER) or their surrounding tissue (hypersensitive response – HR).

To complete our understanding of molecular mechanisms underlying the HR we have been performing transcriptomic analyses of potato leaves infected with PVY¹. However, because only a low number of leaf cells is actually infected in HR, their transcriptional response is masked by the whole leaf transcriptome. To overcome this, we have designed and constructed a modified PVY clone, which includes a tagged potato ribosomal protein that is incorporated in ribosomal complexes of infected potato cells. With a modified TRAP-seq method², we will be able to isolate and analyze mRNAs from infected cells only, maximizing the signal and potentially finding the most important molecular components of the HR in PVY-infected cells.

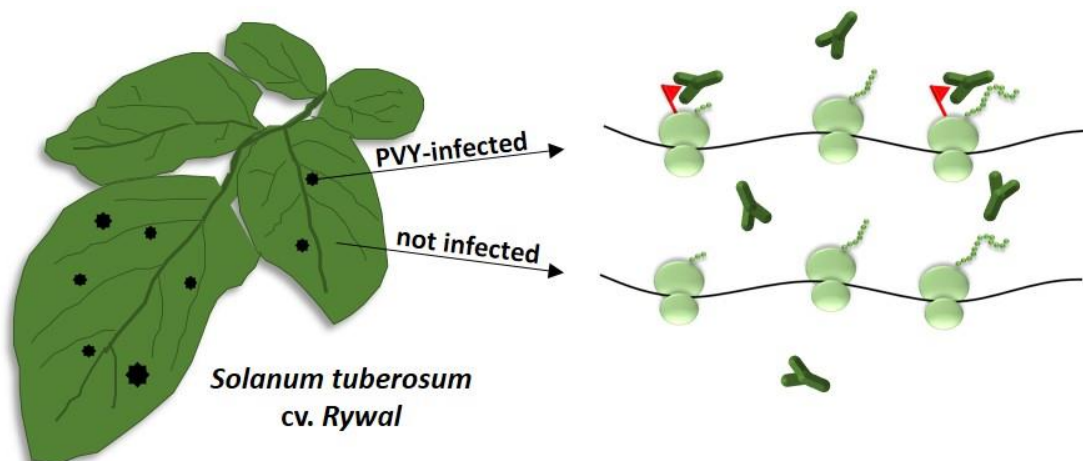


Figure 1: Overview of a modified TRAP-seq method for isolation of mRNA from PVY-infected cells.

1. Baebler, Š.; Witek, K.; Petek, M.; Stare, K.; Tušek-Žnidarič, M.; Pompe-Novak, M.; Renaut, J.; Szajko, K.; Strzelczyk-Zyta, D.; Marczewski, W.; Morgiewicz, K.; Gruden, K.; Hennig, J., Salicylic acid is an indispensable component of the Ny-1-resistance-gene-mediated response against Potato virus Y infection in potato. *J. Exp. Bot.* **2014**, *65*, 1095-1109.
2. Zanetti, M. E.; Chang, I.-F.; Gong, F.; Galbraith, D. W.; Bailey-Serres, J., Immunopurification of polyribosomal complexes of Arabidopsis for global analysis of gene expression. *Plant Physiol.* **2005**, *138*, 624-635.

Enhancing nanobodies as crystallization chaperones with engineered metal-binding sites

Nejc Arh,^{1,2} Gregor Gunčar*¹

¹ Faculty of Chemistry and Chemical Technology, University of Ljubljana, Večna pot 113, SI-1000 Ljubljana, Slovenia, gregor.guncar@fkkt.uni-lj.si

² Faculty of Medicine, Lund University, Sölvegatan 19, SE-22100 Lund, Sweden

X-ray diffraction is the most common method of unraveling the 3D structures of proteins¹. Obtaining protein crystals remains both a key and elusive step in many cases. In this project, we used a computational approach to design modified nanobodies, single-domain antibodies found in camelids, to assist in target protein crystallization. First, we analyzed existing crystal structures containing either nanobodies or metal contacts. In one structure (PDB 5IMO)², we found a symmetrical pair of nanobodies with a large contact surface (Figure 1, left). We tried to reinforce this baseline structure by adding tetrahedral or octahedral metal coordination geometries using a brute-force rotamer search. In this way, we generated thousands of structures belonging to hundreds of mutation sets. With automated sorting and manual analysis, we chose 6 top candidates, out of which we chose “4O3” (one predicted complex shown in Figure I, right) for expression and testing. We successfully purified the modified 4O3 nanobody and showed that it retains binding to the original target – MLKL. While 4O3 did seem to form weak dimers in a solution of cobalt ions, further work is needed to confirm this approach. The script used in this project is already publicly available³, and a general-purpose version for arbitrary protein pairs is in the works.

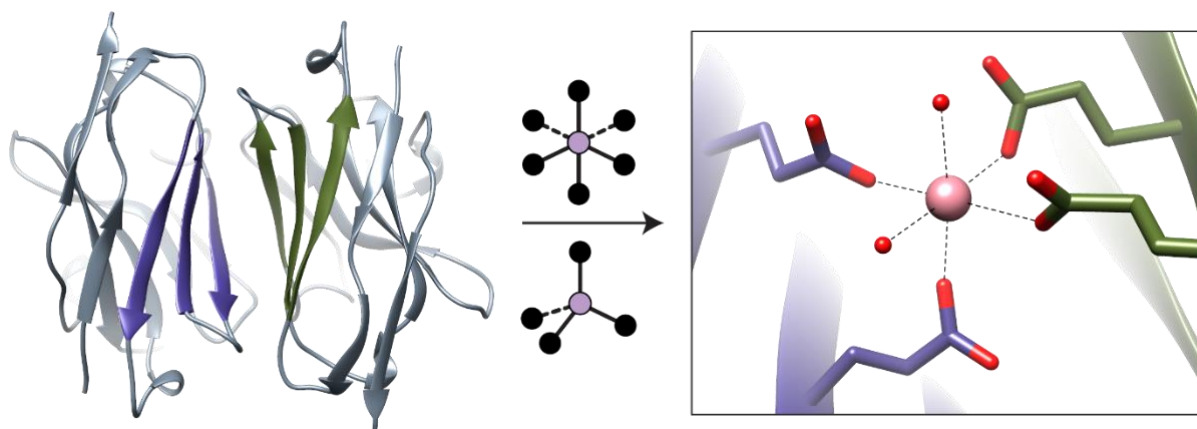


Figure 1: Symmetrical pair of nanobodies and one of the designed metal coordination sites.

1. Berman, H. M.; Westbrook, J.; Feng, Z.; Gilliland, G.; Bhat, T. N.; Weissig, H.; Shindyalov, I. N.; Bourne, P. E. The Protein Data Bank. *Nucleic Acids Res.* **2000**, *28*, 235–242.
2. Wen, Y.; Ouyang, Z.; Schoonooghe, S.; Luo, S.; De Baetselier, P.; Lu, W.; Muyldermans, S.; Raes, G.; Zheng, F. Structural Evaluation of a Nanobody Targeting Complement Receptor Vsig4 and Its Cross Reactivity. *Immunobiology* **2017**, *222*, 807–813.
3. Arh, N. Thesis_nanobody. GitHub. **2018**. https://github.com/nejcarh/thesis_nanobody

Secret biochemical weapon of plants: allelopathy

Katarina Šoln*¹, Jasna Dolenc Koce¹

¹ Biotechnical faculty, University of Ljubljana, Večna pot 111, SI-1000 Ljubljana, Slovenia,
katarina.soln@bf.uni-lj.si

Plants compete for nutrients, water and light. Some plants can release special secondary compounds in the soil, which can inhibit germination and growth of nearby plants. This process is called allelopathy and enables plants to grow faster compared to their plant neighbours¹. Japanese knotweed (*Fallopia japonica*) and Bohemian knotweed (*F. ×bohemica*) are invasive plants, which exploit allelopathic activity to spread across Europe and North America. The aim of our study was to evaluate allelopathic potential of knotweeds rhizome extracts on early growth of seedlings. Seeds of radish (*Raphanus sativus*) were treated with aqueous extracts of knotweed rhizomes in a range of concentrations. Morphological and biochemical changes were analyzed after 3, 5 and 7 days.

Extracts of invasive knotweeds strongly inhibited early growth of radish: root growth was suppressed up to 60%, whereas shoot length of treated plants was up to 20% shorter compared to control plants. Morphological changes can be related to biochemical parameters (total antioxidative capacity, lipid peroxidation, activity of antioxidative enzymes), which changed according to the control treatment. Staining with diaminobenzidine showed increased accumulation of hydrogen peroxide in roots of treated plants. Extracts' mode of action was concentration-dependent and mostly not species specific, which is in accordance with previous study².

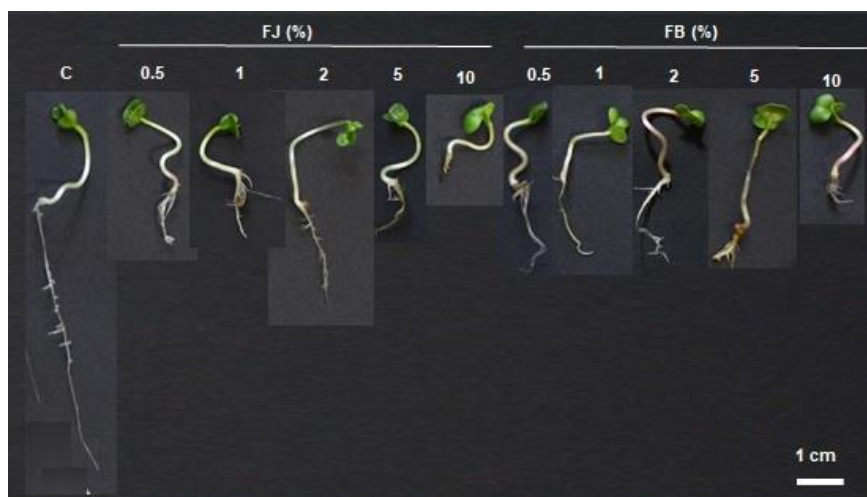


Figure 1: Radish seedlings of control treatment (C) and treatments with extracts of *F. japonica* (FJ) and *F. ×bohemica* (FB) rhizome.

1. Gniazdowska, A.; Bogatek, R., Allelopathic interactions between plants. Multi site action of allelochemicals. *Acta Physiologiae Plantarum* **2005**, *27*, 38, 395-407.
2. Dolenc Koce, J.; Šoln, K., Phytotoxic effects of *Fallopia japonica* and *F. ×bohemica* leaves. *Phyton*. **2018**, *57*, 47-57.

Assessing energy consumption of wastewater treatment plant

Klemen Zupančič^{1*}, Marjetka Levstek², Marjetka Stražar², Andreja Žgajnar Gotvajn¹,

¹ Faculty of Chemistry and Chemical Technology, University of Ljubljana, Večna pot 113, SI-1000 Ljubljana, Slovenia, klemen.zupancic95@gmail.com

² JP CČN Domžale-Kamnik d.o.o., Študljanska 91, SI-1230 Domžale, Slovenia.

Assessing energy consumption of wastewater treatment plant (WWTP) to reduce energy consumption and at the same time increasing production of renewable energy is the first step towards sustainable development and achieving energy neutrality.

The aim of the work was to assess energy consumption for Domžale-Kamnik WWTP, Slovenia using “Benchmarking” method which is fundamental tool in assessing energy consumption and energy conservation potential, by determining the values of process indicators for population equivalents (PE), such as specific electrical energy consumption [kWh/PE_{year}], specific production of electrical energy [kWh/PE_{year}], electrical energy aeration consumption [kWh/PE_{year}], degree of electrical energy consumption for aeration [%], self-sufficiency [%] and specific production of biogas [L/PE_{day}]. Assessment was also made by the method presented as a part of Enerwater project, which is used for developing standard methodology for continuously assessing, labeling and improving the overall energy performance of WWTPs.

The aim of Enerwater project is to establish water treatment energy index (WTEI, Table 1), which assigns WWTPs to different energy labels, that incentive possible optimization.

Table 1: Energy label assignation for WTEI.

Label	WTEI
A	≤0.11
B	0.11 < WTEI ≤ 0.22
C	0.22 < WTEI ≤ 0.33
D	0.33 < WTEI ≤ 0.44
E	0.44 < WTEI ≤ 0.55
F	0.55 < WTEI ≤ 0.75
G	>0.75

1. Maktabifard, M., Zaborowska, E., Makinia, J. Achieving energy neutrality in wastewater treatment plants through energy savings and enhancing renewable energy production. *Reviews in Environmental Science and Bio/Technology* **2018**, 17(4), 655–689.
2. Janičijević, U. Poraba energije v komunalni čistilni napravi. B.Sc. Dissertation, *Faculty of Chemistry and Chemical Technology*, **2016**.
3. Enerwater: Standard method and online tool for assessing and improving the energy efficiency of waste water treatment plants. <http://www.enerwater.eu/wp-content/uploads/2015/10/D3.4-ENERWATER-Oct18-1.pdf>, (accessed Jun 20, 2019).

Identification of volatile compounds in indigenous wines and musts' with headspace GC-MS analysis

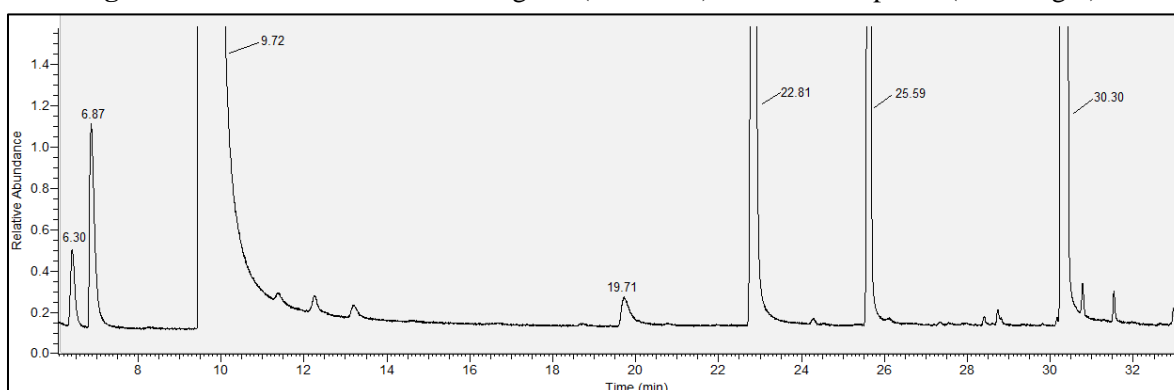
Ema Gričar^{1*}, Jernej Iskra¹, Mitja Kolar¹

¹ Faculty of Chemistry and Chemical Technology, University of Ljubljana, Večna pot 113, SI-1000 Ljubljana, Slovenia, ema.gricar@fkkt.uni-lj.si

With different wine varieties brought to Europe from North America also vine louse (*Viteus vitifoliae*) came that destroyed many vineyards all over Europe.¹ Various hybrids had to be developed to produce vines that were immune to *Viteus vitifoliae* and would survive in European climate. Those indigenous sorts were soon withdrawn from the market because of suspected high methanol content.²

Using headspace GC-MS analysis the volatile compounds in indigenous wines from Dolenjska region were profiled. The samples were acquired at various stages during the fermentation process and were immediately frozen. They were melted right before GC-MS analysis. Using mass spectra library NIST MS Search 2.0, the peaks on the chromatogram were identified (Figure 1). Because of possible high methanol content the determination of methanol was conducted using standard addition method and it was concluded that with the proper production process it does not exceed the permissible limit concentration.³

Figure 1: Section from the chromatogram (6–20 min) with marked peaks (left to right) for



acetaldehyde (6.30 min), methanol (6.87 min), ethanol (9.72 min), 1-propanol (19.71 min), ethyl acetate (22.81 min), isobutyl alcohol (25.59 min) and isoamyl alcohol (30.30 min).

1. Ardenghi, N. M. G.; Galasso, G.; Banfi, E.; Cauzzi, P., *Vitis x novae-angliae* (Vitaceae): systematics, distribution and history of an “illegal” alien grape in Europe. *BIOONE* **2015**, 45,197-207.
2. Breider, H.; Wolf, E., Qualität und Resistenz V. Über das Vorkommen von Biostatica in der Gattung *Vitis* und ihren Bastarden. *Der Züchter* **1966**, 36.
3. Paine, A. J.; Dayan, A. D., Defining a tolerable concentration of methanol in alcoholic drinks. *Human Exp. Toxicol.* **2001**, 20, 563-568.

Oxidation of substituted pyrazolidin-3-ones by photoredox catalysis

Nejc Petek,¹ Bogdan Štefane,^{*1} Uroš Grošelj,¹ Franc Požgan,¹ Jurij Svete¹

¹ Faculty of Chemistry and Chemical Technology, University of Ljubljana, Večna pot 113, SI-1000 Ljubljana, Slovenia, bogdan.stefane@fkkt.uni-lj.si

Pyrazolidin-3-ones react with aldehydes to give azomethine imines **1** which are often used as building blocks for the synthesis of more complex heterocyclic systems. They can, for example, undergo [3+2] cycloaddition with various dipolarophiles.¹ N-substituted pyrazolidinones **2** are prone to oxidation on the site adjacent to N1. We have shown that the oxidation can be achieved by photoredox oxidation with a suitable catalyst under light irradiation with oxygen from air as a terminal oxidant. That leads to the formation of azomethine imines **1**, which can be subsequently transformed to pyrazolo[1,2-*a*]pyrazoles **3** by an *in situ* copper-catalysed [3+2] cycloaddition (Fig. 1). Photoredox catalytical approach, already often employed in the synthesis of organic compounds,² is as such environmentally and economically favourable in oxidation of pyrazolidin-3-ones.

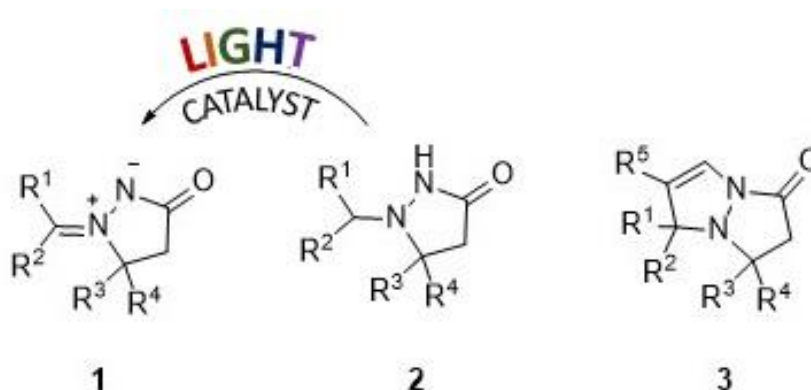


Figure 2: Structures of pyrazolidin-3-ones, oxidation intermediates and cycloaddition products.

1. Nájera, C.; Sansano, J. M.; Yus, M., 1,3-Dipolar cycloadditions of azomethine imines. *Org. Biomol. Chem.* **2015**, *13*, 8596-8636.
2. Marzo, L.; Pagire, S. K.; Reiser, O.; König B., Visible-Light Photocatalysis: Does It Make a Difference in Organic Synthesis? *Angew. Chem. Int. Ed.* **2018**, *57*, 10034-10072.

Organic peroxides and their heteroatom derivatives stabilized with BODIPY scaffold

Griša Grigorij Prinčič,¹ Matic Lozinšek,^{1,2} Jernej Iskra,^{1*}

¹ University of Ljubljana, Faculty of Chemistry and Chemical Technology, Department of Chemistry and Biochemistry, Večna pot 113, SI-1000 Ljubljana, Slovenia, jernej.iskra@fkkt.uni-lj.si

² Jožef Stefan Institute, Jamova cesta 39, SI-1000 Ljubljana, Slovenia

Hydrogen peroxide is a rather simple, unstable inorganic compound mostly used in processes of oxidation and as a polymerization initiator in industry. Reactions of this molecule are, however, not limited only to oxidations. Peroxide bond can also be incorporated into organic scaffolds to produce a rather interesting group of molecules – organic peroxides. This type of compounds has gained a substantial attraction in the past years due to discovery of artemisinin, a peroxide containing natural product with substantial antimalarial activity.¹

Our work mainly focuses on reactions and transformations of organic peroxides mainly *gem*-dihydroperoxides and products of cyclization such as 1,2,4,5-tetraoxanes (TO). TOs are a group of cyclic molecules with 2 O-O bonds and proven antimalarial activity. They can be produced by a condensation reaction of *gem*-dihydroperoxide and a carbonyl compound with an acid catalyst and a fluorinated alcohol as a solvent (template catalysis) (Figure 1). Especially interesting are phenyl substituted TOs due to their antitubercular activity. Electron withdrawing groups on aromatic ring, however, abolish the production of TO so we devised a new synthetic pathway that allows for production of such compounds. During the research, we come to an interesting method that enables synthesis of boron peroxides, a group of compounds with only 5 known structures to date³. Boron-peroxide bond is generally unstable and the key to stability lies in a proper selection of ligand that stabilizes the structure.

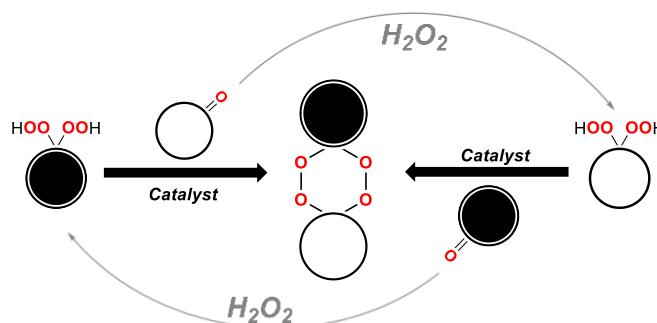


Figure 8: Synthetic scheme for TO production.

1. V.A. Vil, Peroxides with Anthelmintic, Antiprotozoal, Fungicidal and Antiviral Bioactivity: Properties, Synthesis and Reactions. *Molecules*, **2017** 22, 1881-2211.
2. Starkl, K., Activation of aqueous hydrogen peroxide for non-catalyzed dihydroperoxidation of ketones by azeotropic removal of water. *Org. Biomol. Chem.* **2015**, 13, 9369-9372.
3. Tsurumaki, E., Boron Peroxides Stable Boron Peroxides with a Subporphyrinato Ligand. *Angew Chem.* **2016**, 2596-2599.

Organoruthenated nitroxoline inhibitors of cathepsin B with potent antimetastatic properties

Ana Mitrović^{1,2} and Jakob Kljun³, Izidor Sosič¹, Matija Uršič³, Anton Meden³, Stanislav Gobec¹, Janko Kos^{1,2}, Iztok Turel³

¹ Faculty of Pharmacy, University of Ljubljana, Aškerčeva c. 7, SI-1000 Ljubljana, Slovenia

² Department of Biotechnology, Jožef Stefan Institute, Jamova c. 39, SI-1000 Ljubljana, Slovenia

³ Faculty of Chemistry and Chemical Technology, University of Ljubljana, Večna pot 113, SI-1000 Ljubljana, Slovenia; jakob.kljun@fkkt.uni-lj.si

Cathepsin B (EC 3.4.22.1; catB) is a lysosomal cysteine peptidase that belongs to clan CA of the papain family (C1). The proteolytic activity of this enzyme is crucial in the mechanisms of cancer progression. In 2011, we identified antibacterial agent nitroxoline (nxH), a member of 8-hydroxyquinolone (hq) family, as a potent reversible inhibitor of catB.¹ Nitroxoline and its 7-substituted derivatives were found to potently impair tumor progression in both *in vitro* and *in vivo* models and these effects correlated with catB inhibition.^{2,3} We continued the exploration of the chemical space of 5-nitroquinoline scaffold by introducing metal-containing fragments to positions 1 and 8 of the nitroxoline ring.⁴

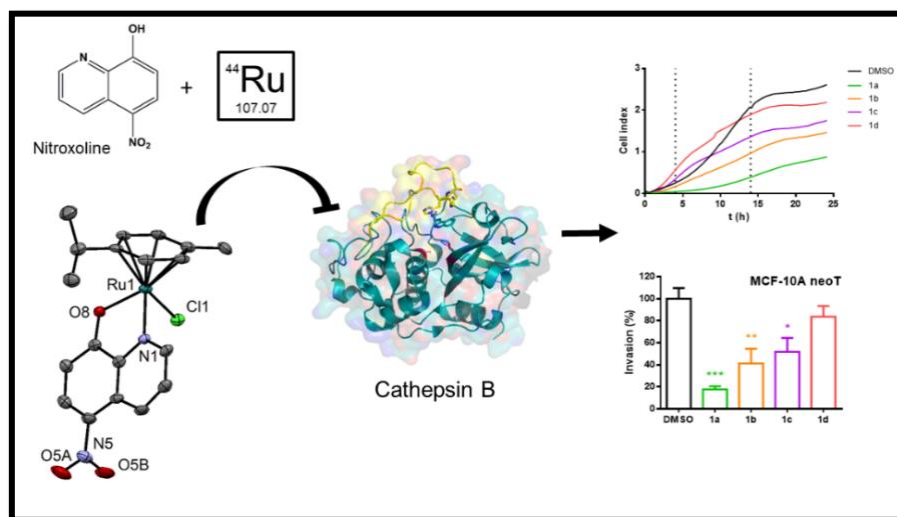


Figure 1: The potency of catB inhibition and tumor invasion depend on the reactivity of the monodentate leaving ligand. **1a** (Cl^-) > **1b** (Br^-) > **1c** (I^-) > **1d** (N_3^-).

1. Mirkovic, B.; Renko, M.; Turk, S.; Susic, I.; Jevnikar, Z.; Obermajer, N.; Turk, D.; Gobec, S.; Kos, J., Novel Mechanism of Cathepsin B Inhibition by Antibiotic Nitroxoline and Related Compounds. *ChemMedChem* **2011**, *6*, 1351-1356.
2. Mirković, B.; Markelc, B.; Butinar, M.; Mitrović, A.; Sosič, I.; Gobec, S.; Vasiljeva, O.; Turk, B.; Čemežar, M.; Serša, G.; Kos, J., Nitroxoline impairs tumor progression *in vitro* and *in vivo* by regulating cathepsin B activity. *Oncotarget* **2015**, *6*, 19027-19042.
3. Mitrović, A.; Sosič, I.; Kos, Š.; Lamprecht Tratar, U.; Breznik, B.; Kranjc, S.; Mirković, B.; Gobec, S.; Lah, T.; Čemežar, M.; Serša, G.; Kos, J., Addition of 2-(ethylamino)acetonitrile group to nitroxoline results in significantly improved anti-tumor activity *in vitro* and *in vivo*. *Oncotarget* **2017**, *8*, 59136-59147.
4. Mitrović, A.; Kljun, J.; Sosič, I.; Uršič, M.; Meden, A.; Gobec, S.; Kos, J.; Turel, I. Organoruthenated nitroxoline derivatives impair tumor cell invasion through inhibition of cathepsin B activity, *Inorg. Chem.* **2019**, *accepted manuscript*

Synthesis of Nickel-Alumina Promoted Transition Metal Catalysts for Hydrodeoxygenation of Hydroxymethylfurfural

Brett Pomeroy¹, Miha Grilc^{*1}, Blaž Likozar¹

¹ Department of Catalysis and Chemical Reaction Engineering, National Institute of Chemistry, Hajdrihova 19, 1000 Ljubljana, Slovenia

Hydroxymethylfurfural (HMF) has been identified as an important platform chemical with tremendous potential that can be produced from renewable feedstocks such as lignocellulosic biomass. As HMF consists of several functional constituents including an aromatic aldehyde, aromatic alcohol, and furan ring, a wide range of bio-based fuels and chemicals can be chemically converted from HMF as an intermediate¹. The most promising catalytic conversion route of HMF is hydrodeoxygenation (HDO). Typically HDO occurs when heating HMF to moderate temperatures (180-250°C), under high hydrogen pressures (30-50 MPa), and in the presence of a heterogeneous catalyst. Transition metal catalysts are desirable for HDO due to their wide availability and low cost, however, generally require additional promoters and/or supports to improve performance and tune product selectivity. Nickel was chosen as the transition metal and catalysts with varying supports were prepared by incipient wetness impregnation and ammonium precipitation. Catalytic activity tests for HDO of HMF were conducted in 75 mL batch reactors at 175°C and 50 bar H₂ pressure for 2 hours and samples were collected to determine concentration of products as a function of time. Liquid-phase products were analysed via GC-MS and a predicted reaction pathway has been presented that demonstrates a major influence on overall conversion and product selectivity towards hydrogenated products with changes in support and promoter addition. Catalyst characterization including temperature-programmed reduction (TPR), temperature-programmed desorption (TPD), and N₂ adsorption will highlight the impact catalyst composition and morphology has on product selectivity towards DMF during HDO of HMF.

Table 11: HMF Conversion and DMF Selectivity.

	Ni/Al	Ni/C	Ni/Si
C _{HMF} (%)	95,7	13,6	30,1
DMF Selectivity (%)	65,1	82,5	0

Acknowledgments: Authors acknowledge financial support by the EU Framework Programme for Research and Innovation Horizon 2020 under Grant agreement no. 814416 (ReaxPro) and the ARRS (Programme P2-0152 and postdoctoral research project Z2-9200).

1. Menegazzo, F., Ghedini, E., Signoretto, M., 5-Hydroxymethylfurfural (HMF) Production from Real Biomasses. *Molecules*. **2018**, *23*, 2201

Synthesis and anticancer activity of methyl-substituted organoruthenium(II)-pyrithionato complexes

Jerneja Kladnik,¹ Jakob Kljun,¹ Hilke Burmeister,² Ingo Ott,² Isolda Romero-Canelón,³ Iztok Turel^{1,*}

¹ Faculty of Chemistry and Chemical Technology, University of Ljubljana, Večna pot 113, 1000 Ljubljana, Slovenia; iztok.turel@fkkt.uni-lj.si

² Institute of Medicinal and Pharmaceutical Chemistry, Technische Universität Braunschweig, 38106 Braunschweig, Germany

³ School of Pharmacy, Institute of Clinical Sciences, University of Birmingham, Edgbaston, Birmingham, B15 2TT, UK

Pyrithione, a cyclic thiohydroxamic acid, binds *via O*- and *S*- atoms to various metal ions, which express broad spectrum of biological activities. Recently, our research group was the first to report the synthesis of organoruthenium(II) pyrithione complex with potent anticancer activity on MFC-7 breast cancer cells and inhibition of enzymes aldo-keto reductases¹ and glutathione-*S*-transferases, both involved in the cancer progression. Besides, the complex is not toxic to non-cancerous cells and possesses no unwanted effects on the neuromuscular system.² As we were interested how minor structural alterations could potentially tune anticancer properties an array of methyl-substituted pyrithiones and their organoruthenium(II)-chlorido and -pta (1,3,5-triaza-7-phosphaadamantane) complexes (**Figure 1**) has been prepared and screened on seven cancer cell lines. Best-performing chlorido and pta complexes with pyrithione ligand with methyl substituent on 3-position were further evaluated for cell cycle analysis, induction of apoptosis, ROS generation, protein binding and thioredoxin reductase inhibition to gain a better insight into underlying mechanism on cellular level.

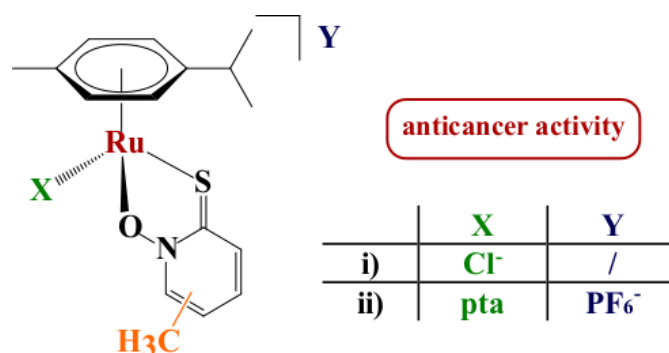


Figure 1: Organoruthenium(II) methyl-substituted-pyrithionato complexes.

1. Kljun, J.; Anko, M.; Traven, K.; Sinreih, M.; Ude, Ž.; Codina, E. E.; Stojan, J.; Lanišnik Rižner, T.; Turel, I., Pyrithione-based ruthenium complexes as inhibitors of aldo-keto reductase 1C enzymes and anticancer agents. *Dalton Trans.* **2016**, 45, 11791-11800.
2. Ristovski, S.; Uzelac, M.; Kljun, J.; Lipec, T.; Uršič, M.; Zemljič Jokhadar, Š.; Žužek, M. C.; Trobec, T.; Frangež, R.; Sepčić, K.; Turel, I., Organoruthenium prodrugs as a new class of cholinesterase and glutathione-*S*-transferase inhibitors. *ChemMedChem* **2018**, 13, 2166-2176.

Nanoparticle Analysis in Biomaterials Using Laser Ablation–Single Particle–Inductively Coupled Plasma Mass Spectrometry

Dino Metarapi,^{1,2} Johannes T. van Elteren,¹ Katarina Vogel-Mikuš,^{3,4} Martin Šala,¹ Vid S. Šelih,¹ Mitja Kolar*²

¹ Department of Analytical Chemistry, National Institute of Chemistry, Hajdrihova 19, 1000 Ljubljana, Slovenia

² Faculty of Chemistry and Chemical Technology, University of Ljubljana, Večna pot 113, 1000 Ljubljana, Slovenia, Mitja.Kolar@fkkt.uni-lj.si

³ University of Ljubljana, Biotechnical Faculty, Jamnikarjeva 101, SI-1000 Ljubljana, Slovenia

⁴ Jožef Stefan Institute, Jamova 39, SI-1000 Ljubljana, Slovenia

In the past decade, the development of single particle–inductively coupled plasma mass spectrometry (SP-ICPMS) has revolutionized the field of nanometallomics¹. SP-ICPMS is able to quantify the nanoparticle (NP) number concentration and determine the NP size². As SP-ICPMS is limited to analysis of NPs in solution, we show how solid sampling by laser ablation (LA) adds spatial-resolution characteristics for localized NP analysis in biomaterials. Using custom-made gelatin standards doped with dissolved gold and gold nanoparticles, LA-SP-ICPMS conditions were optimized for NP analysis. A sunflower-root-sample cross-section, originating from a sunflower plant exposed to gold NPs, was successfully imaged using the optimized LA-SP-ICPMS conditions for localized NP characterization³.

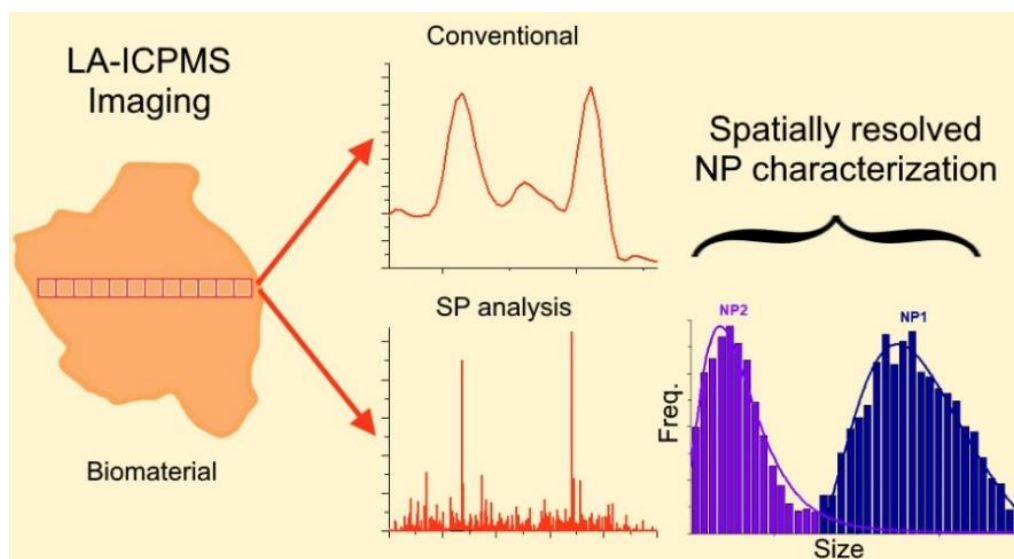


Figure 1: Concept of NP analysis in biomaterials using LA-SP-ICPMS.

1. Degueldre C.; Favarger P.-Y.; Wold S., Gold colloid analysis by inductively coupled plasma-mass spectrometry in a single particle mode. *Anal. Chim. Acta* **2006**, 555, 2, 263-268.
2. Montano M.D.; Olesik J.W.; Barber A.G.; Challis K.; Raneville J.F., Single Particle ICP-MS: Advances toward routine analysis of nanomaterials. *Anal. Bioanal. Chem.* **2016**, 408, 19, 5053-5074.
3. Metarapi D.; Šala M.; Vogel-Mikuš K.; Šelih V.S.; van Elteren J.T., Nanoparticle Analysis in Biomaterials Using Laser Ablation–Single Particle–Inductively Coupled Plasma Mass Spectrometry. *Anal. Chem.* **2019**, 91, 9, 6200-6205.

Formation of ammonia during the synthesis of zinc quinaldinate complexes with alcoholamine ligands in autoclaves

Nina Podjed,¹ Romana Cerc Korošec,¹ Barbara Modec^{1,*}

¹ Faculty of Chemistry and Chemical Technology, University of Ljubljana, Večna pot 113, SI-1000 Ljubljana, Slovenia, barbara.modec@fkkt.uni-lj.si

A great deal of interest in zinc coordination compounds arises from the fact that zinc is an essential trace element that is necessary for all organisms. Previous work was based on zinc(II) complexes with quinaldinate and pyridine-based ligands.¹ Our next goal was preparation of compounds with alcoholamine ligands instead of pyridines. A facile substitution of methanol or water in $[\text{Zn}(\text{quinal})_2(\text{CH}_3\text{OH})_2]^2$ or $[\text{Zn}(\text{quinal})_2(\text{H}_2\text{O})]^3$ (quinal⁻ stands for anion of quinoline-2-carboxylic acid, commonly known as quinaldic acid) with alcoholamine ligand should yield desired complexes. The first ligands of choice were 3-aminopropan-1-ol (abbreviated as 3-AmPrOH) and 2-(methylamino)ethanol (nmea). The syntheses were performed in autoclaves, but instead of desired products, a complex with ammonia, $[\text{Zn}(\text{quinal})_2\text{NH}_3]$, was obtained. Its formation was unambiguously confirmed with single crystal X-ray diffraction (**Figure 1**) and with infrared spectroscopy. The formation of ammonia was confirmed in reaction mixtures in autoclaves with acetonitrile solvent as a prerequisite by means of mass spectrometry (MS) of gas phase. The desired complexes could only be obtained in good yields by using a different solvent and/or carrying out the reaction at room temperature or at reflux.

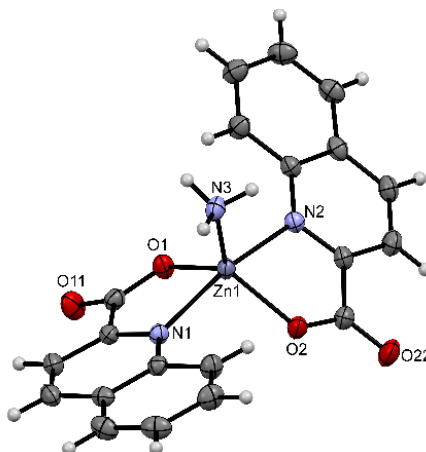


Figure 1: ORTEP drawing of $[\text{Zn}(\text{quinal})_2\text{NH}_3]$. Thermal ellipsoids are shown at 50 % probability level.

1. Modec, B., Crystal chemistry of zinc quinaldinate complexes with pyridine-based ligands. *Crystals* **2018**, *8*, 52-73.
2. Yue, Z. Y.; Cheng, C.; Gao, P.; Yan, P. F., *trans*-Bis-(methanol- κO)-bis(2-quinoline-carboxylato- $\kappa^2 N, O$)-zinc(II). *Acta Cryst. E* **2004**, *E60*, m82-m84.
3. Okabe, N.; Muranishi, Y., Aquabis(quinoline-2-carboxylato- $\kappa^2 N, O$)zinc(II). *Acta Cryst. E* **2003**, *E59*, m244-m246.

Self-healing effect in bio-concrete

Petra Štukovnik², Violeta Bokan Bosiljkov², Andrej Ipavec⁴, Rok Novak¹, Jure Starc², Mojca Legan¹, Luka Stare², Tanja Buh¹, Klavdija Kastelic², Bor Gorjup³, Marjan Marinšek^{1*}

¹ Faculty of Chemistry and Chemical Technology, University of Ljubljana, Večna pot 113, p.p. 3422 SI-1000 Ljubljana, Slovenia, marjan.marinsek@fkkt.uni-lj.si

² Faculty of Civil and Geodetic Engineering, University of Ljubljana, Jamova cesta 2, 1001 Ljubljana, Slovenia

³ School of Economics and Business, University of Ljubljana, Kardeljeva ploščad 17, 1000 Ljubljana, Slovenia

⁴ Salonit Anhovo, d.d., Anhovo 1, 5210 Deskle, Slovenia

Concrete is the most widely used construction material. It is mainly a combination of water, aggregate and cement. Despite concrete's many advantages, it has a high tendency to form cracks, which need to be treated. Active treatment techniques of cracks are also known as self-healing techniques and involve microbial production of calcium carbonate through biomineralization.² In such process biominerals are formed through successful attachment of the positively charged Ca^{2+} ions from the surroundings to the negatively charged microbial cell walls (Fig. 1). Calcium carbonate is produced by microorganisms extracellularly through preferable heterotrophic metabolic pathway. The bacteria use organic compounds as a source of energy. Among several metabolic cycles metabolic conversion of calcium lactate overcomes many drawbacks associated with other metabolic cycles.³ Regarding self-healing effect in bio-concretes some opened questions remain; i.e. potential applicability of some bacteria and their embedding into the concrete, activity of bacteria in different environments, as well as embedding and concentration of nutrients. Finally yet importantly, apart from concrete robustness, bio concrete production cost is another challenge. Experimental work within the project included preparation of bio-concrete using commercial self-healing agent and subsequent deliberately introduced cracks formation. Through the in depth investigations of aged bio-concretes' mechanical properties and their gradually changed microstructure were systematically answered (Fig. 1).

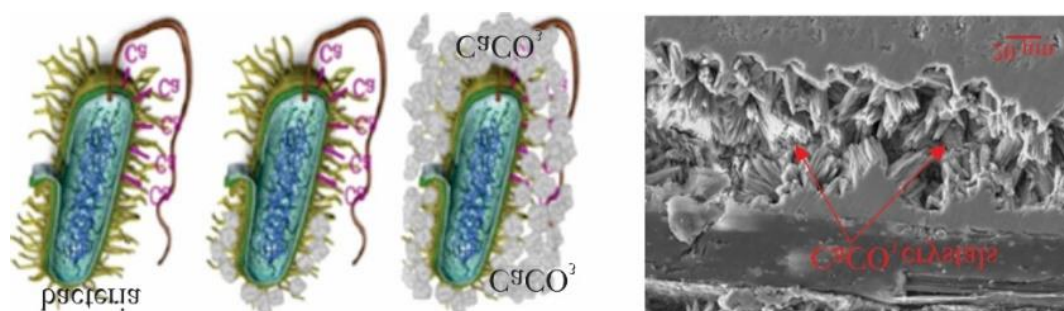


Figure 1 : CaCO_3 formation on bacterial cell wall.¹(left) Crack in bio-concrete filled with CaCO_3 (Right).

1. Vijay K., Murmu M., Deo S.V., Bacteria based self healing concrete – A review. *Construction and Building Materials* **2017**, 152, 1008–1014
2. Seifan M., Semani A.K., Berenjian A., Bioconcrete: next generation of self-healing concrete. *Applied Microbiology and Biotechnology*, **2016**, 100, 2591–2602
3. Khaliq W., Ehsan M.B., Crack healing in concrete using various bio influenced self-healing techniques. *Constr. Build. Mater.*, **2016**, 102, 349-357

Characterization of succinimide amino acid derivatives as allosteric effectors of cathepsin L

Ana Obaha¹, Tjaša Goričan¹, Marko Novinec¹

¹ Faculty of Chemistry and Chemical Technology, University of Ljubljana, Večna pot 113, SI-1000 Ljubljana, Slovenia

Human cathepsin L is a papain-like cysteine endopeptidase expressed in most cells. It is present in lysosomes, where it has crucial roles in protein degradation, antigen presentation and processing of the invariant chain. In lower concentrations it is also found in the nucleus, where it regulates the progression from G1 to S phase in the cell cycle¹. The enzyme is also excessively active in patients with arterosclerosis² and therefore a potential target for its the treatment of this disease. Allosteric inhibitors which bind to sites distant from the active site are a promising emerging strategy for the targeting of papain-like peptidases. With this approach we can achieve greater specificity than with orthosteric inhibitors, since the active sites of all cathepsin L-like peptidases are very similar.

Our research is focused on identifying cathepsin L as an allosteric enzyme and characterizing the effects of potential allosteric inhibitors from a library of amino acid derivatives of succinimide that were synthesized as potential inhibitors of the related cathepsins K and S. By measuring the activity of cathepsin L with synthetic fluorogenic substrate Z-LR-AMC, we determined the effects of 27 potential inhibitors on the activity of recombinant cathepsin L. Ten compounds did not have any effect on enzyme activity. Ten acted as linear inhibitors and are thus likely to bind into the active site. Seven compounds acted as hyperbolic inhibitors and are thus likely to act via allosteric mechanisms. One of them is Su-Gly-L-Phe-NH₂ which lower cathepsin L activity by 60 %. We predicted its binding mode at the proposed allosteric site with molecular docking (Figure 1). With these findings we determined that cathepsin L is likely an allosteric enzyme. Based on our results, novel compounds will be synthesized with the aim of obtaining compounds with better specificity and affinity for cathepsin L.

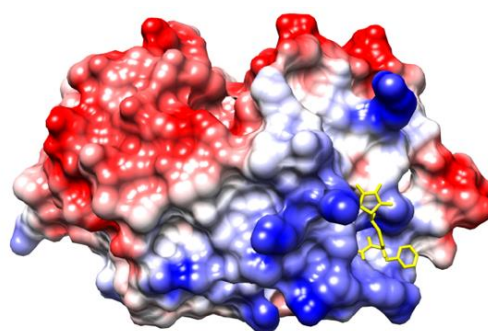


Figure 1: Cathepsin L with active site on top and bound Su-Gly-L-Phe-NH₂. Picture was generated with docking.

1. Kirschke, H. Cathepsin L. *Handb. Proteolytic Enzym.* **2013**, 1808–1817.
2. Liu, J.; Sukhova, G. K.; Yang, J.-T.; Sun, J.; Ma, L.; Ren, A.; Xu, W.-H.; Fu, H.; Dolganov, G. M.; Hu, C.; et al. Cathepsin L Expression and Regulation in Human Abdominal Aortic Aneurysm, Atherosclerosis, and Vascular Cells. *Atherosclerosis* **2006**, *184*, 302–311.

Organoruthenium(II) complex with pyrithione is a potent inhibitor of cholinesterases and glutathione-S-transferase

Samuel Ristovski,¹ Monika Uzelac,¹ Jakob Kljun,² Tanja Lipec,² Matija Uršič,² Špela Zemljič Jokhadar,³ Monika C. Žužek,⁴ Tomaž Trobec,⁴ Robert Frangež,^{4,*} Kristina Sepčić,¹ Iztok Turel²

¹ Department of Biology, Biotechnical Faculty, University of Ljubljana, Jamnikarjeva 101, 1000 Ljubljana, Slovenia

² Faculty of Chemistry and Chemical Technology, University of Ljubljana, Večna pot 113, 1000 Ljubljana, Slovenia

³ Institute of Biophysics, Faculty of Medicine, University of Ljubljana, Vrazov trg 2, 1000 Ljubljana, Slovenia

⁴ Institute of Preclinical Sciences, Veterinary Faculty, University of Ljubljana, Gerbičeva 60, 1000 Ljubljana Slovenia, Robert.Frangez@vf.uni-lj.si

A diverse array of 17 ruthenium(II) compounds with general formula $[\text{Ru}^{\text{II}}(\text{fcl})(\text{chel})(\text{L})]^{\text{n}+}$ (fcl = face capping ligand, chel = chelating bidentate ligand, and L = monodentate ligand) was synthesized and evaluated for their inhibition against human and animal acetylcholinesterases (AChE), butyrylcholinesterase and glutathione-S-transferase (GST) *in vitro*. In a collection of various ruthenium(II) complexes with *N,N*-, *N,O*-, *O,O*- and *S,O*-ligands, only the complex with pyrithione (2-mercaptopyridine-*N*-oxide; **Figure 1**) provided potent competitive inhibition on all above mentioned enzymes. In addition, this compound did not induce inhibitory effect on the AChE in the neuromuscular junction and also any undesirable response on the peripheral neuromuscular system at pharmaceutically relevant concentrations. In these concentrations, this compound did not show any cytotoxic effect against non-transformed cells. Therefore, the compound is interesting for further studies as multitarget drug and can potentially be applicable in veterinary and human medicine.¹



Figure 1: Complex $[(\eta^6\text{-}p\text{-cymene})\text{Ru}(\text{pyrithionato})\text{Cl}]$ – cholinesterase and GST inhibitor.

1. Ristovski, S.; Uzelac, M.; Kljun, J.; Lipec, T.; Uršič, M.; Zemljič Jokhadar, Š.; Žužek, M. C.; Trobec, T.; Frangež, R.; Sepčić, K.; Turel, I., Organoruthenium prodrugs as a new class of cholinesterase and glutathione-S-transferase inhibitors. *ChemMedChem* **2018**, *13*, 2166-2176.

Study of stepped magnesium surface properties with density functional theory

David Ciriković,¹ Anja Kopač Lautar^{2,3}

¹ Faculty of Chemistry and Chemical Technology, University of Ljubljana, Večna pot 113, 1000 Ljubljana, Slovenia

² Department of Materials Chemistry, National Institute of Chemistry, Hajdrihova ulica 19, 1000 Ljubljana, Slovenia

³ Department of Physics, Faculty of Mathematics and Physics, University of Ljubljana, Jadranska ulica 19, 1000 Ljubljana, Slovenia

Understanding the interface stability and morphological changes which occur during continuous stripping and deposition is crucial for further development of batteries.¹ One of the most pressing issues in current battery research is dendrite formation which lead to short-circuiting.² To understand morphology evolution on specific surfaces, we have to look at diffusion barriers with hopping and exchange mechanisms, and surface, adsorption and interaction energies.^{1,3} We have studied the properties of stepped magnesium surfaces ($10\bar{1}9$ and $60\bar{6}4$) using density functional theory and compared the obtained results between stepped and smooth magnesium surface.

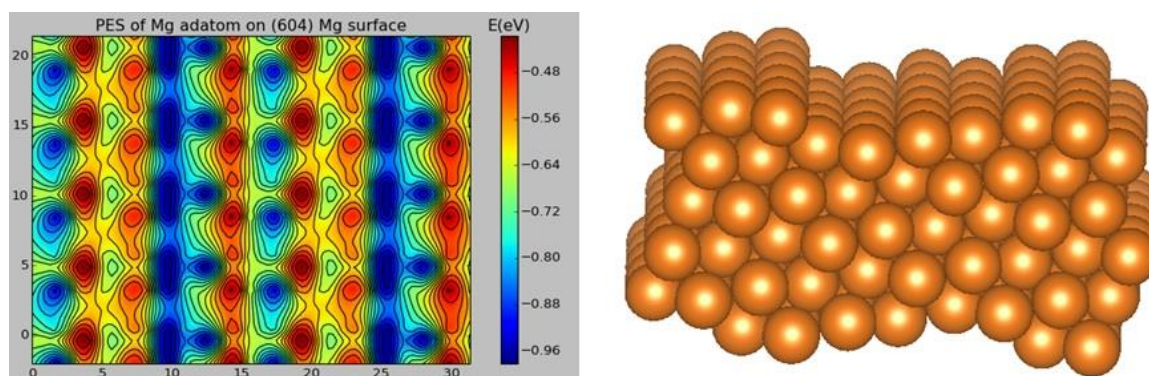


Figure 1: Potential energy surface (PES) result of magnesium stepped surface on the right ($60\bar{4}$).

1. Kopač Lautar, A.; Kopač, D.; Rejec, T.; Bančič, T.; Dominko, R. Morphology Evolution of Magnesium Facets: DFT and KMC Simulations. *Phys. Chem. Chem. Phys.* **2019**, *21*, 2434–2442
2. Jäckle, M.; Groß, A. Microscopic Properties of Lithium, Sodium, and Magnesium Battery Anode Materials Related to Possible Dendrite Growth. *J. Chem. Phys.* **2014**, *141*, 174710
3. Jäckle, M.; Helmbrecht, K.; Smits, M.; Stottmeister, D.; Groß, A. Self-Diffusion Barriers: Possible Descriptors for Dendrite Growth in Batteries? *Energy Environ. Sci.* **2018**, *11*, 3400–3407

Determination of the toxicity of the waterborne epoxy coatings

Leja Pleško^{*,1}, Janez Cerar¹, Andreja Žgajnar Gotvajn¹, Gabriela Kalčikova¹

¹ University of Ljubljana, Faculty of Chemistry and Chemical Technology, Večna pot 113, SI-1000 Ljubljana, Slovenia, plesko.leja@gmail.com

Waterborne epoxy coatings are extensively used, for protection of various surfaces. However they can contain many components that can leach during the lifecycle of the coated product and have negative impact on the environment. The aim of this study was to assess the impact of two-component waterborne epoxy coatings and its components on water flea *Daphnia magna*. The component A contains among others trizinc bis(orthophosphate) and 1-metoxy-2-prophanol, whereas the component B contains zinc oxide and 2-butoxyethanol.

Toxicity tests were carried out separately on the most often used coats (in full composition), as well as separately on their two main components. The respective tests started with the coating of inert glass plate and they were allowed to dry for 24h. Such prepared glass plates with coatings were put in the medium M4 (ISO 10706, 2000) and components were leached, for a period of 24 hours. After leaching the medium was diluted to several concentrations and ten water fleas, not older than 24 hours, were exposed for 48 hours. In case of a good dose-response relationship the results were expressed as 48hEC50.

According to the results component B shows high toxicity, because it contains zinc oxide, which is according to its safety data sheet toxic for water fleas. However, based on our data, it was not possible to determine 48hEC50 in the component B, because inhibition to all tested concentrations was 100%. Component A showed lower toxicity to water fleas the 48hEC50 for it was 22,7 vol.% and is mainly caused by trizinc bis(orthophosphate). Moreover, the result showed that the tested coatings (in full composition) are not as toxic to water fleas as their separate components. Calculated 48hEC50 for tested coating is >100 vol.%.

Table 12: Concentration of the solution and inhibition of water fleas after 48h exposure.

Component A [vol.%]	Inhibition [%]	Component B [vol.%]	Inhibition [%]	Coating [vol.%]	Inhibition [%]
100	90	100	100	100	25
75	85	75	100	75	15
50	65	50	100	50	7,5
25	55	25	100	25	0

1. Piazza, V., Gambardella, C., Garaventa, F., Massanisso, P., Chiavarini, S., Faimali, M., A new approach to testing potential leaching toxicity of fouling release coatings (FRCs). *Marine Environmental Research*. **2018**, 305-312.

Nothobranchius furzeri as a suitable model organism for TDP-43 proteinopathy studies

Jakob Rupert,¹ Alessandro Cellerino,² Annalisa Pastore*,^{2,3,4}

¹ Faculty of Chemistry and Chemical Technology, University of Ljubljana, Večna pot 113, SI-1000 Ljubljana, Slovenia

² Scuola Normale Superiore, Piazza dei Cavalieri 7, Pisa 56126, Italy

³ King's College London, The Strand, London WC2R 2LS, UK

⁴ The Francis Crick Institute, Midland Rd. 1, London NW1 1ST, UK, annalisa.pastore@crick.ac.uk

Several animal models have been developed for the study of TDP-43-mediated diseases, starting from *C. elegans* to mouse, yet one of the limitations is the relatively slow ageing of the animals which dictates the pace by which studies can progress. Recently, a new model was introduced and investigated for the purpose of modelling vertebrate ageing, namely the turquoise killifish *Nothobranchius furzeri*. It has been demonstrated that the remarkably short lifespan of *N. furzeri*, currently the shortest-lived vertebrate available, recapitulates all the hallmarks of vertebrate ageing¹. TAR DNA-binding protein 43 kDa (TDP-43) is an RNA-binding protein involved in RNA metabolism². TDP-43 is mostly studied for its involvement in motor neuron disease amyotrophic lateral sclerosis (ALS), frontotemporal dementia (FTD)³. The comparison of human and *N. furzeri* TDP-43 constructs shows the fish protein behaviour closely resembles the human. *N. furzeri* TDP-43 also binds similar RNA targets and exhibits intriguing alterations of aggregation patterns upon RNA binding (Fig. 1). Our results suggest that *N. furzeri* has the fundamental requirements to be used as model for TDP-43 human biology.

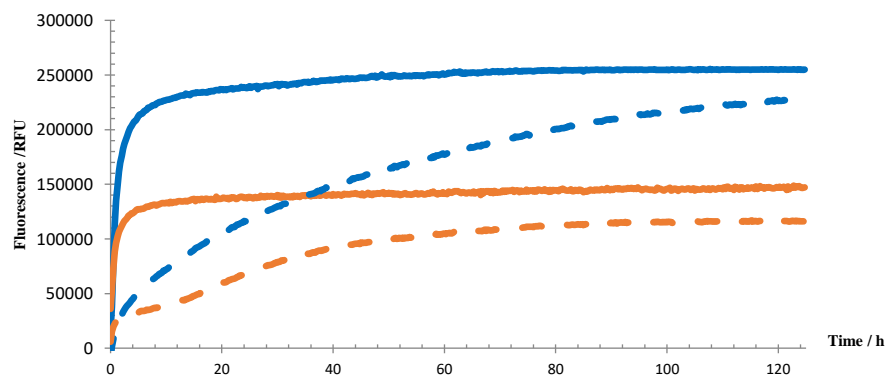


Figure 1. The comparison of human (orange) and *N. furzeri* (blue) N-RRM TDP-43 aggregation in the presence of AUG12 RNA (dash) and without (solid line).

1. Terzibasi, E., Valenzano, D.R., Cellerino, A. The short-lived fish *Nothobranchius furzeri* as a new model system for aging studies. *Exp Gerontol.* **2007**, *42*, 81-89.
2. Lagier-Tourenne, C., Polymenidou, M., Cleveland, D.W. TDP-43 and FUS/TLS: Emerging roles in RNA processing and neurodegeneration. *Hum Mol Genet.* **2010**, *19*, 46-64.
3. Sreedharan, J., Blair, I.P., Tripathi, V., *et al.* TDP-43 Mutations in Familial and Sporadic Amyotrophic Lateral Sclerosis. *Science.* **2008**, *319*, 1668-1672.

Effects of selected metal ions on activity of cathepsin K

Marija Kisilak,¹ Milica Janković,¹ Jakob Kljun,¹ Iztok Turel¹, Marko Novinec,^{1,*}

¹ Faculty of Chemistry and Chemical Technology, University of Ljubljana, Večna pot 113, SI-1000 Ljubljana, Slovenia, marko.novinec@fkkt.uni-lj.si

Cathepsin K is a cysteine protease that is important for bone remodeling. Its increased activity leads to osteoporosis.¹ Many ortho- and allosteric inhibitors are being researched as potential drug candidates.^{2,3} Yet so far, no metal ions have been thoroughly tested to determine their effect on cathepsin K enzymatic activity. We decided to test a scope of metal ions – Zn(II), Pb(II), Cd(II), Ga(II), Ce(IV), Ce(III) and La(III) to determine their inhibition mechanism. Preliminary test were done as kinetic titration experiments, where we determined enzymatic activity of cathepsin K with Z-FR-AMC fluorogenic substrate in the presence of increasing concentrations of metal ions to estimate their K_i or IC_{50} values and inhibition mechanisms. Ions that exhibited hyperbolic inhibition mechanisms were further tested and more exact mechanisms were determined by means of specific velocity plots. Effects on collagenolytic activity were also tested for selected ions.

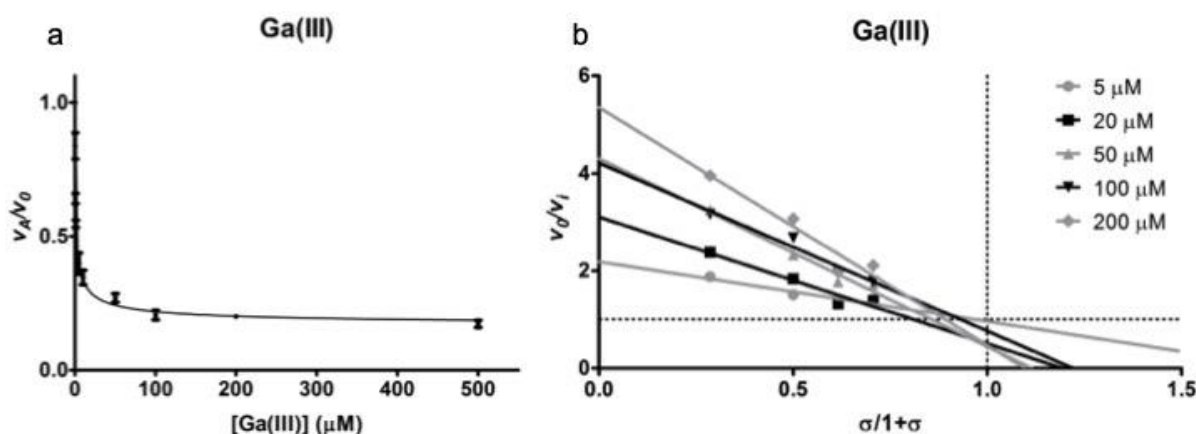


Figure 1: a) Titration curve for Ga(III) ions. Preliminary IC_{50} value was $0,9 \pm 0,1 \mu\text{M}$ and ions displayed a hyperbolic inhibition mechanism. b) Specific velocity plot for Ga(III) ions. Determined K_i was $13 \pm 2 \mu\text{M}$, α was 6 and β was approximated to be 1, which altogether points to a hyperbolic competitive inhibition of cathepsin K by Ga(III) ions.

1. Novinec, M.; Lenarčič, B., Cathepsin K: a unique collagenolytic cysteine peptidase. *Biol. Chem.* **2013**, 394, 1163-1179.
2. Drake, M. T.; et al., Cathepsin K inhibitors for osteoporosis: biology, potential clinical utility and lessons learned. *Endocr. Rev.* **2017**, 38, 325-350.
3. Novinec, M.; Lenarčič, B.; Baici, A., Probing the activity modification space of the cysteine peptidase cathepsin K with novel allosteric modifiers. *PLoS One.* **2014**, 9, e106642.

Alkali carbonate reaction as a self-healing mechanism in concretes

Marjan Marinšek¹, Violeta Bokan Bosiljkov², Rok Novak¹, Petra Štukovnik^{2*}

¹ Faculty of Chemistry and Chemical Technology, University of Ljubljana, Večna pot 113, p.p. 3422 SI-1000 Ljubljana, Slovenia

² Faculty of Civil and Geodetic Engineering, University of Ljubljana, Jamova cesta 2, 1001 Ljubljana, Slovenia, petra.stukovnik@fgg.uni-lj.si

Autogenous healing in concretes is the natural process of repairing concrete cracks that can occur in the presence of moisture or water and fills cracks through hydration of un-hydrated cement particles or carbonation of dissolved calcium hydroxide. In this respect, one has to consider also the so-called alkali-carbonate reaction (ACR) in concretes with dolomite aggregates. The basic concept of the ACR reaction can be described in brief as follows.¹ Dolomite crystals, present in dolomitic limestone aggregates, interact with the alkali hydroxides from the pore solution causing its decomposition and intergrowth of calcite and brucite. The carbonate ions, released during the dedolomitisation, migrate into the hydrated cement paste and assist in portlandite dissolution. Subsequently, released Ca^{2+} ions react with carbonate ions to form a secondary calcite (carbonate halo) around the decaying aggregate grain. Some additional reactions may take place at the phase boundary of a decaying dolomite grains and binding cement paste, i.e. formation of hydrotalcite ($6\text{MgO}\cdot\text{Al}_2\text{O}_3\cdot\text{CO}_2\cdot 12\text{H}_2\text{O}$), formation of Mg-silicate gel ($4\text{MgO}\cdot 6\text{SiO}_2\cdot 7\text{H}_2\text{O}$), and its subsequent reaction with brucite and gibbsite into clinocllore ($5\text{MgO}\cdot\text{Al}_2\text{O}_3\cdot 3\text{SiO}_2\cdot 4\text{H}_2\text{O}$). The newly formed CaCO_3 must (and can) precipitate inside empty space in concrete which in turn may result in pores and cracks filling (Fig. 1). This question has been almost completely overlooked in the literature. However, since spontaneous crack filling is a self-healing mechanism the idea of ACR as a potential self-healing process is worth to be addressed into details. This research investigates the ACR and its influence on self-healing process in concrete with dolomitic aggregate in view of changes in mechanical properties and microstructural characteristics.

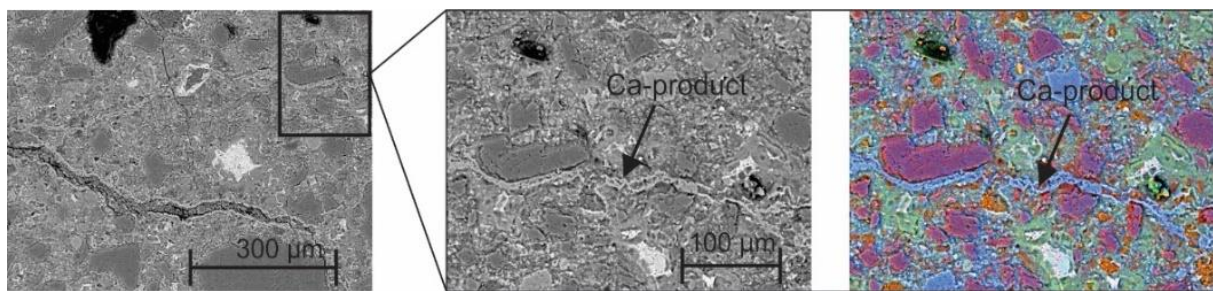


Figure 1: Formation of CaCO_3 around decaying aggregate or inside cracks.

1. (a) Štukovnik, P.; Bokan Bosiljkov, V.; Marinšek, M., Detailed investigation of ACR in concrete with silica-free dolomite aggregate. *Constr. Build. Mater.*, **2019**, *216*, 325-336., (b) Katayama, T., The so-called alkali-carbonate reaction (ACR) - Its mineralogical and geochemical details, with special reference to ASR, *Cement Concrete Res.*, **2010**, *40*, 643-675., (c) Štukovnik, P.; Prinčič, T.; Pejovnik, R.S.; Bokan Bosiljkov, V., Alkali-carbonate reaction in concrete and its implications for a high rate of long-term compressive strength increase. *Constr. Build. Mater.*, **2014**, *50*, 699-709.

Imine formation from acetylenes and anilines catalyzed by palladium complex

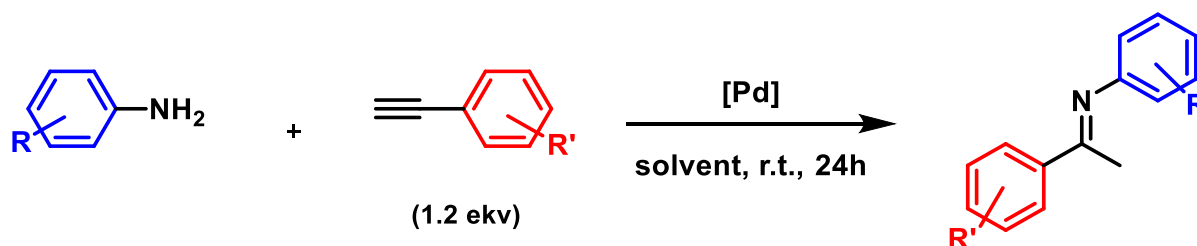
Mateja Mihelač^a, Miha Virant^a, Martin Gazvoda^a, Balazs Pinter^b, Janez Košmrlj^a

¹ Faculty of Chemistry and Chemical Technology, University of Ljubljana, Večna pot 113, SI-1000 Ljubljana, Slovenia, mateja.mihelac@fkkt.uni-lj.si

² Departamento de Química, Universidad Técnico Federico Santa María, Av. España 1680, 2390123 Valparaíso, Chile.

The formation of C–N bond attracts considerable attention in organic synthesis and in industrial chemistry.¹ Imines, an important class of nitrogen containing compound, play evident role as products and intermediates in the synthesis of various biologically active N-heterocyclic compounds and in industrial synthetic processes. Hydroamination, the addition of amine on alkynes, is the most economic process for imine synthesis. Although a wide range of metal catalysts for this transformation have been examined, in most cases the reactions were carried out under elevated temperatures and in the presence of additives.²

We recently discovered a mild and facile Pd-catalyzed intermolecular hydroamination of alkynes with anilines.³ The reactions proceed with excellent regioselectivity and yield. The full scope of the reaction and mechanistic consideration will be presented.



1. Beller, M.; Breindl, C.; Eichberger, M.; Hartung, C. G.; Seayad, J.; Thiel, O. R.; Tillack, A.; Trauthwein, H., *Advances and Adventures in Amination Reactions of Olefins and Alkynes*, *Synlett*, **2002**, *10*, 1579–1594.
2. Huang L., Arndt M., Gooßen K., Heydt H., Gooßen L. J. Late transition metal-catalyzed hydroamination and hydroamidation. *Chem. Rev.*, **2015**, *115*, 2596–2697.
3. Manuscript in preparation.

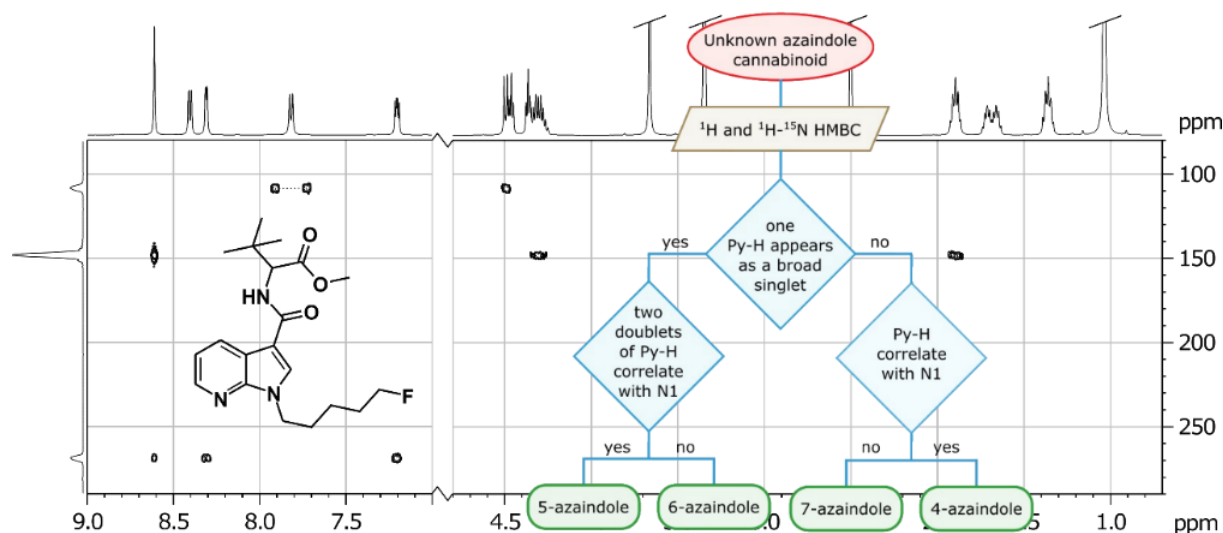
Simple and efficient flow chart diagram for azaindole core determination in new psychoactive substances: The case of 5F-MDMB-P7AICA

Bruno Aleksander Martek,¹ Mateja Mihelač,¹ Sonja Klemenc,² Janez Košmrlj¹

¹ University of Ljubljana, Faculty of Chemistry and Chemical Technology, Večna pot 113, SI-1000 Ljubljana, Slovenia, bruno.aleksander.martek@fkk.uni-lj.si

² National Forensic Laboratory, General Police Directorate, Ministry of the Interior, Vodovodna 95, SI-1000 Ljubljana, Slovenia.

A rapid growth in the number of new synthetic cannabinoid receptor agonists (SCARs) renders this group of new psychoactive substances particularly demanding in terms of detection, identification, and responding. With almost no reference data available, differentiation and structural elucidation of constitutional isomers represents one of the major obstacles¹. Amongst different 2D NMR techniques, HMBC experiment, introduced by Summers and Bax in 1986², become a corner stone in the molecular structure determination process³. Since nitrogen is a common element in biological organic compounds, ¹H–¹⁵N HMBC plays an important role in structural identification. Herein, we present a simple and efficient flow chart diagram, based on ¹H and ¹H–¹⁵N HMBC NMR spectra, for distinguishing between isomeric azaindoles, which is a common heterocyclic framework in new synthetic cannabinoids. The concept was also tested on 5F-MDMB-P7AICA, newly launched on illegal drug market¹.



1. Martek, B. A.; Mihelač, M.; Košmrlj, J.; et al., ¹H–¹⁵N NMR as a tool for rapid identification of isomeric azaindoles: The case of 5F-MDMB-P7AICA. *Drug Test. Anal.* **2019**, *11*, 617–625.
2. Bax, A; Summers, M. F., ¹H and ¹³C Assignments from Sensitivity-Enhanced Detection of Heteronuclear Multiple-Bond Connectivity by 2D Multiple Quantum NMR. *J. Am. Chem. Soc.* **1986**, *108*, 2093–2094.
3. Furrer, J., A robust, sensitive, and versatile HMBC experiment for rapid structure elucidation by NMR: IMPACT-HMBC. *Chem. Commun.* **2010**, *46*, 3396–3398.

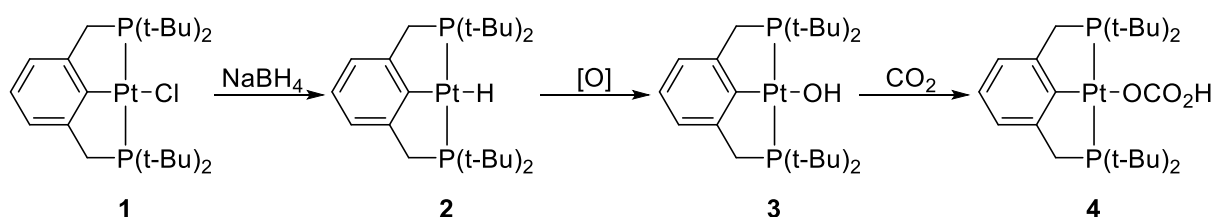
Structural properties and Transformations of Pt(II) PCP Pincer Complexes

Matic Urlep^a, Matic Lozinšek^{a,b}, and Janez Cerkovnik^{*,a}

^a Faculty of Chemistry and Chemical Technology, University of Ljubljana, Večna pot 113, SI-1000 Ljubljana, Slovenia, Janez.Cerkovnik@fkkt.uni-lj.si

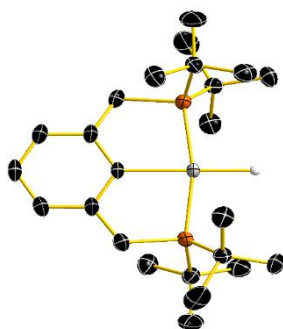
^b Jozef Stefan Institute, Jamova cesta 39, 1000 Ljubljana, Slovenia

PCP pincer complexes were first synthesized by Moulton and Shaw in 1976.¹ Since then a plethora of new pincer complexes with various applications were reported.² We will present the chemistry of PCP pincer complex **1** and its analogues. Hydride **2** was synthesized by reduction of chlorido complex **1** with NaBH₄ and its structure was determined by single-crystal X-Ray diffraction. In the presence of oxygen hydride **2** in solution slowly oxidizes to hydroxide **3**.³ Upon exposure to air hydroxide **3** readily uptakes CO₂ from atmosphere to form a bicarbonato complex **4** whose crystal structure was also elucidated. Until now only one crystal structure with bicarbonate anion as a monodentate ligand on Pt(II) center has been reported.⁴ Crystallization of PCP complexes from acidic chloride solutions leads to the formation of a trinuclear 24-membered macrocyclic complex where [PtCl₂] moieties are bridged by phosphine arms of the pincer ligands.



X-ray crystal structure of **2**

50 % probability thermal ellipsoids



1. Moulton, C. J.; Shaw, B. L. Transition metal–carbon bonds. Part XLII. Complexes of nickel, palladium, platinum, rhodium and iridium with the tridentate ligand 2,6-bis[(di-*t*-butylphosphino)methyl]phenyl. *J. Chem. Soc., Dalton Trans.* **1976**, 1020–1024.
2. Valdés, H.; García-Eleno, M. A.; Canseco-Gonzalez, D.; Morales-Morales, D. Recent Advances in Catalysis with Transition-Metal Pincer Compounds. *ChemCatChem* **2018**, *10*, 3136–3172.
3. Goldberg, K. I. et al. Experimental and Computational Investigation of the Aerobic Oxidation of a Late Transition Metal-Hydride. *J. Am. Chem. Soc.* **2019**, *141*, 10830–10843
4. Ito, M.; Ebihar, M.; Kawamura, T. Preparation and structure of [PhPt(OCO₂H)(PEt₃)₂] and [PhPt(OH₂)(PEt₃)₂]BF₄. *Inorg. Chim. Acta.* **1994**, *218*, 199–202.

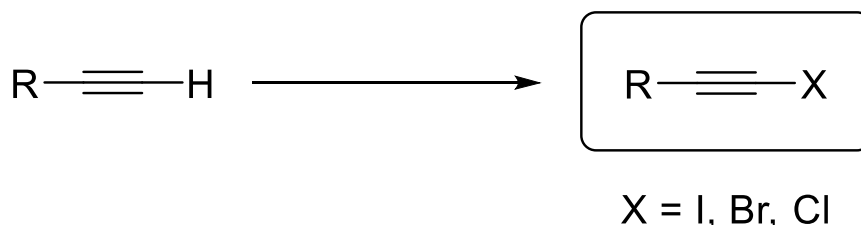
Synthesis of Haloalkynes

Anže Ivančič,^a Janez Košmrlj,^a Martin Gazvoda^{a*}

¹ Faculty of Chemistry and Chemical Technology, University of Ljubljana, Večna pot 113, SI-1000 Ljubljana, Slovenia, Martin.Gazvoda@fkkt.uni-lj.si

Owing to their multifunctionality, haloalkynes are important building blocks in organic synthesis. Because of their both electrophilic and nucleophilic nature¹ they can be used in various addition reactions as well as cycloadditions and cross-coupling reactions². They have found application in many areas of chemistry, including bioorganic chemistry, materials science and in synthesis of natural products and pharmaceuticals¹.

There are many methods for preparation of haloalkynes. Most commonly employed procedures are (i) deprotonation of terminal alkyne with strong base followed by reaction with a source of electrophilic halogen³ and (ii) dehydrohalogenation of 1,1-dihalogenated alkene⁴. Considering relatively harsh reaction conditions of described methods substantial effort has been devoted to developing milder approaches for the synthesis of haloalkynes. For example, decarboxylation of 2-yne-carboxylic acids in presence of halogenating agent⁵, transformation of 1-(trimethylsilyl)alkynes⁶ and halogenation of terminal acetylenes by employing silver (I) salts and electrophilic halogen reagents⁷. Comparison of these methods along with their modifications and improvements will be discussed.



Scheme 1: Synthesis of haloalkynes.

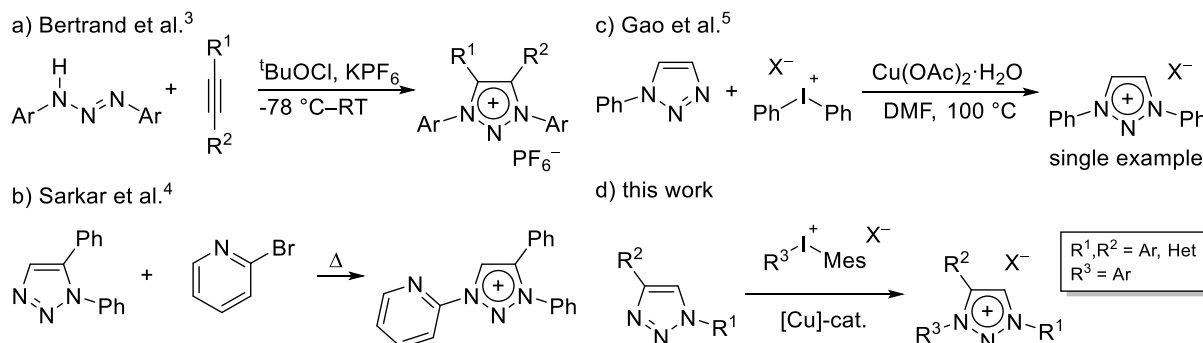
1. Jiang, H., *Haloalkyne Chemistry*. Springer: 2016.
2. Wu, W., Haloalkynes: A Powerful and Versatile Building Block in Organic Synthesis. *Acc. Chem. Res.* **2014**, *47*, 2483-2504.
3. Narayana Rao, M. L., A Simple Convenient Method for the Synthesis of 1-Iodoalkynes. *Synth. Commun.* **1995**, *25* (15), 2295-2299.
4. Grandjean, D., An Improved Procedure for Aldehyde-to-Alkyne Homologation via 1,1-Dibromoalkenes; Synthesis of 1-Bromoalkynes. *Tetrahedron Lett.* **1994**, *35* (21), 3529-3530.
5. Naskar, D., 1-Haloalkynes from Propiolic Acids: A Novel Catalytic Halodecarboxylation Protocol, *J. Org. Chem.* **1999**, *64*, 6896-6897.
6. Nishikawa, T., One Pot Synthesis of Haloacetylenes from Trimethylsilylacetylenes, *Synlett* **1994**, *1994*, 485-487.
7. Shi, D., Silver-Catalyzed Synthesis of 1-Chloroalkynes Directly from Terminal Alkynes, *ChemCatChem* **2015**, *7*, 1424-1426.

Synthesis of triaryl substituted triazolium salts

Miha Virant,^a Janez Košmrlj^{a*}

^a Faculty of Chemistry and Chemical Technology, University of Ljubljana, Večna pot 113, SI-1000 Ljubljana, Slovenia, miha.virant@fkkt.uni-lj.si

Triazolium salts are precursors for *N*-heterocyclic carbenes (NHCs). Abnormal carbenes derived thereof are termed mesoionic and have pronounced σ -donating character as compared to normal, imidazolylidene based carbene counterparts. They have found broad spectrum of applications in coordination chemistry, organic synthesis and catalysis as well as bioactive and medicinal aspects. Among those, triazolylidenes with additional heterocyclic substituents, i.e. pyridine, have displayed attractive catalytic properties when coordinated to transition metals¹. Initially triazolium salts were prepared with alkylation of click triazoles². Examples of triazolium salts with N-3 aryl substituent are rather limited to the procedure developed by Bertrand et al., however it has not been utilized to prepare heterocyclic derivatives³. Those were achieved by Sarkar in the arylation step with 2-bromopyridine⁴. To expand the scope of pyridine appended triazolium salts while exploiting the availability of click triazoles, we have developed an effective, robust, and selective arylation method employing hypervalent iodine reagents as arylating agents. This will enable for a facile preparation of a broad range of designer ligands for the fine-tunable carbenes, their coordination compounds with transition metals and (pre)catalysts with enhanced activity.



1. Gazvoda, M.; Virant, M.; Pevec, A.; Urankar, D.; Bolje, A.; Kočevar, M.; Košmrlj, J. A mesoionic bis(Py-tzNHC) palladium(II) complex catalyses “green” Sonogashira reaction through an unprecedented mechanism. *Chemical Communications* **2016**, 52 (8), 1571–1574.
2. Bolje, A.; Košmrlj, J. A selective approach to pyridine appended 1,2,3-triazolium salts. *Organic Letters* **2013**, 15 (19), 5084–5087.
3. Bouffard, J.; Keitz, B. K.; Tonner, R.; Guisado-Barrios, G.; Frenking, G.; Grubbs, R. H.; Bertrand, G. Synthesis of highly stable 1,3-diaryl-1*H*-1,2,3-triazol-5-ylidenes and their applications in ruthenium-catalyzed olefin metathesis. *Organometallics* **2011**, 30 (9), 2617–2627.
4. Suntrup, L.; Hohloch, S.; Sarkar, B. Expanding the scope of chelating triazolylidenes: mesoionic carbenes from the 1,5-“click”-regioisomer and catalytic synthesis of secondary amines from nitroarenes. *Chemistry – A European Journal* **2016**, 22 (50), 18009–18018.
5. Lv, T.; Wang, Z.; You, J.; Lan, J.; Gao, G. Copper-catalyzed direct aryl quaternization of *N*-substituted imidazoles to form imidazolium salts. *Journal of Organic Chemistry* **2013**, 2013, 78, 5723–5730.

The mechanism of palladium catalyzed alkynylation, formal copper-free Sonogashira cross-coupling reaction

Martin Gazvoda^a, Miha Virant^a, Balazs Pinter^b and Janez Košmrlj^a

^a Faculty of Chemistry and Chemical Technology, University of Ljubljana, Večna pot 113, SI-1000 Ljubljana, Slovenia, martin.gazvoda@fkkt.uni-lj.si

^b Departamento de Química, Universidad Técnico Federico Santa María, Av. España 1680, 2390123 Valparaíso, Chile

Palladium catalyzed alkynylation of aryl halides has become one of the most reliable methods for the construction of sp-sp² carbon-carbon bond.¹ Although the first contributions of this cross-coupling date more than four decades ago, up to now, critical mechanistic questions remained unresolved. Recently, experimental and computational scrutiny of the mechanism revealed, in contrast to the consensus mono-metallic mechanism, a transmetalation-centered tandem Pd/Pd catalytic cycle.^{2,3}

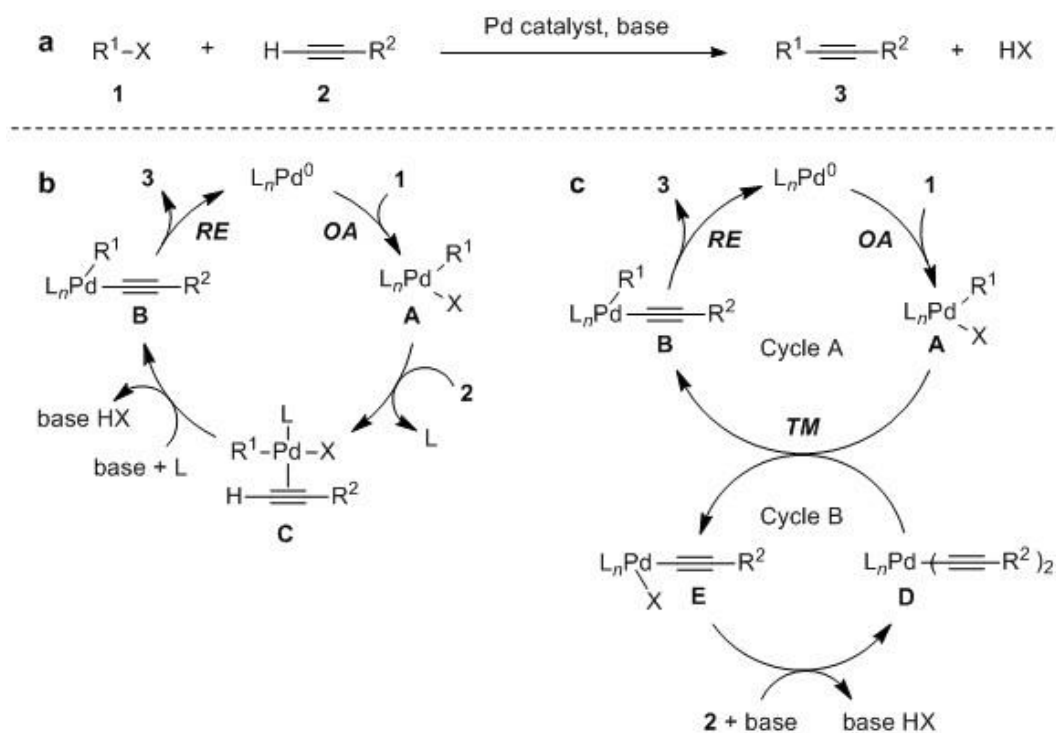


Figure 1: (a) General presentation of Cu-free Sonogashira reaction. (b) Texbook mechanism for Cu-free Sonogashira reaction. (c) Our mechanistic proposal for Cu-free Sonogashira reaction.

1. de Meijere, A.; Bräse, S.; Oestreich, M. (Eds), *Metal Catalyzed Cross-Coupling Reactions and More*. Wiley-VCH, Weinheim, Germany, 2014.
2. Gazvoda, M.; Virant, M.; Pinter, B.; Košmrlj, J., Mechanism of copper-free Sonogashira reaction operates through palladium-palladium transmetalation. *Nat. Commun.* **2018**, *9*, 4814.
3. Gazvoda, M.; Virant, M.; Pevec, A.; Urankar, D.; Bolje, A.; Kočevar, M.; Košmrlj, J., A mesoionic bis(Py-tzNHC) palladium(II) complex catalyses “green” Sonogashira reaction through an unprecedented mechanism. *Chem. Commun.* **2016**, *52*, 1571.

Characterization of Solution's Physical Properties of Bio-based 2,5-Furandicarboxylic Acid (FDCA)

Gašper Virant,¹ Ksenija Kogej,¹ Blaž Likozar,² Miša Mojca Cajnko²

¹ Faculty of Chemistry and Chemical Technology, University of Ljubljana, Večna pot 113, SI-1000 Ljubljana, Slovenia

² National Institute of Chemistry, Hajdrihova street 19, SI-1000 Ljubljana, Slovenia

Plastics such as polyethylene terephthalates (PET) have become an integral part of human life, and world's annual consumption of such plastics is forecasted to increase to over 70 million tons in 2020. Currently, the bulk portion of plastics is derived from fossil carbon sources and increasing usage of oil will inevitably end in exhaustion of world's capacity¹. 2,5-furandicarboxylic acid (FDCA) is great bio-based counterpart of fossil-based terephthalic acid (TA). Polymerization of FDCA with ethylene glycol gives polyethylene furanoate (PEF), 100 % bio-based plastics that even outperform traditional plastics (PET) and is especially suitable for bottle production in beverage industry. Moreover, PEF production can reduce the non-renewable energy usage and greenhouse gas emissions by 40-50 % and 45-55 %, respectively, compared to PET².

FDCA is a small molecule with molecular mass of 156,09 g/mol. However, it has an unusual high melting temperature of 342 °C and very low solubility in most of common solvents (in water only 0.001 g/g at room temperature). That seems to indicate extensive intermolecular bonding which could be achieved via combination of hydrogen bonding between carboxylic groups and pi-pi stacking of aromatic furan rings^{3,4}.

We investigated proposed intermolecular binding with determination of density and viscosity in temperature interval 25 – 55 °C and determination of colligative properties of FDCA solution. Using cryoscopic method for measuring osmotic pressure we identified, that FDCA in water solution is only 18,39 % deprotonated. Thus all carboxylic groups that are not deprotonated (81,61 %) could potentially form H-bonds with neighbouring FDCA molecules and in that fashion bind themselves into di-, tri- or n-meres, as proposed on figure 1.

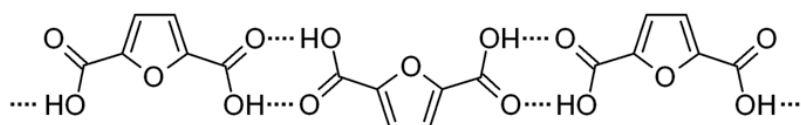


Figure 9: Proposed intermolecular hydrogen bonding between FDCA molecules.

1. Karich, A.; Kleeberg, S.; Ullrich, R.; Hofrichter, M. Enzymatic Preparation of 2,5-Furandicarboxylic Acid (FDCA)—A Substitute of Terephthalic Acid—By the Jointed Action of Three Fungal Enzymes. *Microorganisms*. **2018**, *6*, 1-12.
2. Isikgor, F. H.; Becer, C. R. Lignocellulosic Biomass: A Sustainable Platform for the Production of Bio-Based Chemicals and Polymers. *Polym. Chem.* **2015**, *6*, 4497–4559.
3. Lewkoski, J. Synthesis, Chemistry and Applications of 5 HMF and Its Derivatives. *ARKIVOC* **2001**, *101*, 17–54.
4. Kumar, M.; Sheikh, H. N.; Fraconetti, A.; Zaręba, J. K.; Sahoo, S. C.; Frontera, A. 2,5-Furandicarboxylic Acid as a Linker for Lanthanide Coordination Polymers: The Role of Heteroaromatic π - π Stacking and Hydrogen Bonding. *New J. Chem.* **2019**, *43*, 2179–2195.

Antimicrobial activity of nitrosifying bacteria Nitrosomonas eutropha

Urška Virant¹, Mojca Lunder¹, Maša Močnik Roner¹

¹Faculty of Pharmacy, University of Ljubljana, Aškerčeva cesta 7, SI-1000 Ljubljana, Slovenia

One of the latest trends in the cosmetic industry is cosmetics with probiotics. These are cosmetic products that contain living non-pathogenic organisms which, when administered in adequate amounts, confer a health benefit. Their purpose in cosmetic products is to improve the barrier function of the skin, to inhibit the growth of the pathogen, to stimulate the wound healing process and action of immune cells.¹ One of these products is also the Ao+Mist™, which we tested. During regular application, the skin should be smoother, and conditions of greasy, dry and sensitive skin are supposed to be improved.² It contains nitrosifying bacteria *Nitrosomonas eutropha* D23 (*N. eutropha* D23) that converts ammonia in sweat to nitrite and nitric oxide. In an era of the increasing bacterial resistance to available antibiotics, nitric oxide appears as a promising topical broad-spectrum antimicrobial agent with a small likelihood of resistance



development because of various mechanisms of action on pathogens.^{3,4,5} The main purpose of our work was to test the antimicrobial activity of nitrosifying bacteria *N. eutropha* D23 on *Candida albicans*, *Pseudomonas aeruginosa*, *Staphylococcus aureus*, and *Aspergillus brasiliensis* by the discs diffusion test method. First, we tested if the product contains bacteria *N. eutropha* D23. We also observed how different factors affect the growth and activity of these bacteria. The concentration of bacteria was determined by measuring the optical density at 600 nm. Their activity was determined by measuring the concentration of nitrite spectrophotometrically at 352 nm and 400 nm.

Figure 10: Liquid growth medium after centrifugation. A red pellet is observed (*Nitrosomonas eutropha*).

1. Daniel, C.; Pot, B.; Foligne, B.: Probiotics from research to market: the possibilities, risks and challenges. *Curr. Opin. Microbiol.* **2013**; 16: 284-292.
2. Ao+Mist™. <https://shop.motherdirt.com/product/ao-mist-2/> (accessed Aug 10, 2019)
3. Adler B.L.; Friedman A.J.: Nitric oxide therapy for dermatologic disease. *Future Sci. OA* **2015**; 1: fso.15.37.
4. Ghaffari, A.; Neil, D.H.; Ardakani, A.; Road, J.; Ghahary, A.; Miller, C.C. A direct nitric oxide gas delivery system for bacterial and mammalian cell cultures. *Nitric Oxide - Biology and Chemistry* **2005**; 12: 129–140.
5. Jones, M.L.; Ganopolsky, J.G.; Labbé, A.; Wahl, C.; Prakash, S.: Antimicrobial properties of nitric oxide and its application in antimicrobial formulations and medical devices. *Appl. Microbiol. Biotechnol.* **2010** Sep;88:401-7.

Superhydrophobic aluminium surface with excellent corrosion resistance, self-cleaning and anti-icing properties

Peter Rodič^{*1}, Veronika Bračič², Barbara Kapun¹, Ingrid Milošev¹

¹ Jožef Stefan Institute, Jamova cesta 39, 1000 SI-1000 Ljubljana, Slovenia, peter.rodic@ijs.si

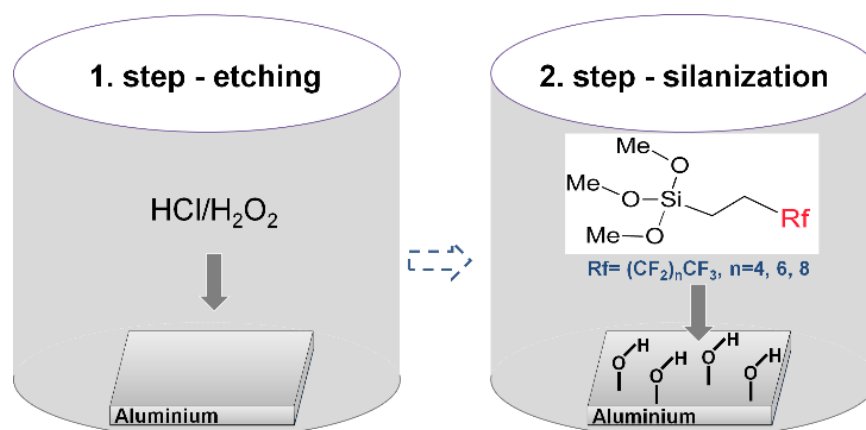
² Faculty of Chemistry and Chemical Technology, University of Ljubljana, Večna pot 113, SI-1000 Ljubljana, Slovenia

Aluminium has excellent mechanical and physical properties, but in chloride-containing corrosive environments, it has low corrosion resistance. One of the options, to suppress this drawback, is reducing the wettability of the aluminium surface by formation of the superhydrophobic film on surface ^{1, 2}.

Superhydrophobicity is generally defined when the contact angle of the water droplet on the surface is greater than 150° and sliding angle is lower than 10°. In such conditions, water droplets exhibit a spherical shape, which roll off from the surface.

In this study, the superhydrophobic surface with hierarchical micro/nano structure was prepared by etching in HCl/H₂O₂ solution ¹, followed by immersion in perfluoro silanes with various chain lengths ², Scheme 1. Electrochemical properties were evaluated in 0.1 M NaCl solution using potentiodynamic measurements. Surface morphology/composition was studied using scanning electron microscopy coupled with energy dispersive spectroscopy (SEM/EDS). Wettability was assessed by measuring the water contact angle using tensiometer.

The treated aluminium surface shows superhydrophobic behaviour, improved corrosion resistance, self-cleaning nature of the surface and anti-icing properties.



Scheme 1: Two-step preparation of the superhydrophobic aluminium surface.

1. Tong, W.; Xiong, D.; Wang, N.; Jan, C.; Tian, T., Green and timesaving fabrication of a superhydrophobic surface and its application to anti-icing, self-cleaning and oil-water separation *Surface and Coatings Technology* **2018**, 352, 609-618.
2. Rodič, P.; Milošev, I., One-step ultrasound fabrication of corrosion resistant, self-cleaning and anti-icing coatings on aluminium, *Surface and Coatings Technology* **2019**, 369, 175-185.

Hybrid sol-gel coating to improve corrosion protection of AA2024-T3 in chloride media

Peter Rodič^{*1}, Jure Lavrič², Barbara Kapun¹, Ingrid Milošev¹

¹ Jožef Stefan Institute, Jamova cesta 39, 1000 SI-1000 Ljubljana, Slovenia, peter.rodic@ijs.si

² Faculty of Chemistry and Chemical Technology, University of Ljubljana, Večna pot 113, SI-1000 Ljubljana, Slovenia

The aluminium alloy 2024-T3 (AA2024-T3) is widely used in the aerospace industry due to its low weight and its passive behaviour in atmospheric conditions. However, due to the presence of alloying elements such as Cu, Fe, Mn, etc., this alloy is highly sensitive to corrosion in chloride-containing solutions.

In the past, better corrosion protection was mainly based on chromate conversion treatments. Unfortunately, due to its negative effect on human health and environment, the use of hexavalent chromium(VI) and other compounds containing chromium have been limited in many countries.

Among possible environmentally acceptable surface treatments, the sol-gel coating is considered as an alternative. The sol-gel chemistry is based on the hydrolysis and condensation reactions of initial organically modified silica and silane reagents.

In this study, the effects of hybrid sol-gel coatings on corrosion performance formulations applied on AA2024-T3 were studied. The synthesis was prepared from organic precursors: 3-(methacryloyloxy)propyl trimethoxysilane and methyl methacrylate. The inorganic one was tetraethyl orthosilicate (TEOS) ^{1,2}. Butyl acetate was used as a solvent. The characterization was performed by Fourier-transform infrared spectroscopy (FTIR) and scanning electron microscopy (SEM). The barrier properties were evaluated by electrochemical measurements and during exposure in the salt spray chamber according to standard ASTM 117.

The results indicated that synthesized hybrid sol-gel coatings are able to form a continuous few micrometres thick film, necessary to provide good barrier properties. Thus, AA2024-T3 shows better corrosion performance in the studied media.

1. Mosa, J.; Rosero-Navarro, N.; C. Aparicio, M., Active corrosion inhibition of mild steel by environmentally-friendly Ce-doped organic-inorganic sol-gel coatings, *RSC Advances*, **2016**, 6, 39577-39586.
2. Rodič, P.; Iskra, J.; Milošev, I., Study of a sol-gel process in the preparation of hybrid coatings for corrosion protection using FTIR and ¹H NMR methods, *Journal of Non-Crystalline Solids*, **2014**, 396–397, 25-35.

We organize this year's conference with
the University Unit for researcher support and promotion
(University Office for research)
within the celebration of the
100th anniversary of University of Ljubljana



in collaboration with



And in partnership with



We are truly grateful to all the sponsors
without whom it would be impossible to make this year's
Cutting Edge happen:



We are especially very honoured that
both coffee breaks were organized by



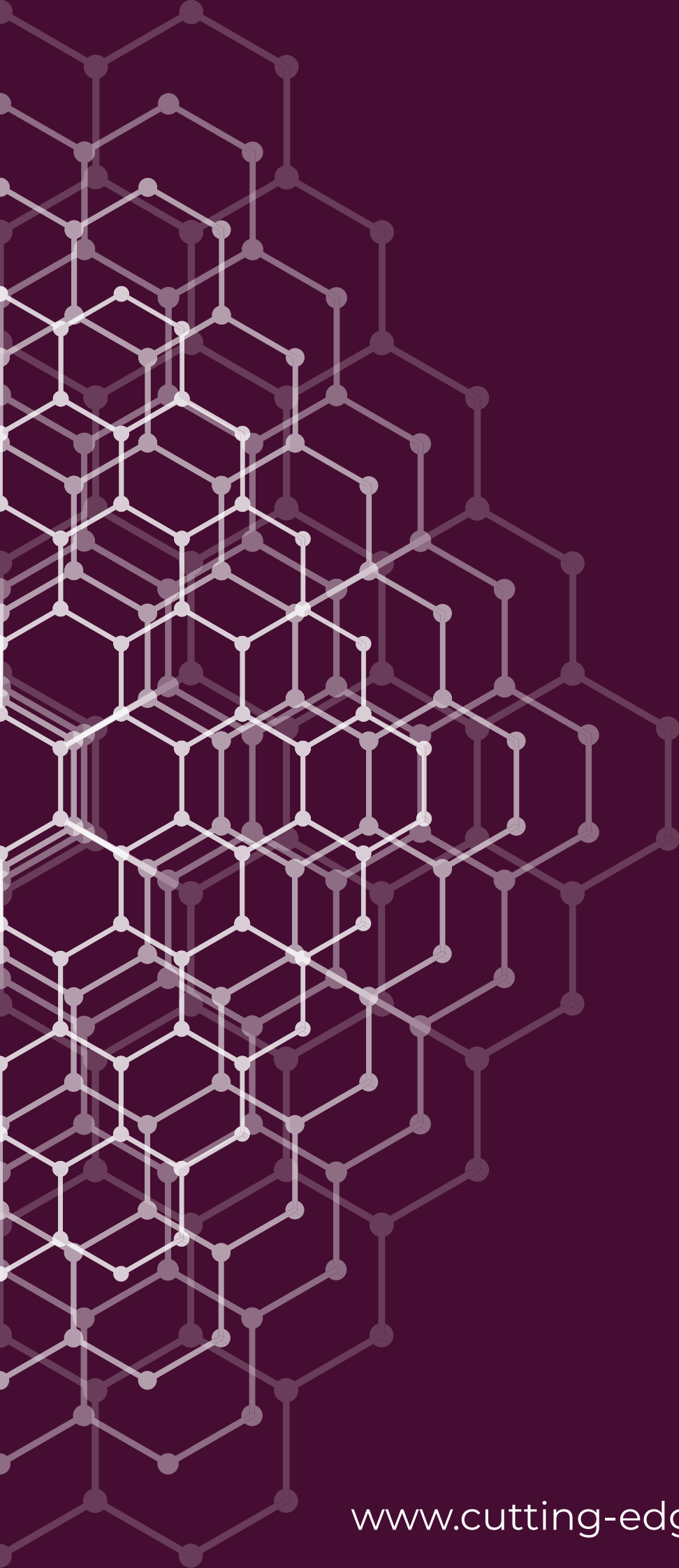
KAMPUS

 **ŠOU**
v Ljubljani

 **stiks**
društveno stičišče ŠOU v Ljubljani

Študentski Kampus je glavno stičišče študentskih idej, aktivnosti in podpornih storitev, ki jih vsak študent potrebuje v času svojega študija. Namen Kampusa je študentom omogočiti platformo, kjer lahko razvijajo svoje potenciale, skupaj ustvarjajo, se športno in umetniško udeležujejo, razvijajo svoje projektne ali podjetniške ideje ter imajo pri tem ustrezno strokovno in infrastrukturno podporo. Kampus vsebuje tudi socialno dimenzijo, s katero želimo s pomočjo subvencioniranih storitev in dejavnosti študentom olajšati njihove finančne težave.

Vizija Študentskega kampusa je postati osrednje stičišče vseh študentov – tako študentov, ki študirajo v Ljubljani, kot tudi študentov iz drugih univerzitetnih središč.



www.cutting-edge.si